



Growth patterns and climate-growth relationships of three *Helichrysum* shrub species  
along an elevation gradient in the Drakensberg Alpine Centre

Tamara Botha



A dissertation submitted to the Faculty of Science, University of the Witwatersrand,  
Johannesburg, in fulfilment of the requirements for the degree of Master of Science.

School of Geography, Archaeology and Environmental Studies

November 2020

ORCID: 0000-0003-1967-1579

## Authorship Declaration

I, Tamara Botha, declare that this research report, apart from the contributions mentioned in the acknowledgments, is my own, unaided work. It is being submitted for the degree of Master of Science by dissertation to the University of the Witwatersrand. It has not been presented before for any degree or examination to any other University.

---

Tamara Botha (1499351)

6 November 2020

Date

## Abstract

Mountains are complex environments owing to environmental lapse rates, varying exposures, changing topography and different microclimatic conditions and, as a result, they act as havens for a variety of ecosystems and high biodiversity. Mountain ecosystems are unique as species remain confined to high elevations compared to areas downslope where vegetation communities occupy broader climatic niches and ranges over wider latitudinal belts. Plant species that grow at these locations are adapted to, or are constrained by, a narrow range of environmental conditions and can be used as possible climate proxies in a changing climate.

This study investigates the growth patterns of *Helichrysum tenuifolium*, *H. trilineatum* and *H. witbergense* species along an elevation gradient in the Drakensberg Alpine Centre (DAC) to determine whether they respond to inter-annual climate variability and how microhabitats may influence their growth patterns. Patterns of ring widths differ between two *Helichrysum* species in the alpine thermal belt (*H. witbergense* and *H. trilineatum*) and the two species located in the upper-montane thermal belt (*H. tenuifolium* and *H. trilineatum*) are evaluated using dendrochronology and AMS radiocarbon dating methods. Data were collected from Kotisephola Pass ( $\pm 3\ 282$  to  $3\ 332$  m a.s.l.), Sani Pass-upper ( $\pm 2\ 859$  to  $2\ 916$  m a.s.l.) and Sani Pass-lower ( $\pm 2\ 514$  to  $2\ 585$  m a.s.l.). Clearly discernable growth rings were identified in all species and ranged from 0.3 mm to 2.4 mm in width. The growth period and age determined using AMS radiocarbon dating confirmed that these three *Helichrysum* species form annual growth rings.

Shrub abundance analyses confirmed that *H. witbergense* were only found at high elevations, in mostly cool and moist areas on south-facing aspects. In contrast, *H. tenuifolium* were only observed at the low elevation study site on eastern aspects. *H. trilineatum* were found at all three study sites and are more abundant on south- and west-facing slopes, except for the Sani Pass-lower study site where they occur only on east-facing aspects. This research confirms that climate, elevation, and aspect all influence their growth patterns and that these species exhibit specific habitat preferences in terms of microhabitats and ecological niches.

There were no consistent statistical trends in shrub growth ring chronologies along the elevation gradient, since shrubs in the alpine and sub-alpine thermal belt have complacent growth patterns. Mean annual temperature, mean growing season temperature and monthly total precipitation rainfall and total growing season rainfall were used for the analysis. Correlation analysis indicated that temperatures in summer had positive correlations with shrub growth (previous December and current January and February for all the sites). Precipitation during the growing season had weak

negative relationships with the all chronologies. However, high precipitation was associated with low temperature in early growing season, further supporting that temperature is a growth-limiting factor. Multiple regression analyses confirmed that a combination of temperature, rainfall, aspect, and elevation influences *Helichrysum* shrub growth. The observed shrub growth response to climate variability increases our understanding of the mechanisms underlying current shrub growth patterns, which is required to predict future climate-driven alpine vegetation patterns.

**Keywords:** *Helichrysum*, Drakensberg Alpine Centre, dendrochronology, AMS radiocarbon dating, climate

## Acknowledgements

I would like to express my sincere gratitude to my supervisors Prof. Stefan Grab, Drs. Stephan Woodborne and Clinton Carbutt for their continued support through this master's project; for their patience, motivation, enthusiasm, and immense knowledge. I cannot imagine having a better team of knowledgeable supervisors.

My sincere thanks go to the team at CE Moss Herbarium for assisting me with the use of the stereo microscope and to the team at NRF iThemba LABS, particularly Mr. Moshabi Silidi, for assisting me with the practical work in the laboratory, the analysis of the AMS results and for their willingness throughout the year in assisting me.

I thank my field assistants, Bianca Kieweg and my mother, Ilse Botha, for their enthusiasm and assistance through my fieldwork and Prof. Stefan Grab and Dr. Clinton Carbutt for showing me the way and making sure I am at ease in the field.

This thesis was made possible through financial assistance from the University of the Witwatersrand, Johannesburg.

Last, I would like to thank my parents and grandfather for the support and continuous words of encouragement throughout the year.



# Contents

<b>Authorship Declaration</b> .....	ii
<b>Abstract</b> .....	iii
<b>Acknowledgements</b> .....	v
<b>List of Tables</b> .....	ix
<b>List of Figures</b> .....	x
<b>List of Plates</b> .....	xii
<b>List of Abbreviations</b> .....	xiii
<b>CHAPTER ONE</b> .....	1
1.1 Aim and Objectives .....	3
1.2 Structure of the research report .....	4
<b>CHAPTER TWO</b> .....	5
2.1 Introduction .....	5
2.2 Climate change .....	5
2.2.1 Climate change impacts on southern Africa .....	6
2.3 Mountains .....	7
2.3.1 Mountain vegetation .....	8
2.3.2 Mountains and climate change .....	8
2.4 The Drakensberg Alpine Centre .....	9
2.4.1 Effects of climate change on the DAC and its associated vegetation .....	11
2.5 Shrub growth ring analysis as a research tool to trace climatic influence .....	13
2.5.1 Dendrochronology .....	15
2.5.1.1 Dendrochronological method .....	16
2.5.1.2 Dendrochronological studies .....	18
2.5.2 AMS Radiocarbon dating .....	23
2.5.3 Advantages and disadvantages of using dendrochronology and AMS radiocarbon dating techniques .....	23
2.5.4 Challenges and potential for dendrochronological research in southern Africa .....	24
2.6 Study overview .....	24
<b>CHAPTER THREE</b> .....	26
3.1. Environmental setting .....	26
3.1.1. Geology and soils .....	27
3.1.2. Climate .....	27
3.1.3. Vegetation .....	28
3.1.4. Shrub abundance .....	32
3.2. Field work .....	32

3.2.1.	Collection of shrub stems.....	33
3.3.	Laboratory work.....	33
3.3.1	Growth patterns.....	33
3.3.2	AMS radiocarbon dating.....	35
3.4	Data sources.....	37
3.5	Statistical Analyses.....	38
3.5.1	Growth patterns.....	38
3.5.2	Growth analysis.....	38
3.5.3	Climate-growth relationships.....	39
3.5.4	Distribution and abundance of shrub species at the study sites.....	39
3.6	Summary.....	40
<b>CHAPTER FOUR</b>	.....	<b>41</b>
4.1	Introduction.....	41
4.2	Growth patterns.....	41
4.2.1	Growth ring characteristics and anomalies.....	41
4.2.2	Growth ring analysis.....	42
4.2.3	Growth chronologies.....	53
4.2.4	Radiocarbon dating.....	59
4.3	Distribution and abundance.....	61
4.3.1	Kotisephola Pass study site.....	61
4.3.2	Sani Pass-upper study site.....	62
4.3.3	Sani Pass-lower study site.....	63
4.4	Climate.....	64
4.4.1	Temperature.....	64
4.4.2	Rainfall.....	67
4.5	Climate-growth relationship.....	68
4.5.1	Pearson correlation coefficients of <i>Helichrysum</i> growth and temperature.....	68
4.5.2	Pearson correlation coefficients of <i>Helichrysum</i> growth and rainfall.....	69
4.5.3	Multiple regression analysis.....	69
4.6	Summary.....	70
<b>CHAPTER FIVE</b>	.....	<b>71</b>
5.1	Growth patterns.....	71
5.2	Growth chronologies.....	72
5.4	Distribution and abundance.....	73
5.5	Climate.....	74
5.6	Climate-growth relationship.....	75
5.7	Key findings.....	76

<b>CHAPTER SIX</b> .....	78
<b>REFERENCE LIST</b> .....	80
<b>APPENDIXES</b> .....	108
Appendix i: Sample information.....	108
Appendix ii: AMS Radiocarbon dating results.....	113
Appendix iii: Mean correlation results.....	114
Appendix iv: Correlation coefficients of <i>Helichrysum</i> shrubs growing at different elevations and aspects .....	115
Appendix v: Multiple regression of climate-growth relationships.....	116
Appendix vi: Summary of shrub abundance .....	120



## List of Tables

Table 2-1: Research themes and questions investigated using shrubs for dendrochronology. .20	
Table 2-2: Summary of dendrochronological and dendroclimatological studies undertaken in southern Africa.....21	
Table 3-1: Summary of the chosen species and their threats (Hilliard, 1963, p. 220; Carbutt and Edwards, 2006).....31	
Table 3-4: Summary of climate datasets used.....38	
Table 4-1: Shrubs affected by woodboring insects. ....41	
Table 4-2: Site information, chronology statistics and common interval (1964–2018) statistics of the three shrub species from the three sampling sites from different elevations. ....42	
Table 4-3: Site information, chronology statistics and common interval (1964–2018) statistics of the three shrub species from the three sampling sites from different elevations and aspects. ....43	
Table 4-4: Growth pattern information of <i>H. trilineatum</i> , <i>H. witbergense</i> and <i>H. tenuifolium</i> . ....44	
Table 4-5: Mean correlations of shrub growth chronologies of shrub species located at different elevations. Significant level of $p < 0.05$ . ....55	
Table 4-6: Pearson correlation coefficients of <i>Helichrysum</i> growth chronologies over a 11-year period from 2007 to 2018. Significant level of $p < 0.05$ . ....58	
Table 4-7: Radiocarbon dates and deduced mean number of rings formed per year. Where $\delta^{13}\text{C}$ = a measurement that indicates the source of the C in the sample, pMC (percent Modern Carbon) - the sample age in standard radiocarbon terms. ....60	
Table 4-8: Pearson correlation analysis results of <i>Helichrysum</i> growth and seasonal temperature. ....68	
Table 4-9: Pearson correlation analysis results of <i>Helichrysum</i> growth and seasonal rainfall...69	

## List of Figures

Figure 2-1: Drakensberg Alpine Centre (DAC) comprising (1) eastern Free State, (2) KwaZulu-Natal Drakensberg, (3) Lesotho Maloti Mountains and (4) Eastern Cape Drakensberg and Witteberge. Where Be = Bergville; E = Elliot; H = Harrismith; Hi = Himeville; K = Kokstad; Ma = Maseru; Mc = Maclear; U = Underberg (adapted from Carbutt and Edwards, 2004). .....10

Figure 2-2: Schematic profile through the Drakensberg showing major thermal belts and associated vegetation classes, and location of the lower–upper montane treeline ecotone (adapted from Carbutt and Edwards, 2015). .....13

Figure 2-3: Schematic representation of the dendrochronological assessment process (adapted from Pignatelli, 2010). .....17

Figure 2-4: Schematic overview of the dendrochronological process for alpine and arctic shrubs (adapted from Myers-Smith *et al.*, 2015). .....18

Figure 3-1: Locality of the three study sites. ....26

Figure 3-2: Layout of the 20m x 20m and 2m x 2m plots. ....32

Figure 4-1: Growth ring analysis of *H. trilineatum* at Kotisephola Pass study site. ....48

Figure 4-2: Growth ring analysis of *H. witbergense* at Kotisephola Pass study site. ....49

Figure 4-3: Growth ring analysis of *H. trilineatum* at Sani Pass-upper study site. ....51

Figure 4-4: Growth ring analysis of *H. tenuifolium* at Sani Pass-lower study site. ....52

Figure 4-5: Growth ring analysis of *H. trilineatum* at Sani Pass-lower study site. ....53

Figure 4-6: Standardised growth chronologies of *Helichrysum* species at the three study sites. ....54

Figure 4-7: Standardised growth chronologies of *H. trilineatum* at different aspects at the Kotisephola Pass study site. ....56

Figure 4-8: Growth chronologies of *H. witbergense* at different aspects at the Kotisephola Pass study site. Ring width index indicates z-scores. ....56

Figure 4-9: Growth chronologies of *H. trilineatum* at the Sani Pass-upper study site. ....56

Figure 4-10: Growth chronologies of *H. trilineatum* at the Sani Pass-lower study site. ....57

Figure 4-11: Growth chronologies of *H. tenuifolium* at the Sani Pass-lower study site. Ring width index indicates z-scores. ....57

Figure 4-12: AMS radiocarbon age versus ring count of *Helichrysum* samples. ....59

Figure 4-13: Aerial cover percentage and preferred aspect for growth of *Helichrysum* growing at the Kotisephola Pass study site. ....61

Figure 4-14: Aerial cover percentage and preferred aspect for growth of *Helichrysum* growing at Sani Pass-upper study site. ....63

Figure 4-15: Mean annual temperatures for Sani Top, Sani Pass-lower and Kotisephola Pass study site.....65

Figure 4-16: Mean minimum temperatures for Sani Top, Sani Pass-lower and Kotisephola Pass study sites.....65

Figure 4-17: Mean maximum temperatures for Sani Top, Sani Pass-lower and Kotisephola Pass study sites.....66

Figure 4-18: Mean annual growing season temperatures for Sani Top, Sani Pass-lower and Kotisephola Pass study site. ....66

Figure 4-19: Total annual rainfall for Giant's Castle, Shaleburn, Mokhotlong and a composite of these three sites.....67

Figure 4-20: Total growing season rainfall for Giant's Castle, Shaleburn, Mokhotlong and a composite of these three sites.....68

## List of Plates

Plate 3-1: a) <i>H. tenuifolium</i> , b) <i>H. witbergense</i> and c) <i>H. trilineatum</i> .....	30
Plate 4-1: Growth rings of <i>H. trilineatum</i> . Arrows indicate direction of growth. ....	42
Plate 4-2: <i>Helichrysum</i> affected by woodboring insects. Arrows indicate wounding. ....	42
Plate 4-3: a) Photograph of the south-western aspect at the Kotisephola Pass study site, with the rock outcrop on the left and <i>H. witbergense</i> and <i>H. trilineatum</i> in close vicinity. b) Photograph of the eastern aspect at the Kotisephola Pass study site.....	62
Plate 4-4: Photograph of the southern aspect at the Sani Pass-upper study site.....	62
Plate 4-5: a) Photograph of the Sani Pass-lower study site located between a gravel road and a gully. b) Photograph of <i>E. tysonii</i> and <i>H. trilineatum</i> at the Sani Pass-lower study site. ....	64

## List of Abbreviations

ABA	Acid-Base-Acid
AMS	Accelerated Mass Spectrometry
AD	Anno Domini
ASL	Above Sea Level
BP	Before Present
°C	Degree Celsius
°C/yr	Degree Celsius per Year
ca.	Circa, Meaning Around or About
CAL	Calendar
DAC	Drakensberg Alpine Centre
e.g.	Exempli Gratia (For Example)
ENSO	El Niño Southern Oscillation
GBIF	Global Biodiversity Information Facility
GS	Growing Season
GST	Growing Season Temperature
HTe	<i>Helichrysum tenuifolium</i>
HTr	<i>Helichrysum trilineatum</i>
HW	<i>Helichrysum witbergense</i>
IPCC	Intergovernmental Panel on Climate Change
LMS	Lesotho Meteorological Services
KHTr	Kotisephola Pass study site <i>Helichrysum trilineatum</i>
KHW	Kotisephola Pass study site <i>Helichrysum witbergense</i>
m a.s.l.	Meters Above Sea Level
MAT	Mean Annual Temperatures
MATmin	Mean Annual Minimum Temperature
MATmax	Mean Annual Maximum Temperature
MAGST	Mean Annual Growing Season Temperature
MAGSTmin	Mean Annual Minimum Growing Season Temperature
MAGSTmax	Mean Annual Maximum Growing Season Temperature
MANGST	Mean Annual Non-Growing Season Temperature

MANGSTmin	Mean Annual Minimum Non-Growing Season Temperature
MANGSTmax	Mean Annual Maximum Non-Growing Season Temperature
MHTr	Sani Pass-upper study site <i>Helichrysum trilineatum</i>
mm	Millimeter
mm/yr	Millimeter Per Year
NH	Northern Hemisphere
NOAA	National Oceanic and Atmospheric Administration
PDB	Pee Dee Belemnite
pMC	Percent Modern Carbon
SH	Southern Hemisphere
SHTe	Sani Pass study site <i>Helichrysum tenuifolium</i>
SHTr	Sani Pass study site <i>Helichrysum trilineatum</i>
SIO	South Indian Oscillation
VPDB	Vienna Pee Dee Belemnite
yr(s)	Year or Years

# CHAPTER ONE

## Introduction

Mountains are an important component of the Earth's ecosystems, hosting an estimated one-third of terrestrial biodiversity and half of the thirty-four global biodiversity hotspots (Beniston, 2003; Spehn *et al.*, 2011; Körner *et al.*, 2017), most likely due to environmental lapse rates, varying exposures, changing topography and different microclimatic conditions typical to mountainous environments (Körner *et al.*, 2017). As a result of biogeographic isolation of mountain ecosystems, many endemic species can be found in mountain biomes (Spehn *et al.*, 2011; Körner *et al.*, 2017). Diverse mountain vegetation is of particular importance as high vegetation cover prevents and/or minimises the impact of soil erosion and mass movement (e.g. landslides) (Körner *et al.*, 2017). Mountain vegetation provides food, fibre, fodder, clean water, and often acts as a tourist attraction due to the natural beauty it adds to associated landscapes (Körner *et al.*, 2017; Ngwenya *et al.*, 2018). Mountain ecosystems have served as refugia for organisms during past climatic change and they are predicted to do so through future climatic change (Körner *et al.*, 2017). However, mountain ecosystems accommodate the effects of climate change through species migration, which leaves them vulnerable to biodiversity loss, spread of invasive species and land degradation (Elsen and Tingley, 2015; Pauchard *et al.*, 2015; IPCC, 2018).

An ecosystem's resilience is not infinite, and its ecological functioning may change in response to climate change. Previous studies have found that mountain ecosystems and associated biota are disproportionately influenced by climate change (Engler *et al.*, 2011; Gottfried *et al.*, 2012; Gentili *et al.*, 2015). Each elevation zone or vegetation belt in a mountain ecosystem is characterised by distinct vegetation and ecosystem functions (Körner *et al.*, 2011, Carbutt, 2012). Understanding the current changes and dynamics of different mountain vegetation types in relation to climatic changes and anthropogenic activities is essential for the development of adaptive strategies to address the challenges posed by both climate change and human activities (Jiang *et al.*, 2017).

Archer *et al.* (2018) mentioned that southern African temperatures have been increasing rapidly at a rate of about twice the global rate. Studies specifically focused on the Lesotho highlands predict warmer summers with frequent droughts (mostly December to January) and delayed, but more intense rainfall seasons, and less snow in winter (Grab *et al.*, 2017; Morris, 2017a; Mukwada and Manatsa, 2018; Bentley *et al.*, 2019). Growing evidence indicates that high-mountain environments experience more rapid changes in temperature than environments at lower elevations at the same location (Gilbert and Vincent, 2013). Climatic changes may impact mountain ecosystem by affecting the abundance of species and communities, biotic interactions, ecosystem functionality, and the geographic ranges

of individual species and biomes (Kerns *et al.*, 2018; Rogora *et al.*, 2018). It may influence vegetation growth patterns, including structural and composition changes of species (Diaz *et al.*, 2003; Kerns *et al.*, 2018). Despite the pressure of climatic changes, African mountains are also facing socio-economic pressures (Nsengiyumva, 2019). Population growth and increased socio-economic development place pressure on water provision and has led to competition over natural resources (Nsengiyumva, 2019). The compound effects of climate change and socio-economic pressures on African mountains affects the wellbeing and livelihoods of people residing in these mountain environments (Nsengiyumva, 2019).

The study region for this M.Sc. project is located in the Drakensberg Alpine Centre (DAC), covering two thermal belts (alpine and upper-montane), with relatively well-partitioned vegetation communities (dominated by dwarf shrubs, C<sub>3</sub> and C<sub>4</sub> grasses) (Carbutt and Edwards, 2015a). According to Carbutt and Edwards (2015a, p. 262), “this tree line ecotone is a key temperature threshold area and is therefore an ideal boundary to use for climate change research.” Predicted increasing air temperatures will potentially impact these temperature-limited plants, as shrubs growing at these high elevations are limited and adapted to a narrow range of environmental conditions (Morris, 2017a). These shrubs may potentially experience a longer growth season as the number of frost days and frequency of severe snowfalls are expected to decrease with predicted increasing air temperatures (Morris, 2017a). In addition to the threats of climate change, the unregulated harvesting of shrubs for fuelwood (Gentili *et al.*, 2015) may pose an even greater threat to these species, particularly if the harvest rate is greater than plant growth rate.

For this study, three woody shrub species (*Helichrysum tenuifolium*, *Helichrysum trilineatum* and *Helichrysum witbergense*) were selected based on their presence in the lower-alpine and upper-montane thermal belts in the DAC (Körner *et al.*, 2011, Carbutt, 2012) and their distinct growth rings (Hilliard, 1977). *Helichrysum trilineatum* and *H. witbergense* are located in the lower-alpine thermal belt (Körner *et al.*, 2011, Carbutt, 2012) and have adapted to extreme cold temperatures associated with that elevation. *Helichrysum witbergense*, in particular, is mostly restricted to high elevations (2 600 – 3 400 m a.s.l.) in moist, shaded areas on south- and west-facing slopes (Pooley, 2003). *Helichrysum trilineatum* has a wide elevational range of 1 200 – 3 400 m a.s.l., but is mostly found at higher elevations (Pooley, 2003). Studying these three shrub species, which are located at the juncture of the two thermal belts along a significant elevation gradient of c. 800 m, aids in the understanding of how growth patterns (including shrub age, growth rate and annual ring widths) are potentially influenced by aspect and elevation zonation, and how growth rates respond to inter-annual climate variability and whether species are confined to certain microhabitats in these mountains. Knowledge of the age, growth rate and mean annual growth of *Helichrysum tenuifolium*, *H. trilineatum*



and *H. witbergense*, and predicted future climate variability, aids in the development of adaptation strategies. It will further assist with the conservation and management of *Helichrysum tenuifolium*, *H. trilineatum* and *H. witbergense* and the associated alpine and montane ecosystems in the DAC.

### 1.1 Aim and Objectives

To investigate the growth patterns and the response to climate of *Helichrysum tenuifolium*, *H. trilineatum* and *H. witbergense* along an elevation gradient in the Drakensberg Alpine Centre (DAC). This study aims to show whether these species respond to inter-annual climate variability and how microhabitats may influence their growth patterns. The study investigates whether the patterns of ring widths differ between the two *Helichrysum* species located in the alpine thermal belt (*H. witbergense* and *H. trilineatum*) and the two species located in the upper-montane thermal belt (*H. tenuifolium* and *H. trilineatum*).

The specific objectives of this study are:

1. To determine whether climate influences the growth patterns of shrub species growing in the high Drakensberg.
  - a. Do *H. tenuifolium*, *H. trilineatum* and *H. witbergense* form annual growth rings?
  - b. What are the temporal ring widths in *H. tenuifolium*, *H. trilineatum* and *H. witbergense*?
  - c. Do ring widths correspond to inter-annual climate (e.g. temperature and precipitation) and its variability in the DAC?
2. To determine how aspect and elevation zonation impact the growth rates of *H. tenuifolium*, *H. trilineatum* and *H. witbergense*.
  - a. Are shrub species richness and abundance affected by elevation and aspect?
  - b. Do ring widths of species differ between and within species on the same and on different aspects and elevations?
  - c. Do growth rates differ between shrubs of the same species and shrubs of different species at the same elevation?
3. To determine if *H. tenuifolium*, *H. trilineatum* and *H. witbergense* occur in unique microhabitats.
  - a. Is there a specific elevation band between 2 400 and 3 300 m a.s.l. to which *Helichrysum tenuifolium*, *H. trilineatum* and *H. witbergense* are confined?

- b. Do microhabitats correlate with the occurrence of specific species?
- c. How do the growth rates for species located in different microhabitats compare across different slopes and elevations?

## 1.2 Structure of the research report

The introductory chapter is followed by Chapter 2 which discusses the relevant literature concerning the topics of mountain vegetation and the impact of climatic changes. This chapter discusses the use of dendrochronological and AMS radiocarbon dating methods with reference to shrub growth patterns. Chapter 3 presents the setting of the study within Lesotho, with reference to the climate, soils, geology, and vegetation of the study region. The chapter also includes an overview of the field and laboratory work that was performed and statistical methods used. Chapter 4 report the results of the studies regarding shrub growth patterns and characteristics, relationships to elevation gradient and aspect. The results are then linked together into a broad discussion to address the project aims and hypotheses (Chapter 5).

# CHAPTER TWO

## Literature Review

### 2.1 Introduction

Mountain environments are characterised by diverse habitat types and provide vital resources and services to plants, animals, and people (Gentili *et al.*, 2015). Mountain ecosystems are particularly fragile, subject to both natural (e.g. global climate change, glacial retreat, upward shift of tree lines, and sub-alpine and alien species invasion) and anthropogenic (e.g. loss of vegetation cover because of land use changes) drivers of change (Gentili *et al.*, 2015). Consequently, mountain environments will show more immediate and noticeable effects from climate change (Morris, 2017a).

Previous research found that the effect of climate change will be unavoidable in mountain ecosystems (Dullinger *et al.* 2012). In addition, the harvesting of specific unpalatable shrubs for fuelwood can intensify the effect of climate change in areas such as the DAC (Letšela *et al.*, 2003; Wikle, 2015). Examples of this may be an increased rate and amount of biodiversity loss, decline in canopy cover, increased density of smaller shrubs as a result of larger stem shrubs being harvested first, land degradation, and increased erosion rates (Twine and Holdo, 2016).

### 2.2 Climate change

Mean annual temperatures (MAT) have increased nearly 1.5 times the observed global average increase of 0.65°C since the 1960s, and are predicted to increase 2–3°C by the end of the 21st century (Ziervogel *et al.*, 2014; Archer *et al.*, 2018; Wilkening *et al.*, 2019). Plant and animal populations, and ecosystems do not respond to the approximated global average temperatures, but rather to regional climate changes (Walther *et al.*, 2002). As a result of the asymmetry in the warming of the earth, the impacts of climate change are not expected to be spatially uniform. Mountain regions at high elevation are expected to experience the effects of a warming climate faster than other regions located at the same latitude (Gilbert and Vincent, 2013).

While the global MAT has increased, diurnal temperature ranges have decreased (Gilbert and Vincent, 2013). This can be attributed to minimum temperatures increasing at a greater rate than maximum temperatures (Gilbert and Vincent, 2013). Consequently, the periods of no snow and ice in mid- and high-latitude regions are longer, and satellite and ground-based measurements reveal a decrease in snow cover, permafrost, and ice extent since the late 1960s (Luo *et al.*, 2017; Connolly *et al.*, 2019; Luomaranta *et al.*, 2019). The intensification of precipitation accompanies increasing global temperatures. Precipitation is neither spatially nor temporally uniform, and may differ not only by region, but by aspect and elevation (Donat *et al.*, 2016). Regardless of uncertainties in total

precipitation changes between regions, the average of extreme daily precipitation has increased for both wet and dry regions since the 1960s (Barros *et al.*, 2015; Donat *et al.*, 2016). Strong trends in temperature extremes and heat waves, frequent heavy rainfalls and consequent flooding, and snow, ice, and permafrost melt during the most recent decades, are some of the direct consequences of climate change. Climate change, however, also indirectly impacts water resources, food security, health, infrastructure, and ecosystem services and biodiversity (Ziervogel *et al.*, 2014).

### 2.2.1 Climate change impacts on southern Africa

All countries in southern Africa are developing nations, which primarily depend on agricultural production and the availability of natural resources (Sithole and Murewi, 2009). These countries are vulnerable to the consequences associated with climate variability and change. Examples of this are less freshwater availability, a decline in natural resources, changing growth seasons and low crop yields as a result of increases in MAT, accompanied by multi-year below-normal summer and winter rainfall (Archer *et al.*, 2018).

According to Engelbrecht *et al.* (2015), annual average surface temperature trends for the interior parts of southern Africa indicated increases of up to 3.2°C per century for the period 1961-1990. Projections indicate that the annual average surface temperature may increase between 4 to 6°C for the period 2071-2100 (Hoffman *et al.*, 2019). Southern Africa's inter-annual rainfall variability is influenced by the El Niño Southern Oscillation (ENSO) (Sithole and Murewi, 2009). Over the past three decades, El Niño events, which are associated with delayed and low rainfall, have become more frequent and climate models project rainfall decreases of up to 20% in some southern African regions (Sithole and Murewi, 2009; Li *et al.*, 2013). Lower rainfall is expected in places where climate change models previously projected an increase in rainfall (Bryan *et al.*, 2009). However, recent studies found that local circulation effects, such as ENSO, are likely to lead to lower rainfall (Bryan *et al.*, 2009; Li *et al.*, 2013). Climate change will not only influence temperature and rainfall patterns, it may also intensify and increase the frequency of extreme weather events (Bryan *et al.*, 2009). For southern Africa, this may include frequent dry spells, intense thunderstorms, tropical cyclones, and heat waves (Serdeczny *et al.*, 2016; Archer *et al.*, 2018). Projections for southern Africa indicate that in addition to increased climate variability, anthropogenic influences may exacerbate these extreme conditions (Kolusu *et al.*, 2019). The most common anthropological influences in developing countries, such as Lesotho, are a combination of "excessive harvesting of common natural resources, through deforestation, overgrazing, and over-cultivation of soils" (Ngwenya *et al.*, 2018, pp. 2). The pressure on the natural system may increase as population growth will lead to an increased need of food, water, fuel, and other necessities.

In response to increasing climate variability and anthropogenic influences, ecosystems and biodiversity may adapt or undergo changes that may include species loss and extinction, species losing part of their climatically determined geographic range, spread of invasive species, degradation and biodiversity loss (Elsen and Tingley, 2015; Bentley, 2016; Foden *et al.*, 2018). The anticipated climate changes coupled with the projected population increase pose threats to natural resources, ecosystems and biodiversity in the area, and food and water security, and public health (Bryan *et al.*, 2009; Sithole and Murewi, 2009). The vulnerability of both natural and human systems to climate-related risks needs to be understood and managed, as it not only depends on the magnitude and rate of warming, but on geographic location, and the ability to adapt and mitigate certain situations. Monitoring the vulnerability of biodiversity and the impacts of climate change on vegetation is a fundamental part of adaptation and mitigation strategies to prevent future biodiversity loss (Foden *et al.*, 2018; Mukwada and Manatsa, 2018).

### 2.3 Mountains

Mountains occupy about one fifth of the earth's terrestrial surface, ~20% of the world's human population resides in mountain environments, and almost 50% of humankind depends on mountain resources (mostly fresh water) (Körner *et al.*, 2005). Mountains comprise a diverse topography and environmental conditions that influence regional climate (Ngwenya *et al.*, 2018). Various mountain ecosystems often host many endemic species, as species that occur at high elevations are mostly isolated compared to species located at lower elevations (Bentley *et al.*, 2019). Mountain ecosystems are thus of prime conservation value. Mountains are a haven to a variety of ecosystems, biodiversity, and endemic species; and form an essential part of the global ecosystem (Stewart and Mitchell, 2018; Bentley *et al.*, 2019). These ecosystems are often regarded as having a high ethnocultural diversity, being spiritually significant. The scenic landscapes and various recreational activities make mountains ideal tourism attractions (Körner *et al.*, 2005).

Mountains are fragile and both natural and anthropogenic drivers of change shape the mountain ecosystem (Gentili *et al.*, 2015). These drivers may include: landslides, flooding, climate change, vegetation loss, seismic events, volcanic eruptions, mining, agricultural and forestry practices (Gentili *et al.*, 2015). The recovery of mountain ecosystems after disturbances is slow or does not take place as the soils are mostly thin, with minimal vegetation cover to keep soil in place on sloping terrain (Körner *et al.*, 2005). Even though mountain ecosystems are fragile, they provide important resources such as refugia for biodiversity (Beniston, 2003). Mountains supply water to nearly 50% of the human population, drive hydroelectricity provision, assist with flood control, and mountain agriculture provides food for almost half a billion people worldwide (Beniston, 2003; Körner *et al.*, 2005; Marsh, 2017;

Ngwenya *et al.*, 2018). Healthy vegetation, slope stability and erosion are crucial in these systems to provide the resources and services continuously (Körner *et al.*, 2005).

Scientists have subdivided mountains vertically by temperature, identifying seven thermal life zones (thermal belts), accounting for the latitudinal change in elevation of thermally similar areas (Körner *et al.*, 2011). These thermal belts were identified as nival, upper-alpine, lower-alpine, upper-montane (previously known as sub-alpine), and lower-montane- with the tree line ecotone positioned between the lower alpine and upper montane thermal belts (Körner *et al.*, 2011). According to Körner *et al.* (2005), the tree line is regarded as the critical bioclimatic reference line that enables global comparison between these regions.

### 2.3.1 Mountain vegetation

The survival of ecosystems, and individual endemic species in the alpine and montane thermal belts, is closely linked to different climatic variables (e.g. temperature, solar radiation, precipitation in the form of rainfall, wind and snow), edaphic properties (e.g. soil type and nutrient availability), invasive species and land-use practices (Cingo, 2015; Knight *et al.*, 2018). These regions are characterised by grassland or low stature shrubland, often with several endemic species, and are resistant to biological invasions (Pauchard *et al.*, 2015). There are several factors (natural and/or anthropogenic) that influence plant growth in these harsh conditions, which include high elevations, low soil depth, variable precipitation, low temperatures, land use, population density and atmospheric CO<sub>2</sub> (eCO<sub>2</sub>) levels (Marsh, 2017).

Climatological, geological, and topographical heterogeneity, such as in the case of South Africa's and Lesotho's mountains, directly influence plant diversity, and the distribution of species (Bentley, 2016). This may result in higher levels of endemism in certain areas of the mountain range than in other parts. Plants growing at high elevations are mostly controlled by direct and indirect influences of low temperatures, radiation, wind, water availability, and soil properties (Bentley, 2016; Knight *et al.*, 2018). An example of this is the vegetation of Europe's major mountain ranges, which have extended their distribution range upslope between the years 2001 and 2008, as a result of a warming climate (Pauli *et al.*, 2012).

### 2.3.2 Mountains and climate change

Climate change will have an impact on the world's mountain regions and may influence the ability of mountains to provide important services (Beniston, 2003). Some of the direct results of climate change may include extreme weather events, such as heat waves, drought, and heavy precipitation, which may lead to flooding and landslides in mountains and extensive flooding in areas downslope (Kohler

*et al.*, 2010; Brönnimann *et al.*, 2014). Examples include: soil erosion, landslides, biodiversity loss and a decrease in natural habitats in mountain regions from the Andes to the Himalayas, and from Southeast Asia to Central and East Africa (Beniston, 2003).

Mountain ranges also act as climate barriers, with prevailing humid conditions on the windward side and dry conditions on the leeward side of mountains due to orographic effects of air uplift and downward flow (Mina *et al.*, 2017; Bentley *et al.*, 2019). Many mountain regions intersect important environmental boundaries, such as tree lines and snow lines, because of their elevational extent (Brönnimann *et al.*, 2014). Direct and indirect climatic changes in these boundaries may affect feedback processes and influence local climate (Thomas, 2010). Retreating snow lines and thawing permafrost, for example, increase the risk of natural hazards such as floods and landslides, accelerated warming trends due to lower reflectance and changes to the carbon and nitrogen cycles (Clifton *et al.*, 2018; Dong *et al.*, 2019; Patton *et al.*, 2019). Changes in these boundaries can alter ecosystems, in particular species' habitats, which may lead to further vegetation changes across the mountain ecosystem (Thomas, 2010).

The impacts of climate change may be more noticeable in alpine and nival vegetation than at lower elevations (Bentley *et al.*, 2019). According to Knight *et al.* (2018), the sensitivity of specifically Afromontane ecosystems, and individual endemic species, to environmental disturbances can be related to changes in climate, soil properties, invasion of alien species and land use/management practices. High mountain plants are generally long-lived and slow-growing, and so changes in vegetation patterns in response to climate change will most likely manifest over the longer-term (over decades), and not short-term climatic oscillations (Pauli *et al.*, 2003). This will result in the decrease of species ranges and possible species extinction (Rogora *et al.*, 2018). Climate change will also affect the growth limits of vegetation above or at the tree line (Diaz *et al.*, 2003). To understand the effects that climate change may have on high mountain vegetation, long-term ecological data are needed (Rogora *et al.*, 2018) (Groffman *et al.*, 2012; Alberto *et al.*, 2013; Lézine *et al.* 2019).

#### 2.4 The Drakensberg Alpine Centre

The DAC covers an area of c. 40 000 km<sup>2</sup> in the greater Drakensberg mountains, which is a mostly continuous mountain range stretching for almost 900 km along the eastern Great Escarpment of southern Africa (Carbutt and Edwards, 2015a, b). The DAC is politico-geographically divided into four areas: the KwaZulu-Natal Drakensberg, the Eastern Cape Drakensberg and Witteberge, the Maloti Mountains of Lesotho, and the highlands of the eastern Free State (Carbutt and Edwards, 2006). Floristically, the DAC is subdivided into the alpine region of the KwaZulu-Natal Drakensberg summit and Maloti Mountains of Lesotho; its outliers (for example the Mahwaqa and Ngeli Mountains); the

northern KwaZulu-Natal Drakensberg scarp; the southern KwaZulu-Natal Drakensberg scarp; the Eastern Cape Drakensberg and Witteberge; and the Sehlabathebe/East Griqualand/Naude's Nek region (Carbutt and Edwards, 2006) and the eastern Free State (Brand *et al.*, 2010) (Figure 2-1). From a palaeoclimatic perspective, the DAC's high elevation and topographic diversity likely reinforced the mountain ranges' susceptibility to late Quaternary climatic shifts, and due to its location above southern Africa's perennially productive sub-tropical coastal forelands, it experiences colder, drier, and more seasonal climatic conditions (Stewart and Mitchell, 2018). This provides an excellent opportunity for exploring potential ecological responses to changing climatic conditions.

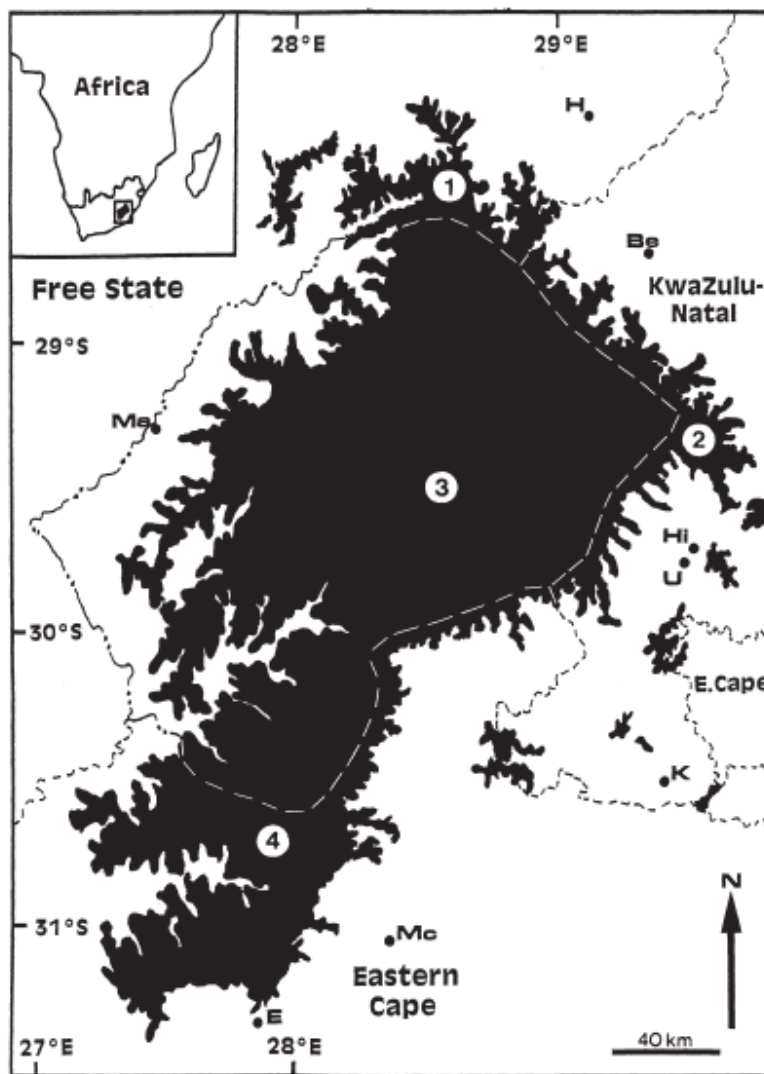


Figure 2-1: Drakensberg Alpine Centre (DAC) comprising (1) eastern Free State, (2) KwaZulu-Natal Drakensberg, (3) Lesotho Maloti Mountains and (4) Eastern Cape Drakensberg and Witteberge. Where Be = Bergville; E = Elliot; H = Harrismith; Hi = Himeville; K = Kokstad; Ma = Maseru; Mc = Maclear; U = Underberg (adapted from Carbutt and Edwards, 2004).



#### 2.4.1 Effects of climate change on the DAC and its associated vegetation

The long-term climate change studies that have been conducted in the Lesotho highlands made use of satellite imagery, international datasets, weather stations and observations by researchers to determine past and predict future climate patterns (Sithole and Murewi, 2009; Morris, 2017a; Archer *et al.*, 2018; Mukwada and Manatsa, 2018). These studies suggest warmer summers with frequent droughts (mostly December to January) and delayed but more intense rainfall seasons, and less snow in winter (Grab *et al.*, 2017; Morris, 2017a; Mukwada and Manatsa, 2018; Bentley *et al.*, 2019). Lesotho will experience increased atmospheric CO<sub>2</sub> (eCO<sub>2</sub>) levels together with increased air temperatures (Lewis and Oosthuizen, 2014; Morris, 2017a). The mean annual temperature (MAT) in Lesotho will increase by up to 0.7°C by 2030 and is expected to rise a further 1.0 – 2.0°C by 2050 and between 2.5 – 3.5°C by 2075 (UNEP, 2016). Global circulation models predict that the western Maloti will experience an increase in MAT of 2.0 – 3.0°C by 2046-2065 and 5.0 – 6.0°C by 2081–2100 (Morris, 2017a). The greatest increase in temperature is projected for the month of September (Lewis and Oosthuizen, 2014). These changes will have a great impact on temperature-limited plants, the number of frost days and the frequency of severe snowfalls (which are expected to decrease). If rising air temperatures are accompanied by precipitation, it can potentially lengthen the growing season (Lewis and Oosthuizen, 2014; Morris, 2017a). However, studies found that drying will mostly occur in southern Africa, even in areas where increasing rainfall is plausible (Engelbrecht *et al.*, 2015). Drastic increasing temperatures lead to lower soil moisture content through increased evaporation, thus leading to shorter growing seasons (Engelbrecht *et al.*, 2015). This will directly impact the growth of natural vegetation, and crops, either through soil water stress or waterlogging (Lewis and Oosthuizen, 2014). Although rainfall patterns of Lesotho have not changed during the last century, a few changes are expected, such as more frequent high intensity events, a shift in the rainfall season from mid- to late-summer (February), and an increase in mean annual precipitation by up to 300 mm by the end of the century (Morris, 2017a).

According to Morris (2017a), the regions at high elevations in Lesotho, where the partial pressure of CO<sub>2</sub> is lower, will experience a greater effect of higher unabated eCO<sub>2</sub>, than other regions at lower elevations. Plants respond differently at higher eCO<sub>2</sub> levels, as some functional groups would be more responsive and therefore better potential indicators of a changing climate (Stock *et al.*, 2004). An example of this is the difference between C<sub>3</sub> and C<sub>4</sub> photosynthetic pathway vegetation. C<sub>3</sub> vegetation is mostly associated with cooler seasons and is less efficient in a low CO<sub>2</sub> environment, which contrasts with C<sub>4</sub> vegetation that is associated with warmer seasons and concentrate carbon in their leaves (Stock *et al.*, 2004; Bentley and Connor, 2018). For this reason, it is predicted that C<sub>3</sub> plants should benefit most from the carbon fertilization effect (CFE), resulting from eCO<sub>2</sub> (McGrath

and Lobell, 2013). In the tropical and subtropical lowlands, C<sub>4</sub> grasses dominate and are restricted to lower elevations in mountains, however, in Lesotho, elevation and topographical limits of C<sub>4</sub> grasses are likely to shift with higher eCO<sub>2</sub>. C<sub>4</sub> grasses will benefit from higher temperatures, in contrast to C<sub>3</sub> grasses, as they are most competitive in regions with a warm growing season (Stock *et al.*, 2004; Bentley and Connor, 2018). Archaeological evidence indicates that the distributions of C<sub>4</sub> and C<sub>3</sub> grasslands have undergone significant elevation shifts, and that these changes correlate to temperature fluctuations during the Holocene, with C<sub>4</sub> grasses moving upslope during warm periods in Lesotho (Bentley and Connor, 2018). Some plant species benefit from the combined influence of eCO<sub>2</sub> and warming, such as the unpalatable C<sub>3</sub> dwarf Karroid shrubs (e.g. *Chrysocoma ciliata* and *Pentzia cooperi*, locally called Sehalahala) that inhabit the Lesotho grasslands when vegetation cover has been reduced through grazing and trampling (Morris *et al.*, 1993; Fitchett *et al.*, 2017; Bentley and Connor, 2018).

The DAC is an excellent test site for determining recent climate change, because cold-adapted shrubs found in the area are likely to be sensitive to global warming (Gentili *et al.*, 2015). Recent observations indicate that many mountain ecosystems (such as the DAC) experience an increase in shrub growth and abundance (Myers-Smith *et al.*, 2015) that is probably driven by climate change (Boscutti *et al.* 2018). Shrub canopy expansion is important as it provides food resources and habitat to species, and alters the litter inputs and nutrient availability, while changing microclimates and influencing soil and permafrost temperatures (Myers-Smith *et al.*, 2015). Shrub growth, abundance and increasing canopy cover are therefore affecting the biodiversity, soil nutrient cycling, carbon storage, water, and energy exchange of the ecosystem (Myers-Smith *et al.*, 2015).

The existence of natural microclimate gradients on mountains at high elevations provide the opportunity to obtain a better understanding of species' responses to small climatic changes, and they enable the evaluation of potential plant responses to future climate changes (Gaire *et al.*, 2013; Bentley *et al.*, 2019). Researchers have focused on the classification of alpine vegetation and vegetation gradients in the DAC (Killick, 1978; Morris *et al.*, 1993; Carbutt and Edwards, 2004; Cingo, 2015, Morris, 2017a) (Figure 2-2). Elevation gradients, along with vegetation gradients, can be a tool for investigating relationships between climate and vegetation (Bentley *et al.*, 2019). Elevation is used as a proxy for temperature in various studies (Grab, 2013; Bentley *et al.*, 2019). For instance, numerical analysis based on field station data has shown that, on average, temperature drops by 0.63°C per 100 m<sup>-1</sup> from mid- to highest- portions along an investigated portion of the KZN Drakensberg (Grab, 2013). In mountain ecosystems, species richness is commonly found to decrease at the tree line where “both stress and competition are intermediate and habitat diversity is high” (Boscutti *et al.*, 2018, p.2). There are sediments and geomorphic features located in the high

Drakensberg from which possible palaeoclimatic records can be obtained (Grab and Mills, 2011; Fitchett *et al.*, 2016; Mills *et al.*, 2017; Lodder *et al.*, 2018; Norström *et al.*, 2018).

The effects of climate change in the DAC is intensified by heavy grazing of the mountain grasslands by cattle (Bentley *et al.*, 2019). Unpalatable shrubs that exist around cattle posts and in overgrazed areas are harvested to supply fuelwood to residents (Morris, 2017b), leading to loss of cover and accelerated soil erosion (Wikle, 2015). This affects hydrological regulatory processes and potentially influences supply of water in Lesotho (Morris, 2017b). Fuelwood harvesting poses a problem in numerous regions in Lesotho (Nüsser and Grab, 2002; Letšela *et al.*, 2003; Wikle, 2015). The rates at which alpine shrubs (including *Helichrysum trilineatum*) are harvested for fuelwood poses a threat to alpine shrub existence, as these shrubs may not grow at the same rate as they are harvested in some areas. Moshoeshoe and Sekantsi (2013) described the problems Lesotho faces in terms of overgrazing, fuelwood harvesting, deforestation and erosion, and what measures need to be taken to combat these issues.

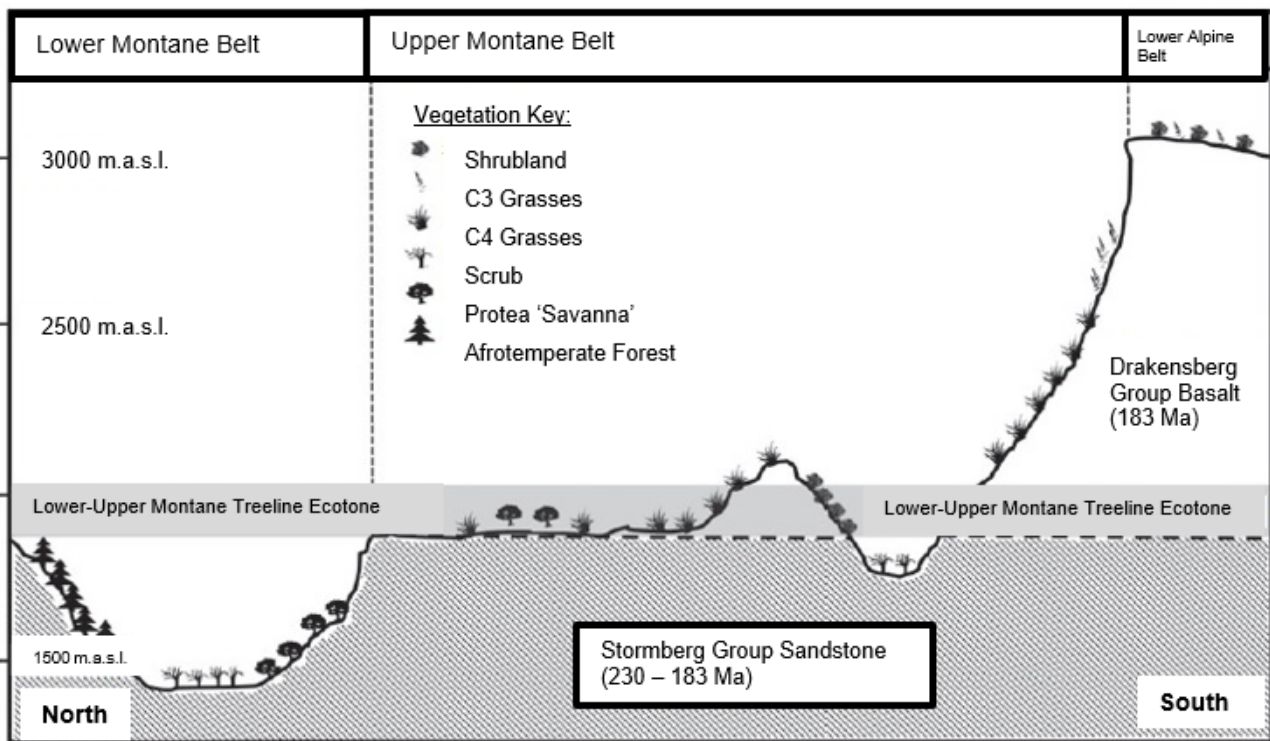


Figure 2-2: Schematic profile through the Drakensberg showing major thermal belts and associated vegetation classes, and location of the lower–upper montane treeline ecotone (adapted from Carbutt and Edwards, 2015).

### 2.5 Shrub growth ring analysis as a research tool to trace climatic influence

Shrubs exhibit a variety of growth forms as a result of their genetic differences or phenotypic plasticity, which relates to the environment in which they grow (e.g. extreme cold, shade, snow cover, soil

movement) (Myers-Smith *et al.*, 2015). This must be considered when measuring and interpreting radial and axial growth of shrubs (Myers-Smith *et al.*, 2015). Shrub growth can be measured in three ways: through radial growth (growth rings), axial growth and stem increments (Myers-Smith *et al.*, 2015). Both the timing and the extent of landscape-level vegetation change, or geomorphic disturbances can be determined by investigating the growth patterns, climate-growth relationships, and examining the wood anatomy of trees and shrubs (Stoffel and Bollschweiler, 2008).

To accurately date the annual growth rings of woody shrubs, such as *Helichrysum tenuifolium*, *H. trilineatum* and *H. witbergense*, the structure and growth of these shrubs must be understood. The stems of woody shrubs consist of the bark tissue on the outside, followed by the cambium and wood tissue on the inside (Schweingruber and Poschlod, 2005). In the cambium, the tissue cells divide to form new phloem and xylem tissue that is responsible for secondary growth of stems and roots (Rathgeber *et al.*, 2016). Phloem conducts sugars and other metabolic products from the leaves, while xylem is supporting tissue that develops inward from the cambium to produce the annual growth increment that transports water (Rathgeber *et al.*, 2016). Every year a shrub's renewed growth starts in the cambium, where large thin-walled cells of early wood forms, which is the inner annual-ring component. The porosity of the wood determines the colour, density, cell-size, and cell-wall thickness of the early wood. The production of late wood cells is influenced by external environmental factors and internal physiological conditions (Schweingruber and Poschlod, 2005). Every year entire annual increments are formed, which include early wood and late wood cells. In a stem, the annual increments are stacked upon increments of preceding years (Schweingruber and Poschlod, 2005). Cross sectioning the stem will intersect the annual increments that will appear as rings (in a seasonal climate). The annual increments, or rings, are mostly continuous and therefore they can be used to date shrub growth (Shroder, 1980). Annual ring width varies significantly between types of shrubs and their location, which allows for comparison and cross-checking, and makes it possible to determine the exact year in which each ring was formed (McCarroll and Loader, 2004). The growth rings are potentially a reliable proxy for past environmental conditions at a particular study site, as the growth rates (Therrell *et al.*, 2007) and the annual ring widths of a shrub are largely influenced by local climate conditions, mainly temperature and precipitation (Suess, 1980).

To understand changes of mountain ecosystems, it is necessary to understand what drives alpine and upper-montane shrub growth, and their population dynamics (Myers-Smith *et al.*, 2015). It is also possible to obtain a multi-decadal record of environmental changes in ecosystems by analysing shrubs (Myers-Smith *et al.*, 2015). Shrub age of living shrubs has been shown to reflect environmental conditions and shrub abundance has been found to be sensitive indicators of environmental change and ecosystem functioning (Boscutti *et al.*, 2018). Studying shrub age distributions and abundance

can improve understanding of ongoing changes in mountain ecosystems and provide insight into the population dynamics of the area. For this reason, researchers are making increased use of tree and shrub dendrochronology and radiocarbon dating to study late Holocene climate variations as it includes data on centennial to decadal time scales at annual or near annual resolution (Esper *et al.*, 2003; Helama *et al.*, 2009; Myers-Smith *et al.*, 2015).

### 2.5.1 Dendrochronology

Dendrochronology is an accurate and precise method for dating tree rings to the year of formation (from either living or non-living trees or shrubs), and to detect environmental signals (Pignatelli, 2010; Gebrekirstos *et al.*, 2014). Dendrochronology was developed by A.E. Douglass at the beginning of the 20<sup>th</sup> century and has since been used worldwide in various professions (Pignatelli, 2010; Torbenson, 2015). Dendrochronology has been used to date archaeological artifacts and ancient architecture, provide calibration during the development of radiocarbon dating, study past ecological and climatic shifts, study geomorphological events and perform climate reconstructions (Pignatelli, 2010; Gao *et al.*, 2013; Torbenson, 2015).

To construct ring-width chronologies, anatomically distinct annual growth rings are a requirement (Gebrekirstos *et al.* 2014). Radial growth is impacted by various factors, such as climate, soil, topography, and competition for resources (Torbenson, 2015). In temperate and boreal latitudes, growth seasons are distinct and climatic conditions force plants into dormancy, forming annual tree rings. In other regions, such as the subtropics, tropics and Mediterranean, seasonal changes in temperature are low and the occurrence of frost is restricted to higher elevations (Gebrekirstos *et al.*, 2014). This, along with precipitation changes, limits growth (Gebrekirstos *et al.*, 2014). Therefore, deciduous tree or shrub species are expected to form growth rings in comparison to evergreen species (Gebrekirstos *et al.*, 2014). Species growing in the same region under similar environmental conditions will most likely display comparable year-to-year variability in growth (Torbenson, 2015). Cross-dated chronologies can therefore be compiled by comparing and matching ring-width patterns between tree species (Torbenson, 2015). These chronologies can then be used to assess growth patterns and growth anomalies and to compare the growth patterns with various datasets, such as climate.

Dendrochronological research is based on nine basic principles and concepts. Cross-dating is regarded as the most important principle as it forms the basis for the analyses of temporal and spatial patterns of the growth-related processes (Fay and de Berker, 2018). This principle focuses on chronology building through comparison, matching, and overlapping of annual growth ring sequences from different trees or shrubs at the same site (Fay and de Berker, 2018). Other important principles

include uniformitarianism, sampling replication, limiting factor principle, ecological amplitude, site selection, and linear aggregate growth modeling. The uniformitarian principle implies that physical and/or biological processes affect tree growth in a similar way today as it would have in the past (Fritts, 1976). This can be used to determine if a relationship between climate variation and tree ring growth exists, and if it does, how it differs from the climate-growth relationships in the past. By using multiple species across various geographical ranges, accuracy of data is improved for better cross-dating and development of an accurate chronology (Fay and de Berker, 2018). The concept of ecological amplitude refers to the factors inherited by species that defines a certain habitat in which a species may grow and reproduce (Fritts, 1976). This links with the principle of limiting factors and the site selection process, based on Liebig's law of the minimum, in which growth is limited by the least available environmental factor (Heinrich and Allen, 2013). Various mathematical and statistical models can be used to predict objective and precise information on how certain shrub or tree species may respond to certain climatic and environmental factors. Cook and Kairiukstis (1990) developed the linear aggregate model acknowledging the importance of taking the various biological and climatic conditions affecting shrub growth into consideration when predicting future outcomes. The schematic diagram shown in Figure 2-3 illustrates the dendrochronological dating process from sampling to dating.

#### 2.5.1.1 Dendrochronological method

Shrubs and dwarf shrubs may produce extremely narrow, discontinuous, or even missing growth rings (Wimmer, 2002; Au and Tardif, 2007; Li *et al.*, 2013; Schweingruber and Börner; 2018). Methodologically, the dating of shrubs and trees is different, since the morphology and growth eccentricity of trees and shrubs is different (Myers-Smith *et al.*, 2015). Myers-Smith *et al.* (2015) discuss the methodological processes with regards to measuring alpine and arctic shrub growth in detail. These authors discussed existing and developing methodologies in terms of the sampling of alpine and arctic shrubs, radial and axial growth measurements, dating of the shrubs and analysing the growth dynamics of the shrubs in relation to environmental variables. The five-step methodological process comprise of sampling strategy, sample preparation, measurement, time-series development, and data analysis (Figure 2-4).

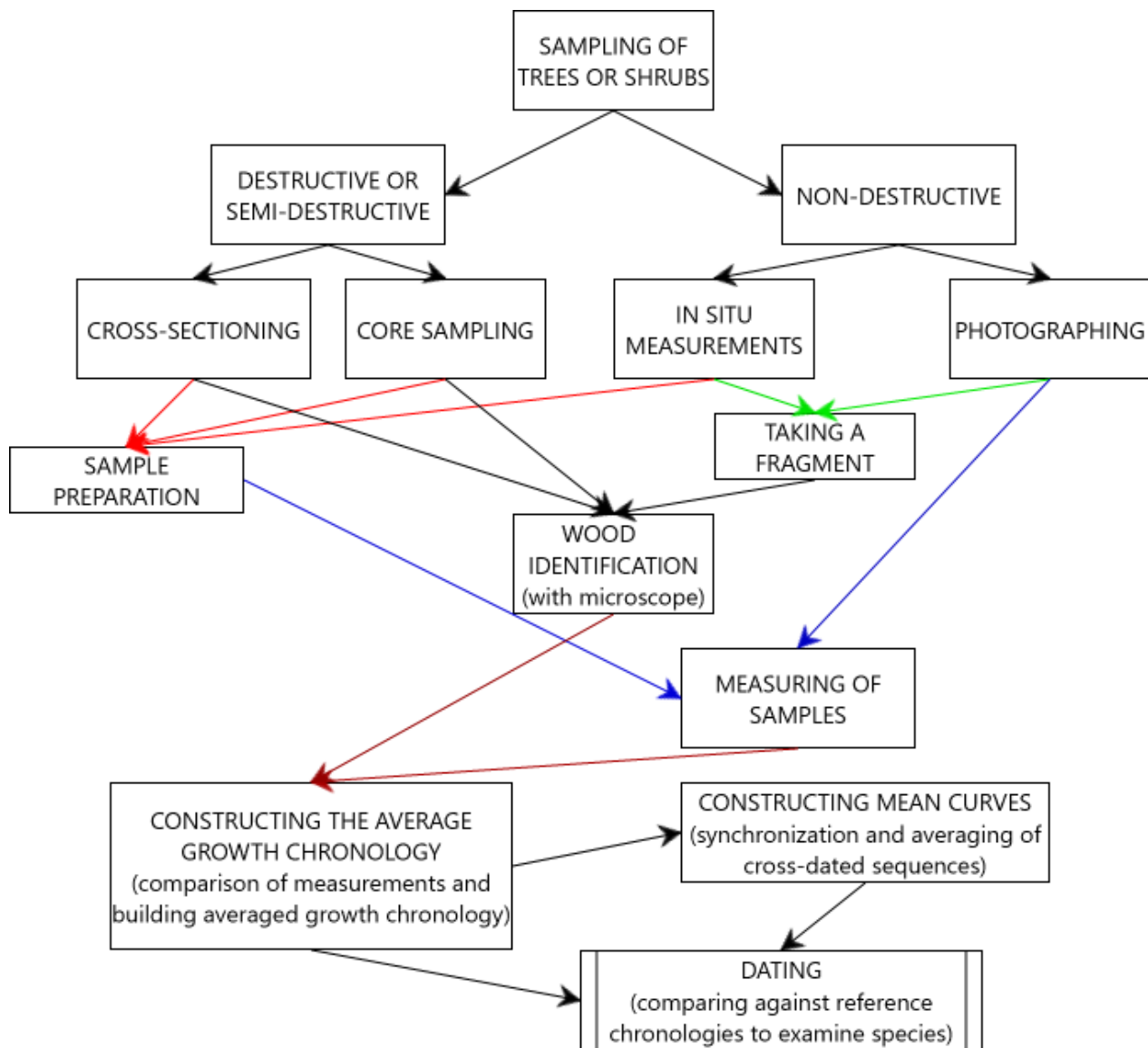


Figure 2-3: Schematic representation of the dendrochronological assessment process (adapted from Pignatelli, 2010).

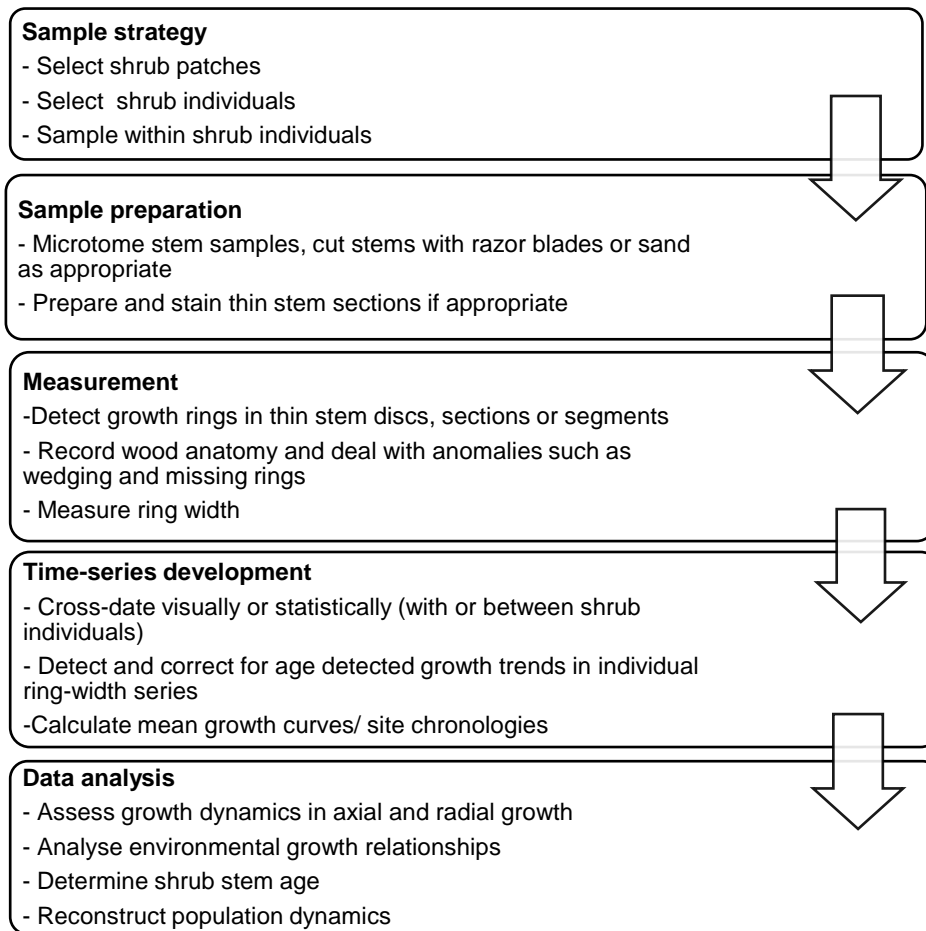


Figure 2-4: Schematic overview of the dendrochronological process for alpine and arctic shrubs (adapted from Myers-Smith *et al.*, 2015).

### 2.5.1.2 Dendrochronological studies

Many tree-ring studies (from trees and shrubs) have been conducted, predominantly in the northern hemisphere (NH) (Bär *et al.*, 2006; Chen *et al.*, 2011; Gao *et al.*, 2013; Lu *et al.*, 2016; Opala-Owczarek *et al.*, 2019). Knowledge of climate variability in southern Africa for periods prior to written and instrumental recording depends mostly on natural paleoclimate proxies, for instance tree rings, lake sediments and pollen (Nash and Adamson, 2014). Regions, such as Europe and North America, have high-resolution and well-dated proxy records covering recent centuries, whereas in most parts of the southern hemisphere (SH), those data sources are relatively scarce or non-existent (Gebrekirstos *et al.*, 2014; Nash and Adamson, 2014). In the SH, historical temperature and rainfall reconstructions have been compiled using tree-ring proxies (e.g. Lopez *et al.*, 2017; Granato-Souza *et al.*, 2019, for the Amazon; Allen *et al.*, 2019; Buckley *et al.*, 2019, for Australia; Lavergne *et al.*, 2017, for eastern slopes of the northern Patagonian Andes; and Lorrey *et al.*, 2016, for New Zealand).



Various shrub and/or tree-ring chronologies were developed for high alpine regions in the NH (Shi *et al.*, 2015; Owczarek and Opała, 2016; Rayback *et al.*, 2017; Carrer *et al.*, 2019). Given that shrubs and trees growing at the tree line are most sensitive to changing environmental conditions, researchers can make use of shrub or tree growth patterns to study environmental and/or climatic changes (Carbutt and Edwards; 2015a; Boscutti *et al.*, 2018). Dendrochronological research at or above the tree line is difficult, since trees are mostly absent and only a limited number of shrub and dwarf shrub species form ring structures that can be used for research purposes. However, in recent years there has been much interest in obtaining dendroecological data from shrubs and dwarf shrubs, likely because alpine regions are well recognised as highly sensitive to contemporary and future climate change (Li *et al.*, 2013; Zimowski *et al.*, 2014; Lu *et al.*, 2015; Lu *et al.*, 2016; Bi *et al.*, 2017; Shetti *et al.*, 2018). Radiocarbon dating has mostly been used as part of shrub dendrochronology to accurately date shrubs and to determine exact dates of extreme climate events and ecological shifts.

Table 2-1 provides a summary of the dendrochronological and radiocarbon research that has been undertaken using shrubs.

Most tree ring studies in southern Africa have used basic ring-width measurements as a tool, but recent advancements in technology and dendrochronological methods have enabled researchers to do a wide variety of analyses. These include dendrometry where measurements provide information on cambial dynamics, seasonal growth and climate variability; micro-coring of the cambium and microscopic analysis of the cell formation process; calculation of stable isotope ratio measurements used to date tree or shrub samples without distinct growth rings; and to study climatic changes taking growth features into consideration (February and Stock, 1999; Tyson *et al.*, 2002; Holmgren *et al.*, 2005; Hall *et al.*, 2008; Norström *et al.*, 2008; Woodborne *et al.*, 2008; Hall *et al.*, 2009; Patrut *et al.*, 2015; Patrut *et al.* 2019; Woodborne *et al.*, 2015; Woodborne *et al.*, 2016; Slotta *et al.*, 2017; Schoeman *et al.*, 2019). Other techniques include wood densitometry (X-ray or Gamma-ray densitometry), and the analysis of wood anatomy to determine if growth anomalies and certain growth features correspond to past environmental conditions and climate extremes (Gourlay and Kanowski, 1991; Gourlay, 1995; Holmgren *et al.*, 2005; Naidoo *et al.*, 2006; Jacobsen *et al.*, 2007; Munalula *et al.*, 2016) (Table 2-2). The results of some of these studies have contributed to the International Tree Ring Databank. Indicating that there are tree and shrub species in southern African that can contribute to the understanding of climatic variability of the recent past.

The dendrochronological and dendroclimatological studies carried out in southern Africa has demonstrated the potential of tree / shrub ring series for use as palaeoclimatic proxies and scope for further research (Table 2-2). Such research allows for a more comprehensive understanding of climate variation in the recent past. There are currently no published studies that have established

*H. trilineatum*, *H. tenuifolium* and *H. witbergense* shrub ring width relations with climate or used such ring widths to reconstruct past climate. To fill this knowledge gap, this study will be the first to build a climate-growth relationship for three *Helichrysum* species along an elevation gradient in the DAC, making use of both dendrochronological and AMS radiocarbon dating methods.

Table 2-1: Research themes and questions investigated using shrubs for dendrochronology.

Theme	Topic	Indicators	Methods	Species	References
<b>Climate</b>	Climate sensitivity of shrub growth	Annual growth rings, stem increments	Dendrochronology, remote sensing	<i>Salix</i> spp., <i>Juniperus</i> spp., <i>Rhododendron</i> spp. and others	Weijers <i>et al.</i> , 2010; Liang <i>et al.</i> , 2011; Li <i>et al.</i> , 2013; Zimowski <i>et al.</i> , 2014; Lu <i>et al.</i> , 2015; Shi <i>et al.</i> , 2015; Lu <i>et al.</i> , 2016; Owczarek and Opała, 2016; Bi <i>et al.</i> , 2017; Shetti <i>et al.</i> , 2018; Buchwal <i>et al.</i> , 2019; Carrer <i>et al.</i> , 2019
	Climate and environment reconstruction	Annual growth rings, leaf scars, wintermark pta			
<b>Vegetation dynamics</b>	Growth dynamics along a slope	Annual growth rings	Dendrochronology, radiocarbon dating	<i>Salix</i> spp., <i>Betula</i> spp., <i>Juniperus</i> spp., <i>Cassiope</i> spp., <i>Erica</i> spp., <i>Spartocytisus</i> spp.	Bär <i>et al.</i> , 2006; Kyncl <i>et al.</i> , 2006; Au and Tardif, 2007; Czimczik and Welker, 2010; Zimowski <i>et al.</i> , 2014; Dearborn and Danby, 2017; Young <i>et al.</i> , 2016; Iturrate-Garcia <i>et al.</i> , 2017; Rayback <i>et al.</i> , 2017; Le Moullec <i>et al.</i> , 2019; Morrissette-Boileau <i>et al.</i> , 2018
	Changes in age distribution	Annual growth rings			
	Advance of the shrub line	Annual growth rings			
<b>Disturbances and landscape change</b>	Dating geomorphological processes, permafrost and glacial history	Annual growth rings	Dendrogeomorphology, radiocarbon dating	<i>Betula</i> spp., <i>Shepherdia</i> spp., <i>Linanthus</i> spp., <i>Potentilla</i> spp., <i>Vaccinium</i> spp., <i>Calluna</i> spp., <i>Alnus</i> spp.	Owczarek, 2010; Röpke <i>et al.</i> , 2011; Franklin, 2013; Owczarek <i>et al.</i> , 2013; Gamm, 2015; Grabowski, 2015; Arzhannikov <i>et al.</i> , 2017; Gamm <i>et al.</i> , 2018
	Herbivory	Annual growth rings, wood anatomy – scaring	Dendrochronology		
	Human-induced ecological changes	Annual growth rings	Dendrochronology, radiocarbon dating		

Table 2-2: Summary of dendrochronological and dendroclimatological studies undertaken in southern Africa

Species	Location	Age (yrs)	Indicators	Method	References
<i>Acacia albida</i> (L.)	South Africa, Zambia, Zimbabwe	Undetermined	–	X–ray densitometry	Gourlay, 1995
<i>Acacia burkei</i> (L.)	South Africa, Zambia, Zimbabwe	Undetermined	–	X–ray densitometry	Gourlay, 1995
<i>Acacia caffra</i> (L.)	South Africa, Zambia, Zimbabwe	Undetermined	–	X–ray densitometry	Gourlay, 1995
<i>Acacia erioloba</i> (L.)	South Africa, Zambia, Zimbabwe	Undetermined	–	X–ray densitometry	Gourlay, 1995
	Kalahari, South Africa	18 – 139 (58); 15-210 (70)*	Decayed, wedging rings, scar tissue, termites, porous	-	Steenkamp <i>et al.</i> , 2008
<i>Acacia galpinni</i> (L.)	South Africa, Zambia, Zimbabwe	Undetermined	–	X–ray densitometry	Gourlay, 1995
<i>Acacia gerrardii</i> (L.)	South Africa, Zambia, Zimbabwe	Undetermined	–	X–ray densitometry	Gourlay, 1995
<i>Acacia goetzei</i> (L.)	South Africa, Zambia, Zimbabwe	Undetermined	–	X–ray densitometry	Gourlay, 1995
<i>Acacia heroensis</i> (L.)	South Africa, Zambia, Zimbabwe	Undetermined	–	X–ray densitometry	Gourlay, 1995
<i>Acacia karroo</i> (L.)	South Africa, Zambia, Zimbabwe	9+	–	X–ray densitometry; marginal parenchyma bands and crystalliferous chains	Gourlay and Kanowski, 1991; and Gourlay, 1995
<i>Acacia nigrescens</i> (L.)	South Africa, Zambia, Zimbabwe	Undetermined	–	X–ray densitometry	Gourlay, 1995
	Hluluwe–Umfolozi, South Africa	46 – 83 (63); 68 – 75 (72)*	Indistinct rings	-	February <i>et al.</i> , 2006
<i>Acacia nilotica</i> (L.)	Hluluwe–Umfolozi, South Africa	29 – 36 (32) 45 – 49 (47)*	Indistinct rings	-	February <i>et al.</i> , 2006
<i>Acacia pilispina</i> (L.)	South Africa, Zambia, Zimbabwe	Undetermined	–	X–ray densitometry	Gourlay, 1995
<i>Acacia polyacantha</i> (L.)	South Africa, Zambia, Zimbabwe	Undetermined	–	X–ray densitometry	Gourlay, 1995
<i>Acacia rehmanniana</i> (L.)	South Africa, Zambia, Zimbabwe	Undetermined	–	Dendrochronology, X–ray densitometry	Gourlay, 1995
<i>Acacia robusta</i> (L.)	South Africa, Zambia, Zimbabwe	Undetermined	–	X–ray densitometry	Gourlay, 1995
<i>Acacia welwischii</i> (L.)	South Africa, Zambia, Zimbabwe	Undetermined	–	X–ray densitometry	Gourlay, 1995
<i>Acacia xanthophloea</i> (L.)	South Africa, Zambia, Zimbabwe	Undetermined	–	X–ray densitometry	Gourlay, 1995
<i>Adansonia digitata</i> (L.)	North–eastern Namibia	1 275	Fusing of stems	–	Patrut <i>et al.</i> , 2007
	Kruger National Park and Skukuza, South Africa	11 – 36 (24)	Indistinct growth rings	Isotopic analysis / radiocarbon dating	Robertson <i>et al.</i> , 2006; Woodborne <i>et al.</i> , 2016
	Zimbabwe	200+		Isotopic analysis / radiocarbon dating	Woodborne <i>et al.</i> , 2015
	Botswana	1300+		Isotopic analysis / radiocarbon dating	Patrut <i>et al.</i> , 2019
<i>Adansonia rubrostipa</i> (L.)	Madagascar	1600+		Isotopic analysis / radiocarbon dating	Patrut <i>et al.</i> , 2015
<i>Brachystegia floribunda</i> (L.)	Zambia	Undetermined	Missing rings	–	Syampungani <i>et al.</i> , (2010)
<i>Brachystegia spiciformis</i> (L.)	Western Tanzania	25–54 (41)	Locally absent rings	–	Trouet <i>et al.</i> , 2001
	Western Zambia	27 – 57 (41)	Wedging rings	–	Trouet <i>et al.</i> , 2006
	Mashonoland Province and Midlands Province, Zimbabwe	Undetermined	High variability of annual rings	–	Grundy, 2006
	South central Africa	43 – 149 (100)	Wedging rings	–	Trouet <i>et al.</i> , 2010
	Zambia	38–50 (46)	–	Cambial growth periodicity	Trouet <i>et al.</i> , 2010

<i>Breonadia salicina</i> (L.)	Limpopo, South Africa	547 – 620 (584)	Missing rings, vague annual rings, lack of samples	Carbon and oxygen isotopic analyses	Holmgren <i>et al.</i> , 2005; Norström <i>et al.</i> , 2008
<i>Burkea africana</i> (L.)	Northern Namibia	60 – 110 (79)	Wedging rings	–	Fichtler <i>et al.</i> , 2004
<i>Eucalyptus grandis</i> (L.)	South Africa	Undetermined		Gamma-ray densitometry and image analysis techniques	Naidoo <i>et al.</i> , 2006
<i>Isoberlinia angolensis</i> (L.)	Zambia	Undetermined	Missing rings	–	Syampungani <i>et al.</i> , 2010
<i>Isoberlinia tormentosa</i> (L.)	Western Tanzania	34 – 70 (44)	Locally absent rings	–	Trouet <i>et al.</i> , 2001
<i>Julbernardia paniculate</i> (L.)	Zambia	Undetermined	Missing rings	–	Syampungani <i>et al.</i> , 2010
<i>Mimusops caffra</i> (L.)	KwaZulu–Natal, South Africa	Undetermined	–	Carbon isotopic analyses, cross-wavelet analysis	Hall <i>et al.</i> , 2009
<i>Pittosporum viridiflorum</i> (L.)	Buffelskloof, Mpumalanga, South Africa			Isotopic analysis / radiocarbon dating	Schoeman <i>et al.</i> , 2019
<i>Podocarpus falcatus</i> (L.)	KwaZulu–Natal Midlands, South Africa	597	–		Hall, 1976
<i>Podocarpus falcatus</i> (L.)	Magoebaskloof, South Africa	128	Inadequately defined, locally absent and converging rings	–	Curtis <i>et al.</i> , 1978
	Witelsbos Forest, South Africa	80 – 205 (152)	Inadequately defined, locally absent and converging rings	–	McNaughton and Tyson, 1979
	Knysna, South Africa	Undetermined	Inadequately defined, locally absent and converging rings	–	February and Stock, 1998
	Midlands, South Africa	774	Missing and false rings	–	Vogel <i>et al.</i> , 2001
	Eastern Cape, South Africa	Undetermined	–	Isotopic analysis	Hall <i>et al.</i> , 2008
<i>Podocarpus latifolius</i> (L.)	Knysna, South Africa	Undetermined	Missing and converging rings	–	February and Stock, 1998
	South Africa, Mozambique, Zambia, Zimbabwe, Botswana	80 – 140 (110)	Wedging rings	–	Therrell <i>et al.</i> , 2007
	KwaZulu–Natal, South Africa	Undetermined	–	Isotopic analysis	Hall <i>et al.</i> , 2008
	South Africa	Undetermined	Inadequately defined, locally absent and converging rings	–	February and Stock, 1998
<i>Protea caffra</i> (L.)	Drakensberg, South Africa	~2400	–	–	February, 1994
<i>Protea roupelliae</i>	Drakensberg, South Africa	~2400	–	–	February, 1994
<i>Prunus africana</i> (L.)	Buffelskloof, Mpumalanga, South Africa			Isotopic analysis / radiocarbon dating	Schoeman <i>et al.</i> , 2019
<i>Pterocarpus angolensis</i> (L.)	Northern Namibia	60 – 79 (70)	Wedging rings	–	Fichtler <i>et al.</i> , 2004
	Zimbabwe	200	–	–	Therrell <i>et al.</i> , 2006
	Botswana, Mozambique, South Africa, Zambia, Zimbabwe	80 – 140 (110)	–	–	Therrell <i>et al.</i> , 2007
	Western Zimbabwe	120-124	Inadequately defined and discontinuous rings	–	Stahle <i>et al.</i> , 1999
<i>Widdringtonia cedarbergensis</i> (L.)	Cape Town, South Africa	412 and 118 – 326 (222)	–	Isotopic analysis	Dunwiddie and LaMarche, 1980; February and Stock, 1998

### 2.5.2 AMS Radiocarbon dating

Most living organisms are in equilibrium with atmospheric  $^{14}\text{C}$  concentration because of their fast turn-over rates of carbon (Van Strydonck, 2016). When an organism dies its metabolic processes, together with the carbon renewal in the organism, will stop and there will be a decrease of  $^{14}\text{C}$  in the remains of the organism as a result of radioactive decay (Van Strydonck, 2016). Since the youngest growth ring is the only living organism in a tree each growth year, the cellulose found in that ring can be considered in equilibrium with the  $^{14}\text{C}$  content in the atmosphere for that growth-season (Ramsey, 2008; Kromer, 2009). Thus, the radiocarbon dating technique entails the comparison of remaining  $^{14}\text{C}$  content in a living organism with atmospheric  $^{14}\text{C}$  content. In other words, calculating the period between the present and when material left the carbon cycle (Van Strydonck, 2016). The year 1950 is defined as the zero year for this method, thus any time before 1950 will be recognised as before present (BP) (Ramsey, 2009; Van Strydonck, 2016). Due to isotopic fractionation, radiocarbon is not evenly produced in the atmosphere, which means that the  $^{14}\text{C}$  content of the plant cellulose has changed in comparison to the atmosphere. Therefore, a correction for the change in concentration is needed (Van Strydonck, 2016). The isotopic fractionation is measured in permil (‰) (Van Strydonck, 2016). The average  $\delta^{13}\text{C}$  value for wood is -25‰. Calibration is then done to convert BP years into calendar years. The Libby half-life is used in this calculation and is expressed in  $\text{BP} \pm 1$  standard deviation ( $\sigma$ ) (Stuiver and Polach, 1977; Van Strydonck, 2016).

### 2.5.3 Advantages and disadvantages of using dendrochronology and AMS radiocarbon dating techniques

AMS radiocarbon dating is used to date trees, to calibrate dendrochronology and to determine growth patterns (Quarta *et al.*, 2005; Biondi *et al.*, 2007; Benedict *et al.*, 2008; Patrut *et al.*, 2015; Fedrigo *et al.*, 2019; McDonald *et al.*, 2019). This dating method is commonly used in southern Africa for paleoenvironmental studies that include climate proxies and dating of different landscapes (Scott *et al.*, 2003; Mills *et al.*, 2009; Strachan *et al.*, 2014; Loftus *et al.*, 2016).

The advantages of dendrochronology include: the ability to date trees based on their annual growth rings, an increase in availability of tree ring chronology networks, existence of large geographic-scale patterns of the same inter-annual variability, and the opportunity to use linear models of climate-growth relationships that can easily be calibrated and tested (Carrer and Urbinati, 2004). The limitations of dendrochronology include: the fact that only certain climate variability information may be captured in the tree-ring records that may reflect multifaceted

biological responses to climatic changes (Carrer and Urbinati, 2004). In addition, plant growth cycles are limited by seasonality and needs to be taken into consideration when dating trees. For instance, in temperate climate zones, plant growth is restricted to discrete growing seasons, which is during spring and summer (Stoffel and Bollschweiler, 2008). Lastly, dendrochronology, as a climate change indicator, assumes that climate-growth relationships are age-dependent, however, studies have found that as trees age, physiological changes take place, causing growth-related climate signals to vary over time (Carrer and Urbinati, 2004).

#### 2.5.4 Challenges and potential for dendrochronological research in southern Africa

One challenge of tree-ring research in southern Africa is that the well-defined annual rings do not remain intact for long enough after death, due to the widespread occurrence of wood-eating insect species such as termites (Nash, 2017). Secondly, the availability of laboratory equipment, especially for AMS radiocarbon dating, as it is a specialised field. Another challenge is securing funding and support from government and private organisations in the field of research and development.

#### 2.6 Study overview

Scientific understanding of the southern African climate system is comparable to other parts of the world. However, interdisciplinary, and international collaborations are needed to extend research projects. There is also a need for the development of extended regional and sub regional climate models that include ecological or climatological factors. The previous sections have demonstrated the potential of dendrochronological and radiocarbon dating techniques in different research projects and at different locations globally. Various species show datable annual growth rings and reach a considerable age, and some show wood-anatomical properties that can indicate climatic variability. Linking dendrochronology and radiocarbon dating with other methods (e.g. remote sensing, modelling, other palaeoclimatic reconstructions and plant physiology) is a valuable approach to draw comprehensive scientific conclusions across temporal and spatial scales.

The locality of the study site and the scale of the study may influence the results when studying the relationship between elevation and species richness (Boscutti *et al.*, 2018). Therefore, individual shrub species and the entire plant community along an elevation gradient should be considered (Boscutti *et al.*, 2018). Elevation studies mostly include features such as shrub age and other dendrochronological, morphological, and physiological parameters. Studies that focused on the effects of elevation only used a single species and studied its acclimation

strategies (Bhattarai and Vetaas, 2003; Chen *et al.*, 2011; Panthi *et al.*, 2018; Opala-Owczarek *et al.*, 2019). However, a need to study the effects of multiple elevations and climate changes on multiple species and communities at the same and different locations exist (Boscutti *et al.*, 2018).

This research aims to answer questions related to the applications of dendrochronology to climatology. The study presents new growth chronologies from *Helichrysum trilineatum*, *H. tenuifolium* and *H. witbergense* in the DAC. The chronologies extend from as early as 1964 to 2018. These *Helichrysum* chronologies from the DAC are remarkably important in the field of dendroclimatology for their length and possible reliable climate reconstructions and other climate related investigations. The newly constructed chronologies are used to test the hypothesis that a relationship exists between climate and shrub growth patterns. Establishing separate shrub growth ring chronologies for different species at different elevations was necessary to address the question of whether shrub growth is limited to species and whether elevational changes affect shrub growth. Testing for a significant correlation between climate variables and shrub ring widths was needed to determine the role temperature and precipitation plays in shrub growth. To do this, temperature and precipitation needs to be correlated and thereafter a relationship between the shrub ring widths and both temperature and precipitation may be established or eliminated. Separate shrub growth ring chronologies for different species at different elevations and aspect was necessary to address the question of whether shrub growth is affected by slope aspect and/or elevation. Correlation analyses between shrub growth of different shrub species at the same or different aspects and elevation from the newly established chronologies was necessary to determine the role aspect and elevation plays in shrub growth. The research focus is thus interdisciplinary in approach, bringing the disciplines of geography, dendroclimatology, and ecology together to test several hypotheses that relate to shrub ecophysiology and dendroclimatology.

# CHAPTER THREE

## Materials and Methods

### 3.1. Environmental setting

The study area is located in the Drakensberg Alpine Centre (DAC), which accounts for the highest elevations along the Great Escarpment, at the border between KwaZulu-Natal Province, South Africa, and eastern Lesotho (Grab, 2000) (Figure 2-1). Three study sites are included in this study: (1) a lower elevation site referred to as Sani Pass-lower (29°34'12" S; 29°16'12" E; ± 2 514 to 2 585 m a.s.l.); (2) one at the crest of Sani Pass (referred to as “Sani Pass-upper” as it is located midway between the lower and upper sites) (29°33'56.58" S; 29°15'23.30" E; ± 2 859 to 2 916 m a.s.l.); and (3) a high elevation site at Kotisephola Pass in Lesotho, in an area known as the ‘Black Mountain’ (29°30'51.78" S; 29°13'8.7" E; ± 3 282 to 3 332 m a.s.l.) (Figure 3-1). Kotisephola and Sani Pass-upper study site are located in the lower-alpine belt, while the Sani Pass-lower study site is located in the upper-montane (previously known as sub-alpine) thermal belt (Killick, 1978; Körner *et al.*, 2011; Carbutt, 2012; Carbutt and Edwards, 2015a).

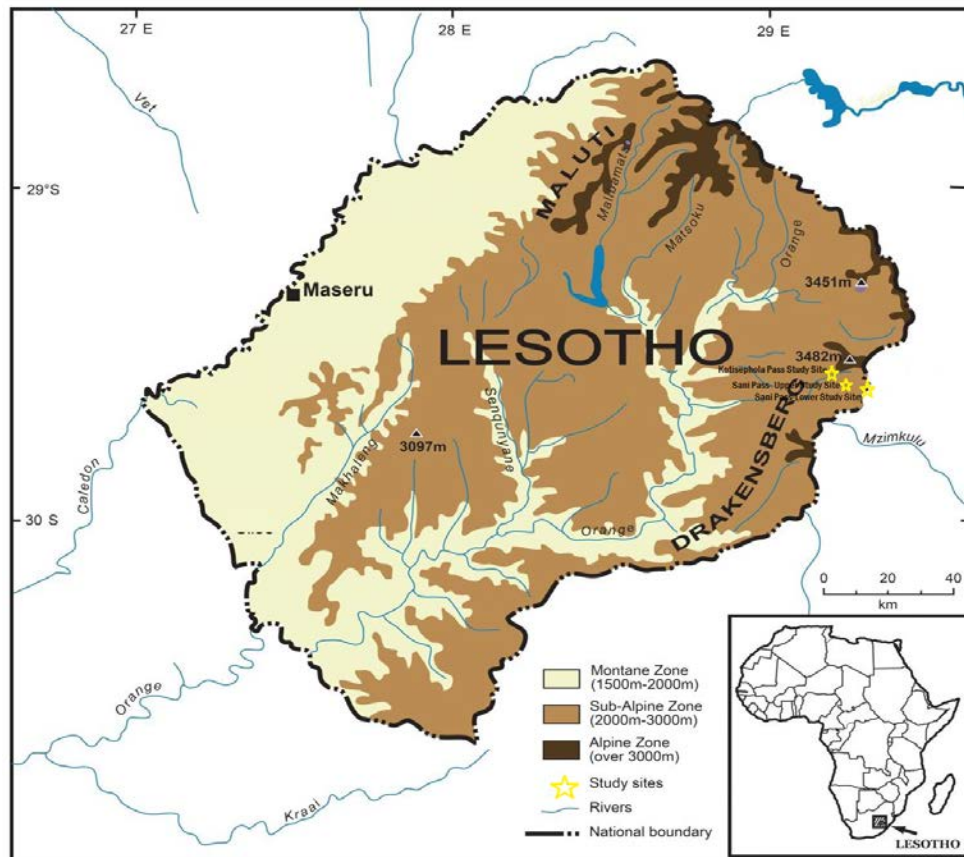


Figure 3-1: Locality of the three study sites.



### 3.1.1. Geology and soils

Geology of the low-altitude section of the Drakensberg (up to 2 200 m a.s.l.) is dominated by the Stormberg Group, which includes the Upper Beaufort rocks, Molteno beds of the Molteno Formation at the base, followed by the Red beds of the Elliot Formation, then the Clarens Formation - which is the youngest, and highest in elevation (Kitching and Raath, 1984; Mucina and Rutherford, 2006; Mills *et al.*, 2017; Lodder *et al.*, 2018) (Figure 2-2). Above 2 200 m a.s.l., the alpine region, is a thick basaltic cap characterised by dark soils as a result of basaltic lava from past volcanic activity (Kitching and Raath, 1984; Bentley and O'Connor, 2018; Brand *et al.*, 2019). Soils of the Elliot Formation are mostly derived from low-altitude mudstones, sandstones and siltstones (Kitching and Raath, 1984). The Molteno Formation comprises coarse-grained, fairly shallow sandstones, and greyish mudstone layers (Bordy *et al.*, 2005). The Clarens Formation hosts fine to medium-grained sandstones with mudstone layers at lower parts in the formation (Kitching and Raath, 1984).

### 3.1.2. Climate

The DAC is located in the summer precipitation zone of southern Africa and is associated with a distinct seasonal alpine climate, cool wet summers and cold dry winters (Grab, 2010; Mills *et al.*, 2017). The DAC receives more than 80% (> 2 000 mm) of its mean annual total precipitation between October and April each year (Grab *et al.*, 2017; Norström *et al.*, 2018). Despite the unknown long-term annual precipitation trends for the lower-alpine belt, Sene *et al.* (1998) and Grab (2010) mentioned that the mean annual precipitation at Sani Top is estimated to vary between 800 and 1 600 mm.yr<sup>-1</sup>. Mean monthly air temperature for the lower-alpine belt varies between 4.0°C to 11.0°C (Brand *et al.*, 2019). May to August are the four coldest months, with mean monthly minimum temperatures ranging from -1.0 °C to -5.4 °C (Brand *et al.*, 2019). Most snowfalls (< 5 cm) occur during mid-winter (June and July) and between 5 and 10 contemporary snowfalls occur over the Lesotho Highlands per annum (Grab *et al.*, 2017; Brand *et al.*, 2019). These snowfalls in the Lesotho Highlands are mostly caused by frontal perturbations and associated infrequent cut-off lows (Grab *et al.*, 2017). Lesotho experiences its strongest winds (mean wind speed of 6.0 to 8.0 m.s<sup>-1</sup>) during late winter/early spring (August to October) due to the influence of frontal systems (Grab, 2010). In summer, east and northeasterly winds are present, whereas in winter predominantly northwesterly winds occur (Grab, 2010; Fitchett, 2015). Berg winds can be present in the winter months as a result of large prefrontal disturbances (Fitchett, 2015). Ground frost occurs ± 180 days a year between April and October (Grab, 2010).

### 3.1.3. Vegetation

#### 3.1.3.1. Vegetation in the DAC

The lower-alpine, lower- and upper-montane thermal belts of the Drakensberg are the floristic basis for the DAC (Killick, 1963; Carbutt and Edwards, 2015a). The DAC has high plant species diversity and is home to over 2 800 taxa of which 13% of the angiosperm species are endemic (Carbutt and Edwards, 2006; Knight *et al.*, 2018). In this region, many of the endemic angiosperms are rare and habitat specific with respect to elevation and slope aspect (Knight *et al.*, 2018). The native angiosperm flora of the DAC contains 134 families, 630 genera and 2 520 species, with an additional 6% exotics (Carbutt and Edwards, 2004). The ten most common families in the DAC are Asteraceae, Poaceae, Fabaceae, Scrophulariaceae, Orchidaceae, Cyperaceae, Iriaceae, Asclepiadaceae, Hyacinthaceae and Asphodelaceae (Carbutt and Edwards, 2004).

Van Wyk and Smith (2001) defined the DAC to extend from between 1 800 m a.s.l. to the Drakensberg's highest point (Thabana Ntlenyana at 3 482 m a.s.l.). As discussed previously, the lower-alpine belt in the Drakensberg has since been redefined to represent the area above 2 800 m a.s.l. (Carbutt and Edwards, 2015b). Vegetation between 1 800 and 2 800 m a.s.l. in the DAC was previously defined by Killick (1963) as the sub-alpine thermal belt, while areas below 1 800 m a.s.l. as the montane thermal belt. Körner *et al.* (2011) introduced a new elevational distinction, suggesting the use of seven thermal belts and using the tree line as the main reference, as discussed previously. The alpine zone, as defined by Killick (1963), equates to the lower-alpine thermal belt of Körner *et al.* (2011) ( $< 6.4^{\circ}\text{C}$  mean growing season temperature (MGST); growing season (GS)  $< 94$  days). The sub-alpine zone is now referred to as the 'upper-montane' zone ( $> 6.4 \leq 10^{\circ}\text{C}$  MGST; GS  $> 94$  days), and montane as the 'lower-montane' zone ( $> 10 \leq 15^{\circ}\text{C}$  MGST; GS  $> 94$  days). The lower-alpine zone is characterised by the presence of *Erica-Helichrysum* heathland, with dwarf shrubs at the highest peaks ( $> 3 400$  m a.s.l.) where vegetation cover may be limited in places (Killick, 1963, 1978, Carbutt and Edwards, 2004, 2006, 2015a). The upper-montane zone is characterised by the presence of *Erica* and  $C_4$  tussock-forming *Themeda triandra* grassland at its lower limits, and towards its upper limits by  $C_3$  tussock-forming *Festuca-Merxmullera-Pentaschistis* grassland ( $> 2 600$  m a.s.l.) (Killick, 1963, 1978; Carbutt and Edwards, 2004, 2006, 2015a). In the lower-montane belt, Afrotemperate forests can be found on the south and south-east facing aspects, whereas *Protea* woodlands can occupy north-facing slopes and boulder bed scrub alongside rivers near valley bottoms (Killick, 1963, 1978; Carbutt and Edwards, 2004, 2006, 2015a). For this study, the focus will be on the

genus *Helichrysum* Mill., which is part of the Asteraceae family, and which grows in the lower-alpine, upper- and lower-montane thermal belts. According to Carbutt and Edwards (2015a), the tree line ecotone is a key temperature threshold area. Thus, the tree line ecotone can be regarded as a boundary in terms of temperature and can be used in climate change research in the DAC (Carbutt and Edwards, 2015a).

#### 3.1.4.2 Genus *Helichrysum* Mill.

*Helichrysum* Mill. is a large, morphologically variable genus that belongs to the Asteraceae family, tribe Inuleae and subtribe Gnaphaliinae. *Helichrysum* consists of approximately 500 to 600 species, comprising both annual and perennial plants that include herbs, shrubs, and sub-shrubs (Bayer *et al.*, 2007; Lourens *et al.*, 2008, Glennon and Cron, 2015). This M.Sc. dissertation specifically examines *Helichrysum tenuifolium*, *H. trilineatum* and *H. witbergense* (Plate 3-1).

*H. tenuifolium* (Plate 3-1a) is a twiggy, rounded shrub with white woolly branches that can reach 2 m in height (Britten *et al.*, 1954; Hilliard, 1963) and grows in the upper- and lower-montane ( $\pm 1\ 300 - 2\ 750$  m a.s.l.) thermal belts (Körner *et al.*, 2011, Carbutt, 2012). It has darkish-green, linear leaves (Britten *et al.*, 1954) that are glabrous above and woolly below (Hilliard, 1977). The heads are heterogamous, with woolly bases, many in compact terminal corymbose clusters (Hilliard, 1963). The flowers' involucral bracts are closely imbricate, and colours may vary from "brown often tipped reddish or orange when young, to bright canary-yellow" (Hilliard, 1963, p. 220-221). *H. tenuifolium* flowers mainly in mid-November to February (Britten *et al.*, 1954; Hilliard, 1977). This shrub is used in the traditional medicine industry to treat a variety of problems, such as nervousness, hysteria, chest problems, colds and flu, nausea, back pain, headaches, and wound care (Lourens *et al.*, 2008) (Table 3-1).

*H. trilineatum* is also known as 'Alpine Everlasting' (Plate 3-1c) (Killick, 1990). It is found in the alpine, upper- and lower-montane thermal belts ( $\pm 1\ 300 - 3\ 480$  m a.s.l.) (Körner *et al.*, 2011; Carbutt, 2012). *H. trilineatum* is a "twiggy, rounded shrub" (Hilliard, 1963, p. 219), which is much-branched (Hilliard, 1963). It has "linear or oblong" (Hilliard, 1963, p. 219), "cobwebby or greyish-white woolly" (Hilliard, 1963, p. 219) leaves (Hilliard, 1963, p. 219) with gland dots on the upper leaf surface and can grow between 150 mm to 1 m high (Hilliard, 1963). Its medium sized head is heterogamous that is often "woolly or cobwebby at the base" (Hilliard, 1963, p. 219), and has "bright canary-yellow flowers" (Hilliard, 1963, p. 219), which are receptacle honeycombed (Hilliard, 1963). Flowering season for *H. trilineatum* is mainly from August to February but can be found in flower throughout the year (Hilliard, 1963, 1977). *H. trilineatum* is not eaten by stock and

is used as fuelwood given that the green branches burn easily (Hilliard, 1963; Lourens *et al.*, 2008) (Table 3-1).

*Helichrysum witbergense* (named after the Witteberg in the Barkley East district) (Hilliard, 1963) occurs exclusively in the alpine thermal belt (2 750 to 3 480 m a.s.l.) (Körner *et al.*, 2011; Carbutt, 2012). It is a “spindly shrub” (Hilliard, 1963, p. 220) that has grey-woolly leaves, the upper leaf surface is “lightly cobwebby” (Hilliard, 1963, p. 220) which broadens at the base (Plate 3-1b) (Hilliard, 1963). This shrub can grow up to 900 mm high (Hilliard, 1963). Its medium sized head is heterogamous and has light brown bracts that are often white-woolly at the base (Hilliard, 1963) and has “bright canary-yellow flowers” (Hilliard, 1963, p. 220), which are “receptacle honeycombed” (Hilliard, 1963, p. 220). *H. witbergense* flowers mainly between November and February (Hilliard, 1963, 1977). *H. tenuifolium*, *H. trilineatum* and *H. witbergense* are all perennial (Hilliard, 1977), for this reason growth rings can be dated and measured on these shrubs (Table 3-1).

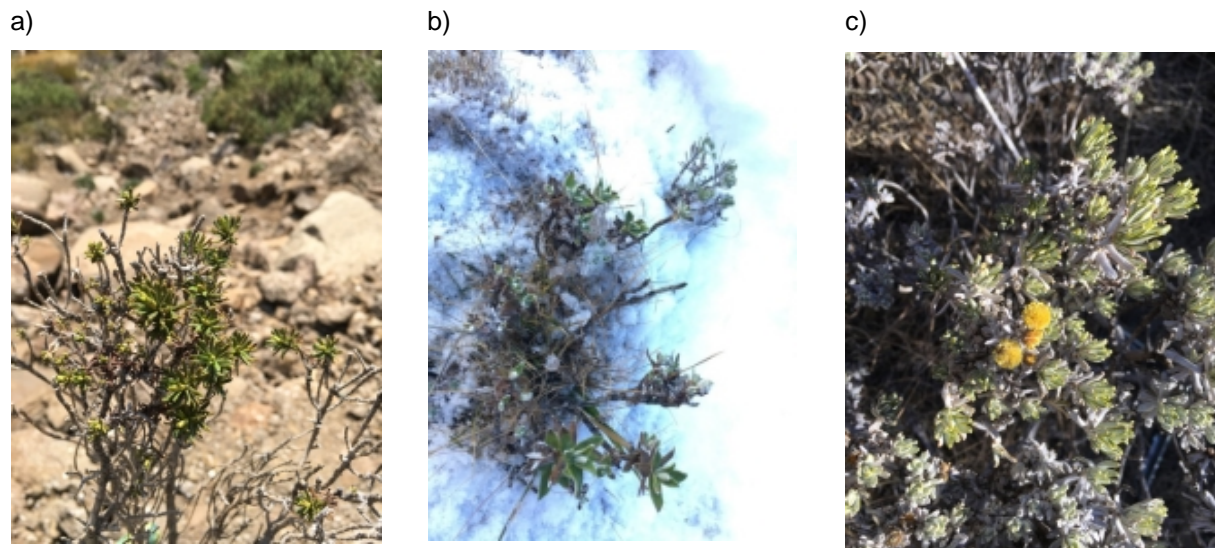


Plate 3-1: a) *H. tenuifolium*, b) *H. witbergense* and c) *H. trilineatum*.

To the knowledge of the author, the wood anatomy of two of the studied species (*H. witbergense* and *H. tenuifolium*) is investigated for the first time in this Masters study. Between the three studied species, only the dendrochronology of *H. trilineatum* was previously examined by the author during her B.Sc. Honours degree, to explore possible climatic signals stored in this species' growth ring records at Mafadi summit, Drakensberg. No previous dendrochronological analyses have yet been undertaken on *H. witbergense* and *H. tenuifolium*.

Table 3-1: Summary of the chosen species and their threats (Hilliard, 1963, p. 220; Carbutt and Edwards, 2006).

Taxon	Orange List Category	Major threat(s)	History of threat
<i>Helichrysum tenuifolium</i> Killick	Rare – Sparse (RS)	Incorrect burning regime; soil erosion, harvesting for medicinal purposes	Past, current and future
<i>Helichrysum trilineatum</i> DC.	Rare – Sparse (RS)	Harvesting for firewood, soil erosion	Current and future
<i>Helichrysum witbergense</i> Bolus	Rare – Sparse (RS)	Harvesting for firewood, soil erosion	Current and future

### 3.1.4.3 Growing season

Various climatic, environmental, and topographical variables contribute to the conditions that affect plant growth in mountain regions (Lewis and Oosthuizen, 2014). Ever-changing climatic conditions in alpine ecosystems restricts plant growth to periods with the most favourable conditions, for this reason growing seasons in these regions are unpredictable (Billings, 1974). Plant growth in alpine ecosystems, such as the DAC, is generally restricted by temperature and available moisture (Edmond *et al.*, 1957; Hatfield and Prueger, 2015, Marsh, 2017). Researchers found that small rainfall events aid respiration of biological crust carbon, whereas larger rainfall events enhance the respiration process of root and microbial-carbon (Schwinning *et al.*, 2004). Excess precipitation can cause unfavourable conditions for plant growth and development (Edmond *et al.*, 1957). Air temperature affects the rates of photosynthesis and respiration, and the phenological stages such as pollination and germination (Edmond *et al.*, 1957). Low temperatures and frost events can limit plant growth as species may enter a dormant state or adopt morphological, physiological or phenological qualities to protect themselves, and to assist the adaptation to the unfavourable growth season conditions (Marsh, 2017).

Slopes with higher insolation are warmer and have higher evaporation rates. For this reason, slopes with higher insolation, north-facing slopes in the southern hemisphere, are associated with greater plant growth rate, whereas plant growth rates are lower on south-facing slopes with a lower insolation (Mata-González *et al.*, 2002). For this reason, plants at higher elevations germinate faster than those at lower elevations, depending on solar radiation incidence and plants adapting to shorter or longer growth seasons (Marsh, 2017). The growing season of individual plants differ as their growth patterns are mostly related to the conditions they are exposed to. According to Nüsser (2002), the growing season in this study region extends from October to March, which is mostly the period between first rains and the first frost (Letšela *et al.*, 2003; Carbutt and Edwards, 2004).

### 3.1.4. Shrub abundance

*H. tenuifolium*, *H. trilineatum* and *H. witbergense* were counted along four transects directed northwards (north transect), southwards (south transect), eastwards (east transect) and westwards (west transect) at each study site. At the Kotisephola study site, transects were measured from the bottom of the rock outcrop (approximately 3 330 m a.s.l.) to 3 000 m a.s.l. elevation. Transects at Sani Pass-upper study site were measured downslope from  $\pm$  2 900 to 2 800 m a.s.l. and at Sani Pass-lower study site transects were measured downslope from  $\pm$  2 600 to 2 500 m a.s.l. Quadrat analyses were used to calculate the abundance of *H. tenuifolium*, *H. trilineatum* and *H. witbergense*. This was done by means of systematic sampling, using 2 m x 2 m quadrats (Figure 3-2) arranged in four transects totaling sixteen 2 m x 2 m quadrats (Figure 3-2). A quadrat size of 2 m<sup>2</sup> was considered as an optimal size given the size of the study area and the study site characterized by sparse alpine grassland and heathland. *H. tenuifolium*, *H. trilineatum* and *H. witbergense* that were located within the 2 m x 2 m plots were visually observed, counted and GPS coordinates documented for record purposes.

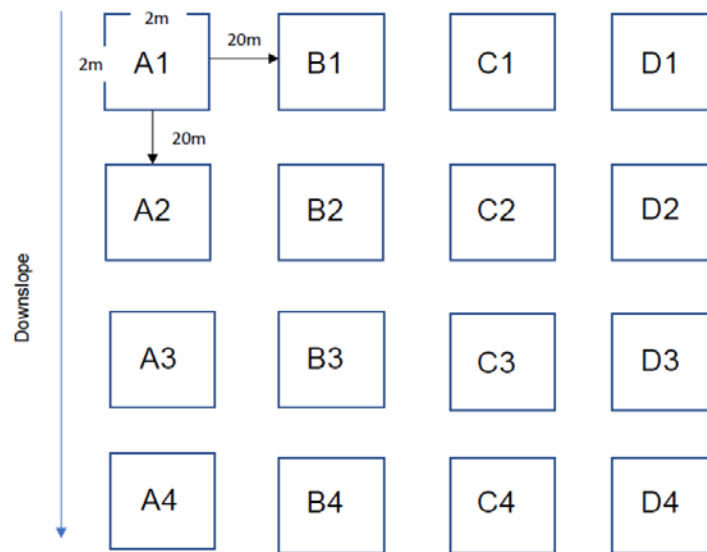


Figure 3-2: Layout of the 20m x 20m and 2m x 2m plots.

### 3.2. Field work

Two field sampling efforts were conducted in May and September 2018 respectively. *H. tenuifolium*, *H. trilineatum* and *H. witbergense* were pre-identified using 'Mountain flowers: a field guide to the flora of the Drakensberg and Lesotho' by Pooley (2003) and confirmed by a plant specialist in the field. Shrub stems that are the largest and presumably the oldest shrubs

with no visible damage to crowns or stems were selected in the 2 500 to 3 330 m a.s.l. elevation range, on all four aspects where available, at the Kotisephola study site, the Sani Pass-upper study site and the Sani Pass-lower study site (Figure 3-1). An import permit was obtained from the Department of Agriculture, Forestry and Fisheries, South Africa, for the import of *H. trilineatum* and *H. witbergense* stems that were collected in Lesotho.

### 3.2.1. Collection of shrub stems

Shrub stem samples were randomly selected (Myers-Smith *et al.*, 2015) with the aim of selecting the largest and presumably the oldest shrubs based on their availability and within the 2 500 to 3 330 m a.s.l. elevation range and on all four slope aspects (north, east, south, and west). Samples were taken from rock outcrops, between rocks where some *Helichrysum* are found, to as much as 100 m downslope from rock outcrops. This ensured that shrubs located in predominantly shaded and predominantly sun-exposed micro-sites were included. Distance from the rock outcrop and GPS (Global Positioning System) coordinates were measured and recorded for each sampled shrub stem. Less than 1% of the total approximate population of *H. trilineatum* (total of 34) and *H. witbergense* (total of 9) were sampled from the Kotisephola Pass site during May 2018. Similarly, less than 1% of *H. trilineatum* (total of 20) were sampled from the Sani Pass-upper study site and *H. tenuifolium* (total of 27) and *H. trilineatum* (total of 9) from the Sani Pass-lower site in September 2018.

Shrubs were cut in such a way as to capture the thickest primary stem portions, and to ensure that maximum growth was accounted for. Samples were taken from shrubs with thin and thicker looking stems, which enabled the study of samples that consist of a broad age range, from juveniles to mature adults. Two stem discs, on average, were collected from each of the sampled shrubs. Only location data (GPS coordinates, aspect, and elevation) were recorded on-site. Samples were stored in plastic bags in a cool dry place and handled individually in a clean workshop.

## 3.3. Laboratory work

### 3.3.1 Growth patterns

Shrub stems were air dried at room temperature and cut into smaller discs for handling purposes. Stem discs were polished using progressively finer sandpaper to achieve a polished finish to increase visibility of growth rings using a microscope. Sanding was done with a handheld electric sander with grains of sandpaper ranging progressively from 80 to 1 200 grit (80, 120, 240, 360,

600, 800, 1 000 and 1 200 grit). Stem discs with high quality rings, based on ring visibility, were analysed and photographed under low magnifications (0.63 X and 1.5 X) using the Zeiss Discovery V.12 stereomicroscope. Growth rings were counted under the microscope and ring widths were measured using the Zeiss Axiovision 4.8.2 software. Ring widths were measured along three radii per sample to account for growth irregularities (uniform, irregular or variable growth) (Myers-Smith *et al.*, 2015). Radii were drawn on the 0.63 X resolution images taken of the stem discs using the Zeiss Axiovision 4.8.2 software. Rings were counted from the pith to the inner edge of the bark and measured perpendicularly to the rings along a reticule, for better accuracy (Fichtler *et al.*, 2004). Measurement resolution was to the nearest 0.01 mm, ensuring a high level of precision.

A range of old and young stem discs collected from various locations were used for growth analyses. This enabled the comparison of growth patterns of *H. tenuifolium*, *H. trilineatum* and *H. witbergense* from the same species or between different species, and at the same and different locations. Rings had to be cross-dated to be included in the master chronology (Lindholm *et al.*, 2000). For this study, the three radii that were measured from one stem disc were cross-dated to assign the correct calendar year to each ring (Lindholm *et al.*, 2000; Myers-Smith *et al.*, 2015). Ring width data from the Zeiss Axiovision 4.8.2 software were exported to Microsoft Excel 2019, where graphs were drawn of the three radii measurements per shrub sample and for all shrub species samples for comparison. This measured series was then cross-dated by visual comparison of ring-width graphs. Visual cross-dating results were then checked by computing cross-correlations between individual series and the master chronology.

Standardisation was done in GraphPad Prism 8.1.0 using the z-score as the main parameter, in order to remove long-term growth trends from individual curves. A mean growth curve was produced for each shrub by averaging the cross-dated indexed curves. As no relevant reference chronology exists for Lesotho, shrubs were cross-dated against one another so that a reliable index chronology could be developed (Fichtler *et al.*, 2004; Trouet *et al.*, 2006). Shrubs that were successfully cross-dated were combined to create a mean site chronology. This resulted in the transformation of the time series into indexed curves.

The wounding that appears on many of the sampled shrubs (see Plate 4-1 for an example) may be the result of intense frost action and/or wind action and/or extreme drought and/or competition for resources, particularly light and water (Schweingruber, 2005; Gardiner *et al.*, 2016; Schweingruber and Börner, 2018), but the exact cause for wounding would require a separate focused study and is not part of the scope of this Masters project. Wounding can occur as



woodboring insects bore through the stem of the shrub, eventually killing the shrub (Drees *et al.*, 1994; Schweingruber and Börner, 2018) (Plate 4-2). These wounds cause the rapid death of parenchyma cells near the wound which in turn may lead to the formation of indistinct, missing, and discontinuous rings (Drees *et al.*, 1994).

### 3.3.2 AMS radiocarbon dating

For this study AMS radiocarbon dating was performed on 25 shrub rings. Two samples per species at each site were selected, and one to two rings were selected from each sample for dating. Samples comprised of the core ring and another from approximately half-way between the core and the outer ring. This serves as a cross-dating method, to eliminate missing or false rings in the sample.

Samples were stored in plastic bags and were later handled individually in a clean laboratory. All instruments and implements used during the process were rigorously pre-cleaned. The surfaces of a whole wood samples were removed mechanically before the wood was shaved into smaller fragments and 10 mg of each sample was weighed and added to 30ml glass test tubes. Cellulose samples were then pretreated using the Acid-Base-Acid (ABA) and  $\alpha$ -cellulose methods (Olsson, 1986; Loader *et al.*, 1997) to remove acid and base soluble organic material respectively, using sodium chlorite (NaOH), concentrated hydrochloric acid (HCl) and distilled water (H<sub>2</sub>O). The tubes were filled with 20 ml of HCl solution. The samples were left to stand in this solution, in a beaker to boiling it at 50°C for one hour, after which they were centrifuged and rinsed twice with distilled water. 15 ml of NaOH were then added to the tube, which were left to stand in this solution, in a beaker to boiling it at 50°C for one hour, after which they were centrifuged and rinsed twice with distilled water. Finally, clean samples were covered and allowed to dry in their respective test tubes in an oven at 70°C overnight. These steps were carried out to remove acid and base soluble organic material, respectively.

Cellulose samples were combusted to CO<sub>2</sub> using the closed tube combustion method (Sofer, 1980; Vandeputte *et al.*, 1996) and CO<sub>2</sub> reduced to graphite with an iron catalyst in a hydrogen atmosphere (Vogel *et al.* 1984). The combustion and graphitization procedures were carried out as described by Bird *et al.* (1999), however combustion time of the last step (900°C) was increased from 1 hour to 6 hours. Ensuring the complete reaction of other contaminant gases with the silver wire in the combustion test tube, as the iron powder catalyst may be poisoned by some unremoved product at a shorter combustion time. Graphite targets were made from CO<sub>2</sub> produced at 900°C temperature combustion.

The graphite-plus-iron powder targets were pressed into 1 mm diameter copper sample holders. These are loaded, together with three to four standard samples, into a sample wheel for insertion into a multi-sample negative ion source. Radiocarbon measurements were performed at iThemba LABS AMS facility of the National Research Foundation in Johannesburg, South Africa with a 6MV Tandem Linear Accelerator.

The method for calculating radiocarbon age from the atomic abundance count followed the approach by Zoppi (2010). The radiocarbon dating technique entails comparing the remaining  $^{14}\text{C}$  content within an organism with the current  $^{14}\text{C}$  content in the atmosphere. By using of the decay curve one can calculate the specific time period that has passed since the material left the carbon cycle when the plant died (equation 1).

$$A = A_0 \times e^{-\lambda t} \quad (1)$$

Where A refers to the activity of the sample,  $A_0$  to the activity of the modern atmosphere, t equals time and  $1/\lambda = T/\ln 2$ , when T = half-life.

Arnold and Libby (1951) were the first to assume that the half-life of radiocarbon was  $5568 \pm 30$  years, later the Cambridge half-life of  $5730 \pm 40$  was derived and is thought to be a more accurate reflection of the half-life of radiocarbon (Godwin, 1962). Suess (1955) found that the  $^{14}\text{C}$  in the atmosphere was lower due to the influence of fossil-fuel derived  $\text{CO}_2$  than originally assumed. An artificial modern radiocarbon standard created by Suess was based on the pre-industrial radiocarbon content of the atmosphere for this reason the year 1950 was chosen as the zero year for this method, thus any time before 1950 will be recognised as before present (BP). Therefore, 1900 BP (Before Present) is supposedly 50 AD (Anno Domini) (Van Strydonck, 2016).

Since isotopic fractionation takes place in almost all chemical reactions a correction is needed. Van Strydonck (2016) described isotopic fractionation as the changes that take place in the  $^{13}\text{C}$  and  $^{12}\text{C}$  ratio ( $^{13}\text{C}/^{12}\text{C}$ ) as a result of chemical reactions. For example,  $^{13}\text{C}/^{12}\text{C}$  that is available in both atmospheric  $\text{CO}_2$  and carbon of the cellulose. The same is true for  $^{14}\text{C}/^{12}\text{C}$ , which means that the  $^{14}\text{C}$  content of the plant cellulose has changed in comparison to the atmosphere; therefore, a correction (equation 2) for the change in concentration is needed (Van Strydonck, 2016). The isotopic fractionation is measured in permil (‰).

$$\Delta t = (\delta^{13}\text{C} + 25) \times 16 \text{ year}(\delta^{13}\text{C}) \quad (2)$$

Once the correction for isotopic fractionation is done, the conventional radiocarbon date needs to be determined, which entails a radiometric age calculation where the “radiocarbon content of a sample is compared to that of the NBS oxalic acid standard, both normalized for isotopic fractionation” (Van Strydonck, 2016; pp.12). The Libby half-life is used in this calculation (equation 3) and is expressed in BP  $\pm$  1 standard deviation ( $\sigma$ ) (Stuiver and Polach, 1977; Van Strydonck, 2016).

$$t = 8033 \cdot \ln \frac{A_{on}}{A_n} (BP) \quad (3)$$

Where  $\ln$  is the logarithm,  $A_{on}$  is the normalised activity of the modern standard and  $A_n$  refers to the normalised activity of the sample.

The rate of  $^{14}\text{C}$  production can experience either short-term or long-term variations (Van Strydonck, 2016). Short-term variations are also known as the De Vries-effect, which is the result of sunspot activity (Stuiver, 1961), whereas the long-term variations may be driven by changes in the strength of the earth’s magnetic field. Therefore, radiocarbon results need to be calibrated. The effect of the nuclear bombing should also be considered when doing the calibration, in the paper of Reimer *et al.* (2004) the calculations are outlined and discussed in detail. Nowadays, calibration programmes exist that incorporates the calibration factors into its age calculations, the most popular ones being OxCal, INTCAL and CALIB (Stuiver and Reimer, 1993, Ramsey 2001; Heaton *et al.*, 2009). For this study, fraction modern values were calibrated and converted into calendar ages with the online software program CALIB (calibomb.org), by using the SHCal13 and SHZ1\_2 atmospheric data set (Reimer *et al.*, 2004; Hogg *et al.*, 2013). Some of the graphite targets were very small and provided low current beams, which resulted in larger statistical errors for those samples.

### 3.4 Data sources

Temperature data for the region of the study sites are only available for Sani Top and were obtained from the Lesotho Meteorological Services and Prof. Stefan Grab’s personal dataset. This dataset was used as a baseline and the international lapse rate ( $0.6^\circ\text{C}$  per  $100\text{m}^{-1}$ ) was used to extrapolate temperature datasets for both the Kotisephola Pass and Sani Pass-lower study sites. Sani Top data were used as an indication of the climate at the Sani Pass-upper study site as it is located at the same elevation. Rainfall data were obtained for the 20-year period (1994 - 2014) from three weather stations in closest proximity to the study sites: Shaleburn and Giants Castle in South Africa, and Mokhotlong in Lesotho. Data were obtained from the Lesotho

Meteorological Services and Prof. Stefan Grab's personal dataset. Shaleburn (1614 m a.s.l.) and Giants Castle (1759 m a.s.l.) are within the lower-montane thermal zone, while Mokhotlong (2209 m a.s.l.) is in the upper-montane thermal zone. These weather station datasets were chosen as they best represent relative rainfall amounts and patterns for two of the three thermal zones. Unfortunately, monthly data are incomplete and thus had to be omitted. When one month of the growing season was not present the whole growing season was removed, as this would give inaccurate results.

Table 3-4: Summary of climate datasets used.

Weather station	Temperature data	Rainfall data
Sani Top	2000 –2018 period, missing 2008 dataset (the 1999 – 2018 growth years)	
Mokhotlong	-	1992 – 2010 (the 1993 – 2019 growth years)
Giant's Castle	-	1993 – 2017 (the 1994 – 2016 growth years)
Shaleburn	-	1992 – 2016 (the 1993 – 2016 growth years)

### 3.5 Statistical Analyses

#### 3.5.1 Growth patterns

Statistical analyses of shrub age and ring widths were used to do a comparison between different species at the same and at different elevations and for the same species at different and the same elevations, and to assess the inter-annual growth variability of all *Helichrysum* stem discs and comparisons were made between different species at the same and different elevations and for the same species at different and the same elevation.

Average, minimum, and maximum shrub diameter of all *Helichrysum* stem discs were determined and comparisons were made between different species at the same and different elevations and for the same species at different and the same elevation.

#### 3.5.2 Growth analysis

Standardised shrub growth chronologies were used to assess the similarity among chronologies and any potential differences due to changes in elevation, relationships among the chronologies were analysed using correlation analysis. As shrubs grow, there may be an associated decrease in radial growth over time, thus radial growth of younger shrubs is faster than that of older shrubs, resulting in heteroscedastic variance in shrub growth chronologies (Cook and Kairiukstis, 1990; Myers-Smith *et al.*, 2015). By means of standardization, non-climatic variations from shrub growth chronologies are removed, and only climatic variations common to all shrubs remain (Lehejček,

2015; Myers-Smith *et al.*, 2015, Allen *et al.*, 2018). Standardised shrub growth chronologies, therefore, represent the amount of radial growth produced each year by a shrub, provided climatic variation associated with the shrub growth remained constant (Lehejček, 2015).

Several standardised tree ring series can therefore be averaged together to produce a master chronology that is suitable to study past climate changes (Cook and Kairiukstis, 1990, Lehejček, 2015). For this study, the ratio of every shrub growth chronology to the trend line is calculated for every point. The ratio will be larger than 1.0 when the shrub growth chronology is above the trend line and is below 1.0 when the shrub growth chronology is below the trend line. Each shrub growth chronology is reduced to a series of dimensionless indices and an equal variance (Myers-Smith *et al.*, 2015).

It should be noted that standardisation may result in inaccurate chronology values (Myers-Smith *et al.*, 2015), as it may remove information and cause the underestimation of natural climatic variability. For this reason, considerations based on available shrub growth ring data, such as for the purposes of the current study, are important when deciding whether to detrend shrub growth chronologies using a standardisation technique (Myers-Smith *et al.*, 2015).

### 3.5.3 Climate-growth relationships

According to Myers-Smith *et al.* (2015), dendroclimatic analyses of growth make use of standardised growth data that provide an index of relative inter-annual growth. However, analysing raw ring width data instead of standardised data can provide a better understanding of shrub growth patterns and the drivers of change over time (Myers-Smith *et al.*, 2015). Pearson's correlation coefficients were calculated between the chronologies to assess which variables were significantly related to shrub growth ( $p < 0.05$ ). Climatic variables used in this study measured monthly mean temperature at all sites and monthly total rainfall. Correlation analyses between shrub growth and climatic variables were compared during the growing season (October to March). The study period was set from 2000 to 2018, so as to make the climate–growth relations comparable between sites. Multiple regression analysis was carried out by considering shrub growth and both temperature and rainfall variables for the growing months.

### 3.5.4 Distribution and abundance of shrub species at the study sites

The Shannon-Wiener Diversity Index ( $H'$ ) is a measure of diversity that combines species richness (the number of species in a given area) and their relative abundances. Where  $n_i$  = number of individuals or amount (e.g. biomass) of each species (the  $i^{\text{th}}$  species) and  $N$  = total number of individuals (or amount) for the site, and  $\ln$  = the natural log of the number.

$$H' = - \sum \left[ \left( \frac{n_i}{N} \right) \times \ln \left( \frac{n_i}{N} \right) \right]$$

Pielou's Evenness Index is a measurement of equitability among species in the community. Where  $H'$  = Shannon-Wiener Diversity Index ( $H'$ ),  $H_{max} = \ln(s)$  species diversity under maximum equitability conditions,  $s$  = number of species in the community.

$$E = \frac{H'}{H_{max}}$$

### 3.6 Summary

A physical description of the study site and the methods used in this research has been detailed. The field techniques and laboratory procedures used to undertake this research included collection and preparation of stem discs, age determination, shrub abundance calculations, AMS radiocarbon dating and correlation analyses. These preparations and analyses facilitate the producibility of a master chronology and improved comparisons between sites. Many of the difficulties faced with methodological processes are valuable lessons also for future studies in the region, as this essentially forms a pioneering study for high elevation dendrochronological work in the DAC.

# CHAPTER FOUR

## Results

### 4.1 Introduction

This chapter presents and describes the results of growth ring identification and measurement, age determination, radiocarbon dating and correlation analyses of the responses of growth rings to climate and shrub abundance along the altitudinal gradient.

### 4.2 Growth patterns

#### 4.2.1 Growth ring characteristics and anomalies

All *Helichrysum tenuifolium*, *H. trilineatum* and *H. witbergense* samples displayed distinct growth rings (Plate 4-1). The wounding that appears on fifty-nine shrub samples (see Plate 4-1 for an example) may be the result of intense frost action and/or wind action and/or extreme drought (Schweingruber, 2005; Gardiner *et al.*, 2016; Schweingruber and Börner, 2018), however this requires more substantive research to be verified. Wounding can also occur as woodboring insects bore through the stem of the shrub, eventually killing the shrub (Drees *et al.*, 1994; Schweingruber and Börner, 2018) (Plate 4-2). Wounding by woodboring insects occurred mostly on *H. tenuifolium* located at the Sani Pass-lower study site, but also affected *H. trilineatum* at the Sani Pass-upper study site (Table 4-1). Woodboring insects were found in the samples during the cutting of stems, type of woodboring insect species will need to be studied separately.

Table 4-1: Shrubs affected by woodboring insects.

Study site	Shrub species	Number of samples	Number of samples damaged by woodboring insects	Sample names of damaged samples
Kotisephola Pass study site	<i>H. trilineatum</i>	34	0	-
Kotisephola Pass study site	<i>H. witbergense</i>	9	0	-
Sani Pass-upper study site	<i>H. trilineatum</i>	20	3	CN4, CS4, CS5
Sani Pass-lower study site	<i>H. trilineatum</i>	9	0	-
Sani Pass-lower study site	<i>H. tenuifolium</i>	27	7	D12, D14, D17, D18, D20, D22, D23

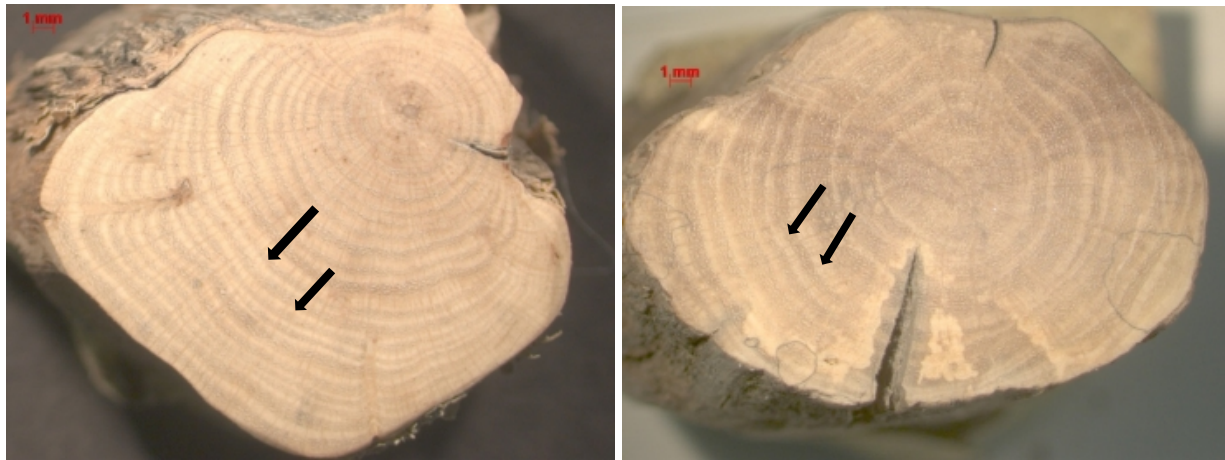


Plate 4-1: Growth rings of *H. trilineatum*. Arrows indicate direction of growth.

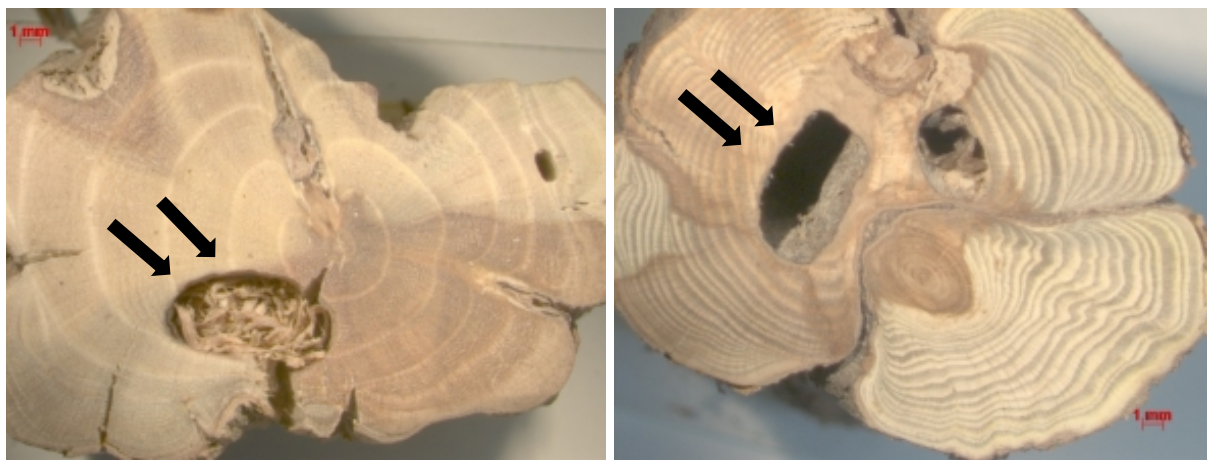


Plate 4-2: *Helichrysum* affected by woodboring insects. Arrows indicate wounding.

#### 4.2.2 Growth ring analysis

In total, 99 shrub samples were studied, and of these, nine were *H. witbergense*, 63 were *H. trilineatum* and 27 *H. tenuifolium*. Site information and statistics of the sampled shrubs are presented in Table 4-2 and Table 4-3.

Table 4-2: Site information, chronology statistics and common interval (1964–2018) statistics of the three shrub species from the three sampling sites from different elevations.

	Kotisephola Pass		Sani Pass - upper	Sani Pass - lower	
	<i>H. trilineatum</i>	<i>H. witbergense</i>	<i>H. trilineatum</i>	<i>H. tenuifolium</i>	<i>H. trilineatum</i>
No. of shrubs sampled	34	9	20	27	9
Time span	1964-2018	1968-2018	1991-2018	2000-2018	2003-2018
First order autocorrelation (AC)	0.01	0.05	0.01	0.01	0.01



Variance explained by the first principal component (PC1%)	0.52	0.18	0.38	0.29	0.29
Average inter-annual variance in growth (mm)	0.10	0.12	0.19	0.56	0.43

Table 4-3: Site information, chronology statistics and common interval (1964–2018) statistics of the three shrub species from the three sampling sites from different elevations and aspects.

Kotisephola Pass study site								
	<i>H. trilineatum</i>				<i>H. witbergense</i>			
Elevation (m a.s.l.)	3330				3330			
Latitude	29°31'5"S				29°31'5"S			
Longitude	29°11'57"E				29°11'57"E			
	North	East	South	West	North	East	South	West
Sample size	2	9	13	10			8	1
Time span	1986 - 2018	1985 - 2018	1964 - 2018	1974 - 2018			1968 - 2018	1994 - 2018
First order autocorrelation (AC)	0.82	0.78	0.82	0.70			0.63	0.03
Variance explained by the first principal component (PC1%)	0.80	0.26	0.68	0.24			0.59	0.44
Average inter-annual variance in growth (mm)	0.07	0.16	0.08	0.10			0.12	0.12
Sani Pass-upper study site								
	<i>H. trilineatum</i>							
Elevation (m a.s.l.)	2800							
Latitude	29°34'20"S							
Longitude	29°15'59"E							
	North		East		South		West	
Sample size	6		5		5		4	
Time span	1991 - 2018		1998 - 2018		1992 - 2018		1993 - 2018	
First order autocorrelation (AC)	0.70		0.73		0.12		0.26	
Variance explained by the first principal component (PC1%)	0.55		0.44		0.39		0.63	
Average inter-annual variance in growth (mm)	0.22		0.19		0.18		0.13	
Sani Pass study site								
	<i>H. trilineatum</i>				<i>H. tenuifolium</i>			
Elevation (m a.s.l.)	2600				2600			
Latitude	29°35'27"S				29°35'27"S			
Longitude	29°17'43"E				29°17'43"E			
	North	East	South	West	North	East	South	West
Sample size		9				27		
Time span		2003 - 2018				2000 - 2018		
First order autocorrelation (AC)		0.71				0.51		
Variance explained by the first principal component (PC1%)		0.29				0.29		
Average inter-annual variance in growth (mm)		0.43				0.56		

\*\*Aspects were grouped into four groups: north (incl. north (N), north north west (NNW), north north east (NNE), north east (NE)); east (incl. east north east (ENE), east (E), east south east (ESE) and south east (SE)); south (south (S), south south east (SSE) and south south west (SSW), south west (SW)); and west (incl. west (W), west south west (WSW), west north west (WNW) and north west (NW)).

Table 4-4: Growth pattern information of *H. trilineatum*, *H. witbergense* and *H. tenuifolium*.

	Aspect																
	Combined	NNW	N	NNE	NE	ENE	E	ESE	SE	SSE	S	SSW	SW	WSW	W	WNW	NW
<b>Kotisephola Study Site</b>																	
<b>Species: <i>H. trilineatum</i></b>																	
Sample size	34	2	-	-	-	-	2	2	2	3	3	5	5	4	5	1	-
Average ring count (shrub age) (yr)	27	29	-	-	-	-	22	30	14	24	26	26	37	32	22	41	-
Minimum ring count (shrub age) (yr)	3	25	-	-	-	-	21	26	8	20	22	15	23	19	14		-
Maximum ring count (shrub age) (yr)	54	32	-	-	-	-	23	33	33	28	32	38	54	44	32	27	-
Average ring width (mm)	0.59	0.42	-	-	-	-	0.57	0.63	0.52	0.61	0.60	0.62	0.41	0.75	0.59	0.30	-
Minimum ring width (mm)	0.26	0.33	-	-	-	-	0.54	0.60	0.41	0.50	0.50	0.48	0.26	0.35	0.41		-
Maximum ring width (mm)	1.41	0.51	-	-	-	-	0.59	0.67	1.14	0.66	0.70	0.94	0.49	1.41	0.91	1.41	-
Pearson correlation between shrub age and shrub growth rate (p < 0.05)	-0.58		-	-	-	-											-
Average shrub diameter (mm)	20.17	15.82	-	-	-	-	18.30	24.90	13.30	19.99	21.44	20.51	20.66	20.92	19.08		-
Minimum shrub diameter (mm)	11.53	11.59	-	-	-	-	16.64	23.11	18.43	19.10	19.14	17.97	14.61	18.36	15.22		-
Maximum shrub diameter (mm)	26.95	20.05	-	-	-	-	19.95	26.68	21.47	21.32	23.61	26.95	26.95	26.79	22.50	26.95	-
Pearson correlation between shrub age and shrub diameter (p < 0.05)	0.07		-	-	-	-											-
Average inter-annual shrub growth variability (mm)	0.10	0.07	-	-	-	-	0.19	0.16	0.12	0.13	0.07	0.08	0.05	0.09	0.11		-
Minimum inter-annual shrub growth variability (mm)	0.04	0.05	-	-	-	-	0.16	0.14	0.10	0.11	0.07	0.05	0.04	0.07	0.06		-
Maximum inter-annual shrub growth variability (mm)	0.26	0.09	-	-	-	-	0.22	0.18	0.26	0.15	0.08	0.10	0.07	0.16	0.16	0.05	-
Pearson correlation between shrub age and inter-annual shrub growth variability (p < 0.05)	-0.56	-	-	-	-	-											-
<b>Species: <i>H. witbergense</i></b>																	
Sample size	9	-	-	-	-	-	-	-	-	-	-	-	-	-	-	-	-
Average ring count (shrub age) (yr)	26	-	-	-	-	-	-	-	-	-	-	22	23	37			
Minimum ring count (shrub age) (yr)	12	-	-	-	-	-	-	-	-	-	-	12	22	24			
Maximum ring count (shrub age) (yr)	50	-	-	-	-	-	-	-	-	-	-	32	24	50			
Average ring width (mm)	0.70	-	-	-	-	-	-	-	-	-	-	0.77	0.69	0.52			
Minimum ring width (mm)	0.42	-	-	-	-	-	-	-	-	-	-	0.65	0.65	0.42			
Maximum ring width (mm)	0.96	-	-	-	-	-	-	-	-	-	-	0.96	0.74	0.62			

Pearson correlation between shrub age and shrub growth rate ( $p < 0.05$ )	-0.77	-	-	-	-	-	-	-	-	-	-	-	-	-	-	-	-
Average shrub diameter (mm)	20.79	-	-	-	-	-	-	-	-	-	-	0.77	0.69	0.52			
Minimum shrub diameter (mm)	15.98	-	-	-	-	-	-	-	-	-	-	0.65	0.65	0.42			
Maximum shrub diameter (mm)	26.33	-	-	-	-	-	-	-	-	-	-	0.96	0.74	0.62			
Pearson correlation between shrub age and shrub diameter ( $p < 0.05$ )	0.67	-	-	-	-	-	-	-	-	-	-						
Average inter-annual shrub growth variability (mm)	0.12	-	-	-	-	-	-	-	-	-	-	0.13	0.11	0.10			
Minimum inter-annual shrub growth variability (mm)	0.42	-	-	-	-	-	-	-	-	-	-	0.10	0.09	0.09			
Maximum inter-annual shrub growth variability (mm)	0.17	-	-	-	-	-	-	-	-	-	-	0.17	0.13	0.12			
Pearson correlation between shrub age and inter-annual shrub growth variability ( $p < 0.05$ )	-0.54	-	-	-	-	-	-	-	-	-	-						
<b>Sani Pass-upper Study Site</b>																	
<b>Species: <i>H. trilineatum</i></b>																	
Sample size	20		4	2			3	2			2	2		2	3		
Average ring count (shrubs age) (yr)	17		16	20			15	17			11	24		17	18		
Minimum ring count (shrubs age) (yr)	10		11	12			13	14			10	22		13	12		
Maximum ring count (shrubs age) (yr)	27		20	27			19	20			23	26		20	25		
Average ring width (mm)	0.62		0.67	0.66			0.76	0.55			0.45	0.42		0.54	0.60		
Minimum ring width (mm)	0.36		0.50	0.37			0.54	0.49			0.45	0.36		0.45	0.43		
Maximum ring width (mm)	0.95		0.85	0.95			0.94	0.61			0.90	0.48		0.62	0.73		
Pearson correlation between shrub age and ring width ( $p < 0.05$ )	-0.90																
Average shrub diameter (mm)	21.37		20.42	21.25			21.23	21.15			13.46	23.49		19.28	23.79		
Minimum shrub diameter (mm)	15.74		16.95	19.78			18.86	17.86			15.74	20.24		17.97	19.82		
Maximum shrub diameter (mm)	26.74		23.48	22.72			23.68	24.43			24.65	26.74		20.59	26.30		
Pearson correlation between shrub age and shrub diameter ( $p < 0.05$ )	0.39																
Average inter-annual shrub growth variability (mm)	0.19		0.22	0.23			0.18	0.21			0.23	0.10		0.16	0.16		
Minimum inter-annual shrub growth variability (mm)	0.05		0.14	0.12			0.16	0.00			0.08	0.08		0.05	0.06		

Maximum inter-annual shrub growth variability (mm)	0.37		0.36	0.33			0.21	0.00			0.37	0.12		0.26	0.30		
Pearson correlation between shrub age and inter-annual shrub growth variability ( $p < 0.05$ )	-0.82																
<b>Sani Pass-lower Study Site</b>																	
<b>Species: <i>H. tenuifolium</i></b>																	
Sample size	27	-		-	-		27										
Average ring count (shrub age) (yr)	11	-		-	-		11										
Minimum ring count (shrub age) (yr)	7	-		-	-		7										
Maximum ring count (shrub age) (yr)	18	-		-	-		18										
Average ring width (mm)	1.22	-		-	-		1.22										
Minimum ring width (mm)	0.72	-		-	-		0.72										
Maximum ring width (mm)	1.34	-		-	-		1.34										
Pearson correlation between shrub age and shrub ring width ( $p < 0.05$ )	-0.63	-		-	-		-0.63										
Average shrub diameter (mm)	24.26	-		-	-		24.26										
Minimum shrub diameter (mm)	16.16	-		-	-		16.16										
Maximum shrub diameter (mm)	40.20	-		-	-		40.20										
Pearson correlation between shrub age and shrub diameter ( $p < 0.05$ )	0.36	-		-	-		0.36										
Average inter-annual shrub growth variability (mm)	0.40						0.40										
Minimum inter-annual shrub growth variability (mm)	0.20						0.20										
Maximum inter-annual shrub growth variability (mm)	0.93						0.93										
Pearson correlation between shrub age and inter-annual shrub growth variability ( $p < 0.05$ )	27																
<b>Species: <i>H. trilineatum</i></b>																	
Sample size	9	-		-	-		9										
Average ring count (shrub age) (yr)	9	-		-	-		9										
Minimum ring count (shrub age) (yr)	3	-		-	-		3										
Maximum ring count (shrub age) (yr)	15	-		-	-		15										
Average ring width (mm)	1.31	-		-	-		1.31										
Minimum ring width (mm)	0.65	-		-	-		0.65										

Maximum ring width (mm)	2.37	-		-	-		2.37										
Pearson correlation between shrub age and shrub ring width ( $p < 0.05$ )	-0.86	-		-	-		-0.86										
Average shrub diameter (mm)	20.76	-		-	-		20.76										
Minimum shrub diameter (mm)	16.16	-		-	-		16.16										
Maximum shrub diameter (mm)	25.26	-		-	-		25.26										
Pearson correlation between shrub age and shrub diameter ( $p < 0.05$ )	0.74	-		-	-		0.74										
Average inter-annual shrub growth variability (mm)	0.56						0.56										
Minimum inter-annual shrub growth variability (mm)	0.21						0.21										
Maximum inter-annual shrub growth variability (mm)	1.34						1.34										
Pearson correlation between shrub age and inter-annual shrub growth variability ( $p < 0.05$ )	-0.49						-0.49										

#### 4.2.2.1 Kotisephola Pass study site

A total of 43 shrubs, consisting of two species (*H. trilineatum* and *H. witbergense*) were sampled at the Kotisephola study site in May 2018 at the start of the non-growing season (Table 4-2). Of these 43 shrubs, 34 are *H. trilineatum* and nine *H. witbergense*. Ages of the *H. trilineatum* samples range between three and 54 years, with an average age of 27 years; and the ages of *H. witbergense* range between 12 and 50 years, with the average age being 26 years (Table 4-2). Growth ring widths of *H. trilineatum* range from relatively wide (1.4 mm in width) to extremely narrow rings (0.3 mm in width), and *H. witbergense* growth ring widths varied between 0.4 mm and 1.0 mm (Table 4-2). *H. trilineatum* have an average diameter of 20.2 mm; similarly, *H. witbergense* stem discs have an average diameter of 20.8 mm. It can be noted that an inverse relationship exists between the ages of *H. trilineatum* and *H. witbergense* and average ring widths (*H. trilineatum*:  $r = -0.6$ ;  $p < 0.05$ ; *H. witbergense*:  $r = -0.8$ ;  $p < 0.05$ ).

#### *H. trilineatum* at Kotisephola Pass study site

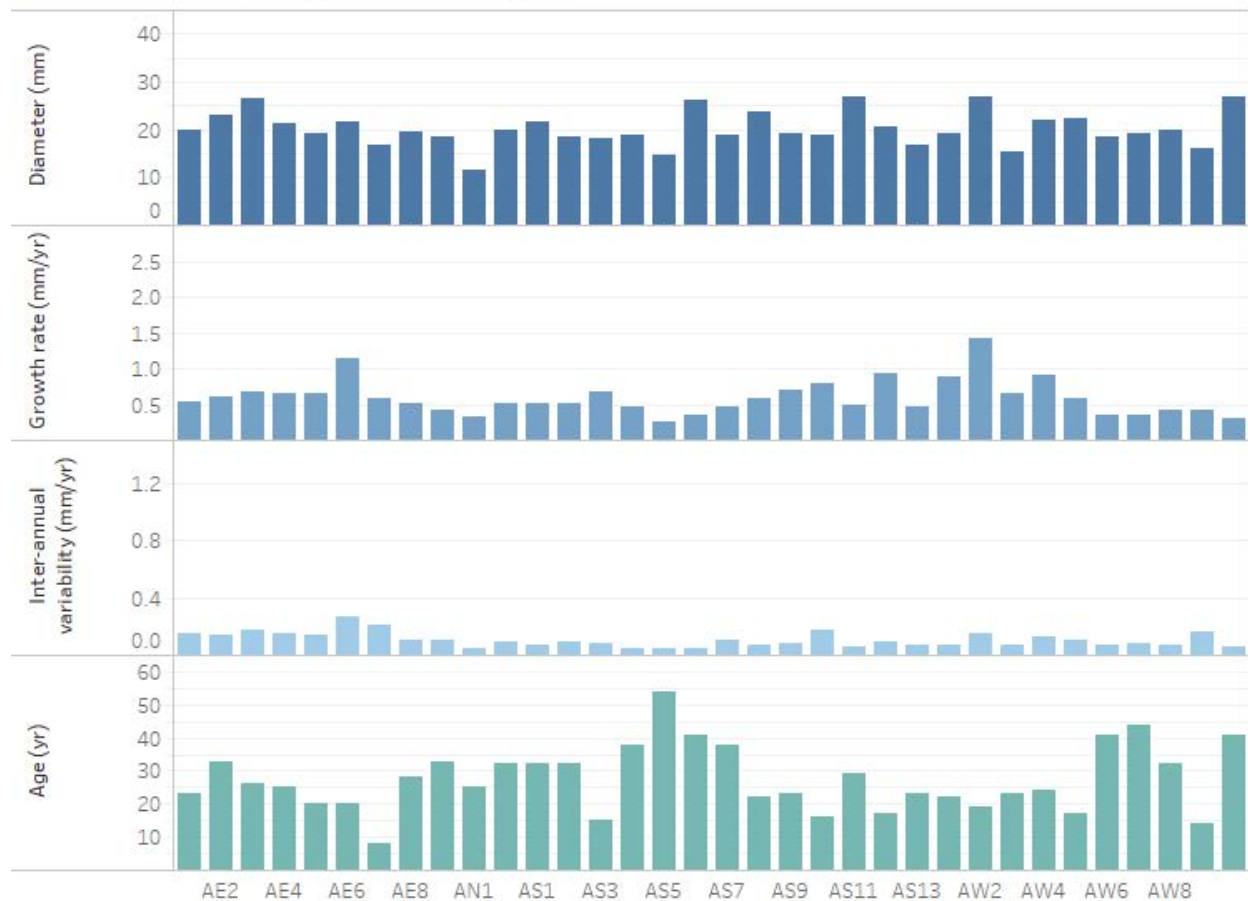


Figure 4-1: Growth ring analysis of *H. trilineatum* at Kotisephola Pass study site.

*H. witbergense* at Kotisepholo Pass study site

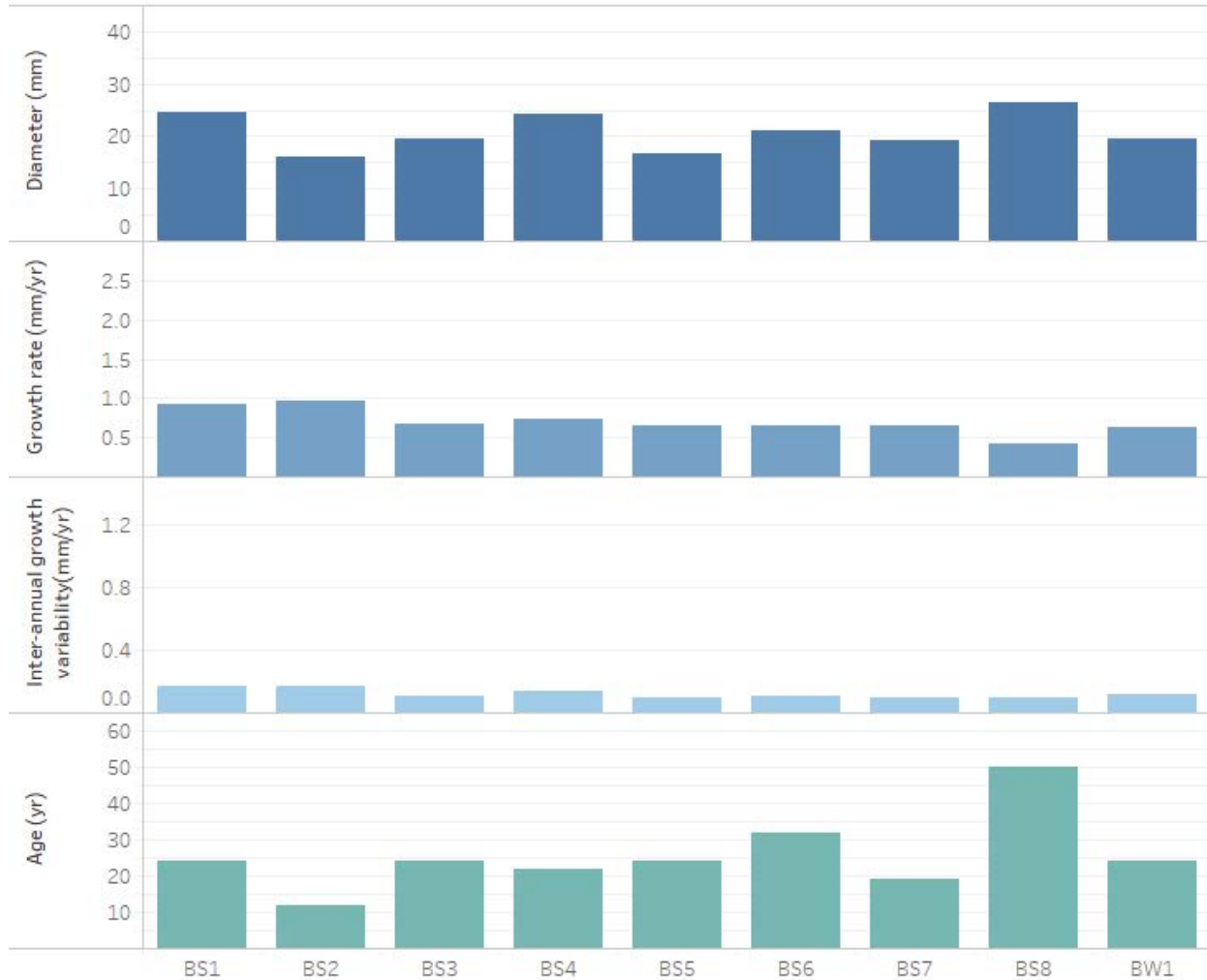


Figure 4-2: Growth ring analysis of *H. witbergense* at Kotisepholo Pass study site.

*H. trilineatum* sample with the greatest maximum ring width was sampled on the western aspect of the Kotisepholo Pass study site, whereas the shrub with the lowest minimum ring width was sampled on the southern aspect (Figure 4-1). In contrast, the greatest average ring width (0.7 mm) (Table 4-2) was measured on *H. witbergense* shrub BS2, which was sampled from the southern aspect (Figure 4-2). The shrub with the lowest average ring width is BS8 (0.6 mm) (Table 4-2), sampled from the western aspect (Figure 4-2). There exists an inverse relationship between shrub age and inter-annual growth variability (*H. trilineatum*:  $r = -0.6$ ;  $p < 0.05$ ; *H. witbergense*:  $r = -0.5$ ;  $p < 0.05$ ) (Figure 4-1, Figure 4-2, Table 4-2). The inter-annual shrub growth variability of the sampled *Helichrysum* shrubs from the Kotisepholo Pass study site varied between 0.0 to 0.3 mm/yr (Figure 4-1 and Figure 4-2). *H. trilineatum* have the greatest diameter between the two species at the Kotisepholo Pass study site (Figure 4-1). The oldest *H. trilineatum* (AS5) had a diameter of 14.6 mm,

whereas the youngest *H. trilineatum* AE7 had a diameter of 16.64 mm (Figure 4-2). The greatest diameter (27.0 mm) was measured on *H. trilineatum* AS11, sampled from the south south western aspect, whereas the *H. trilineatum* AN1 with the smallest diameter (12.0 mm) was sampled from the north north western aspect (Table 4-2). A positive relationship ( $r = 0.7$ ;  $p < 0.05$ ) is observed between *H. witbergense* shrub age and shrub diameter (Figure 4-2), thus the younger the shrub the smaller the diameter. Thus, the oldest *H. witbergense* BS8 had the greatest diameter (26.3 mm) and was sampled from the west south western aspect, whereas the youngest *H. witbergense* BS2 had the smallest diameter (21.1 mm) and was sampled from the south south western aspect (Table 4-2).

#### 4.2.2.2 Sani Pass-upper study site

Twenty *H. trilineatum* were sampled from the Sani Pass-upper study site. The ages ranged between 10 and 27 years (Table 4-2). The average age for these *H. trilineatum* samples was 17 years. The samples had clear visible growth rings, with growth rates ranging from 0.4 mm/yr to 1.0 mm/yr (Figure 4-3, Table 4-2). The *H. trilineatum* with the greatest maximum ring width (1.0 mm) was sampled on the northern aspect, whereas the shrub with the lowest minimum ring width (0.4 mm) was sampled on the southern aspect (Table 4-2). It is noted that an inverse relationship exists between the ages of *H. trilineatum* and average ring widths (Figure 4-3) ( $r = -0.9$ ;  $p < 0.05$ ). *H. trilineatum* stem discs have an average diameter of 21.73 mm and the shrub diameters range between 15.7 mm to 26.7 mm (Table 4-2). The oldest *H. trilineatum* (CN5) had a diameter of 19.8 mm, whereas the youngest shrub (CS3) had a diameter of 15.7 mm (Figure 4-3, Table 4-2). The greatest diameter (26.7 mm) was measured on the *H. trilineatum* CS2, sampled from the south south western aspect (Figure 4-3, Table 4-2), whereas *H. trilineatum* CS3 had the lowest diameter (15.7 mm) and was sampled from the southern aspect (Figure 4-3, Table 4-2). A positive relationship between shrub age and shrub diameter is noticeable ( $r = 0.4$ ;  $p < 0.05$ ) (Table 4-2). An inverse relationship between shrub age and inter-annual growth variability exists ( $r = -0.8$ ;  $p < 0.05$ ) (Figure 4-3). The inter-annual growth variability of the *H. trilineatum* from the Sani Pass- upper study site varied between 0.1 to 0.4 mm/yr (Figure 4-3).



*H. trilineatum* at Sani Pass-upper study site

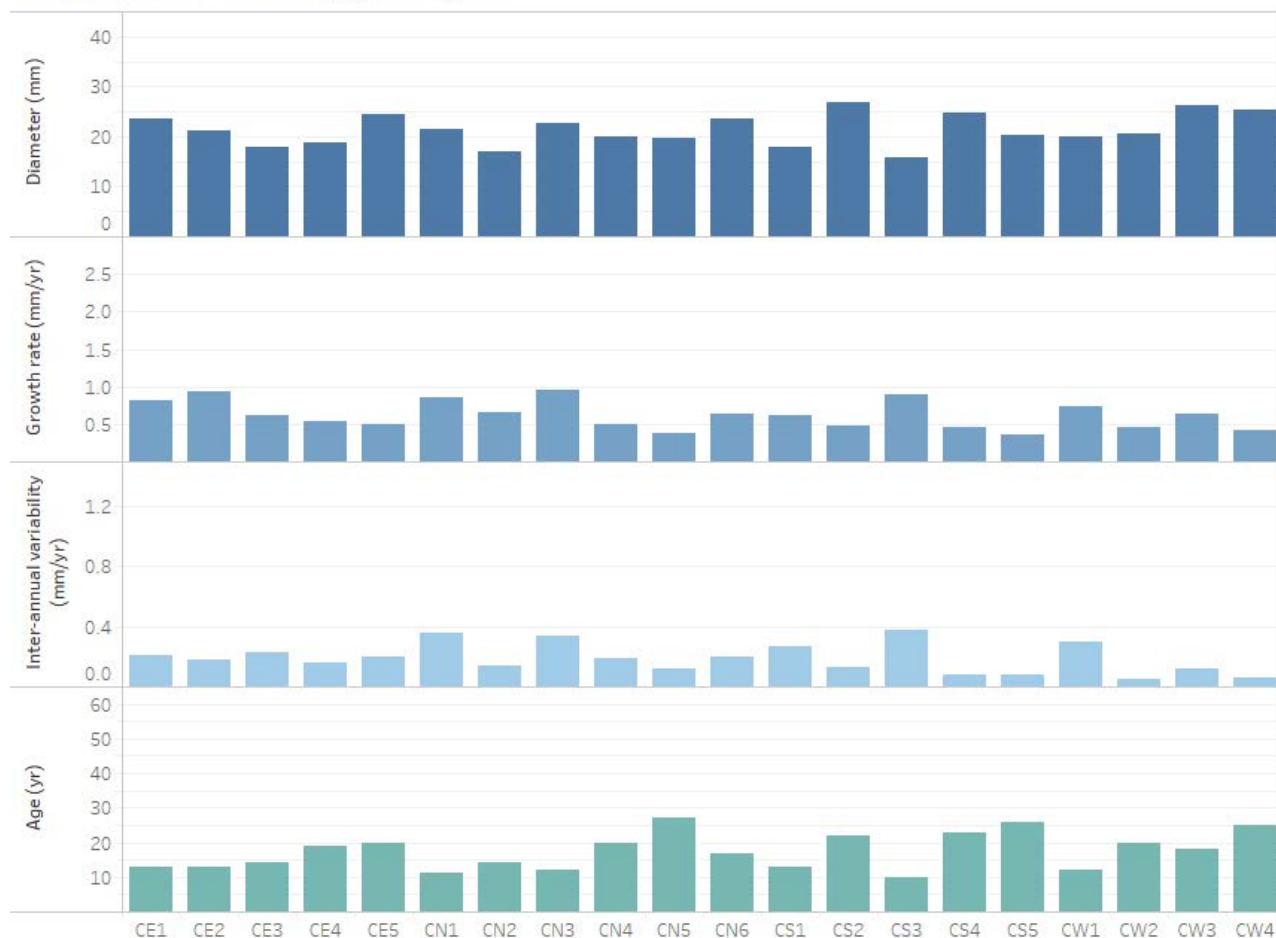


Figure 4-3: Growth ring analysis of *H. trilineatum* at Sani Pass-upper study site.

4.2.2.3 Sani Pass-lower study site

A total of 36 shrubs, consisting of two species (*H. tenuifolium* and *H. trilineatum*), were sampled at the Sani Pass-lower study site in May 2018 at the start of the non-growing season (Table 4-2). All *H. tenuifolium* and *H. trilineatum* were sampled from the eastern aspect of the Sani Pass-lower study site. Of these 36 shrubs, 9 were *H. trilineatum* and 27 were *H. tenuifolium* (Table 4-2). The ages of the sampled *H. trilineatum* ranged between 3 and 15 years, with an average age of 9 years and the *H. tenuifolium* ranged between 7 and 18 years, with an average age of 11 years (Table 4-2). Growth ring widths of the *H. tenuifolium* varied between 0.7 mm and 1.9 mm, and *H. trilineatum* growth ring widths varied between 0.7 mm to 2.4 mm (Table 4-2). *H. tenuifolium* had an average diameter of 24.3 mm, while *H. trilineatum* stem discs had a similar average diameter of 20.8 mm (Table 4-2). An inverse relationship exists between the ages of *H. tenuifolium* and *H. trilineatum* and average ring width (*H. trilineatum*:  $r = -0.9$ ;  $p < 0.05$ ; *H. tenuifolium*:  $r = -0.6$ ;  $p < 0.05$ ). *H. trilineatum* E9 was

the youngest (three years) and had the greatest average shrub ring width (2.4 mm). In contrast, the oldest *H. tenuifolium* D22 (18 years) had the smallest average shrub ring width (1.00 mm) (Table 4-2). An inverse relationship exists between shrub age and inter-annual growth variability (*H. trilineatum*:  $r = -0.8$ ;  $p < 0.05$ ; *H. tenuifolium*:  $r = -0.5$ ;  $p < 0.05$ ) (Table 4-2). Inter-annual shrub growth variability of the sampled *Helichrysum* varied between 0.2 to 1.3 mm/yr (Table 4-2). The *H. tenuifolium* samples had the greatest diameter between the *H. trilineatum* and *H. tenuifolium*. A positive relationship can be seen between shrub age and diameter (*H. trilineatum*:  $r = 0.7$ ;  $p < 0.05$ ; *H. tenuifolium*:  $r = 0.4$ ;  $p < 0.05$ ) (Figure 4-4, Figure 4-5, Table 4-2).

*H. tenuifolium* at Sani Pass-lower study site

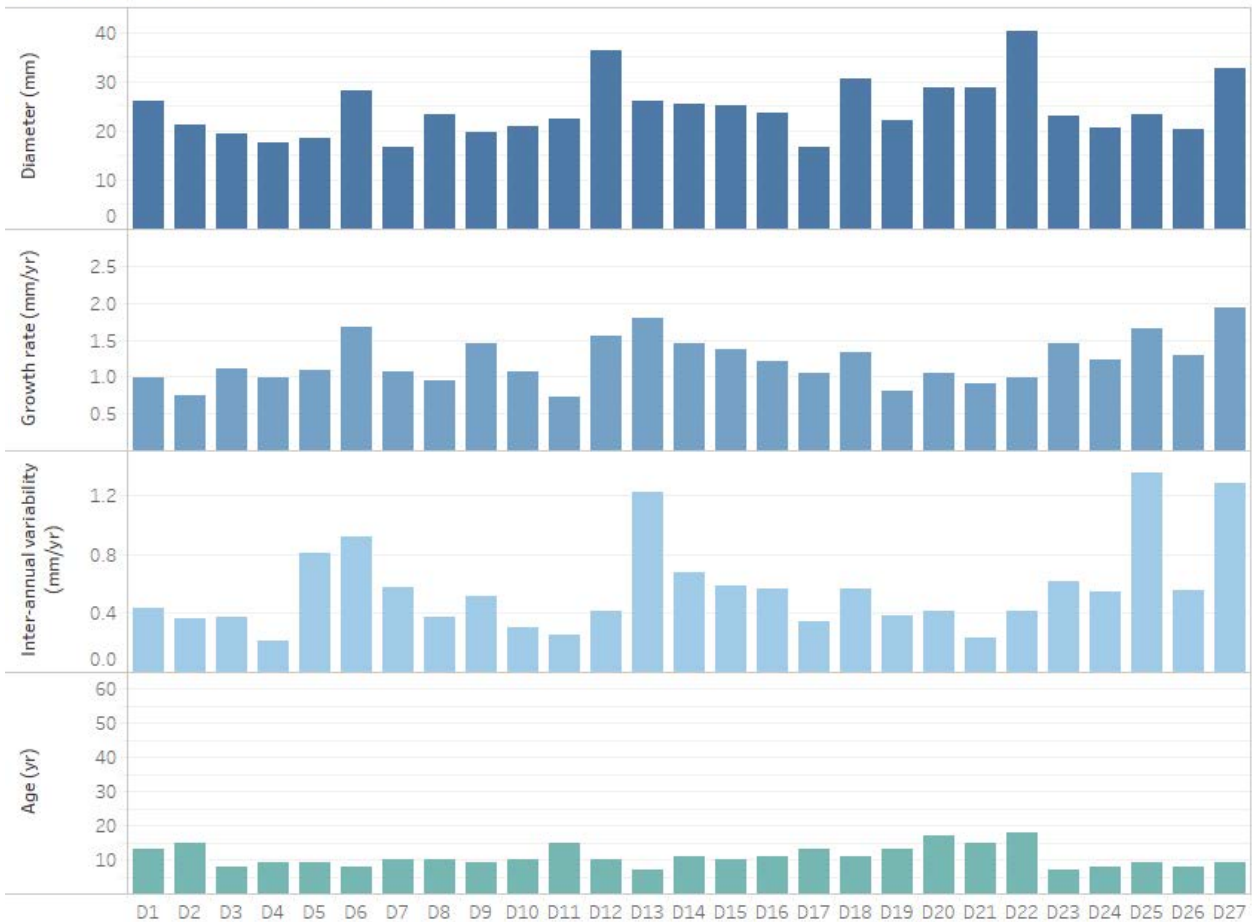


Figure 4-4: Growth ring analysis of *H. tenuifolium* at Sani Pass-lower study site.

*H. trilineatum* at Sani Pass-lower study site

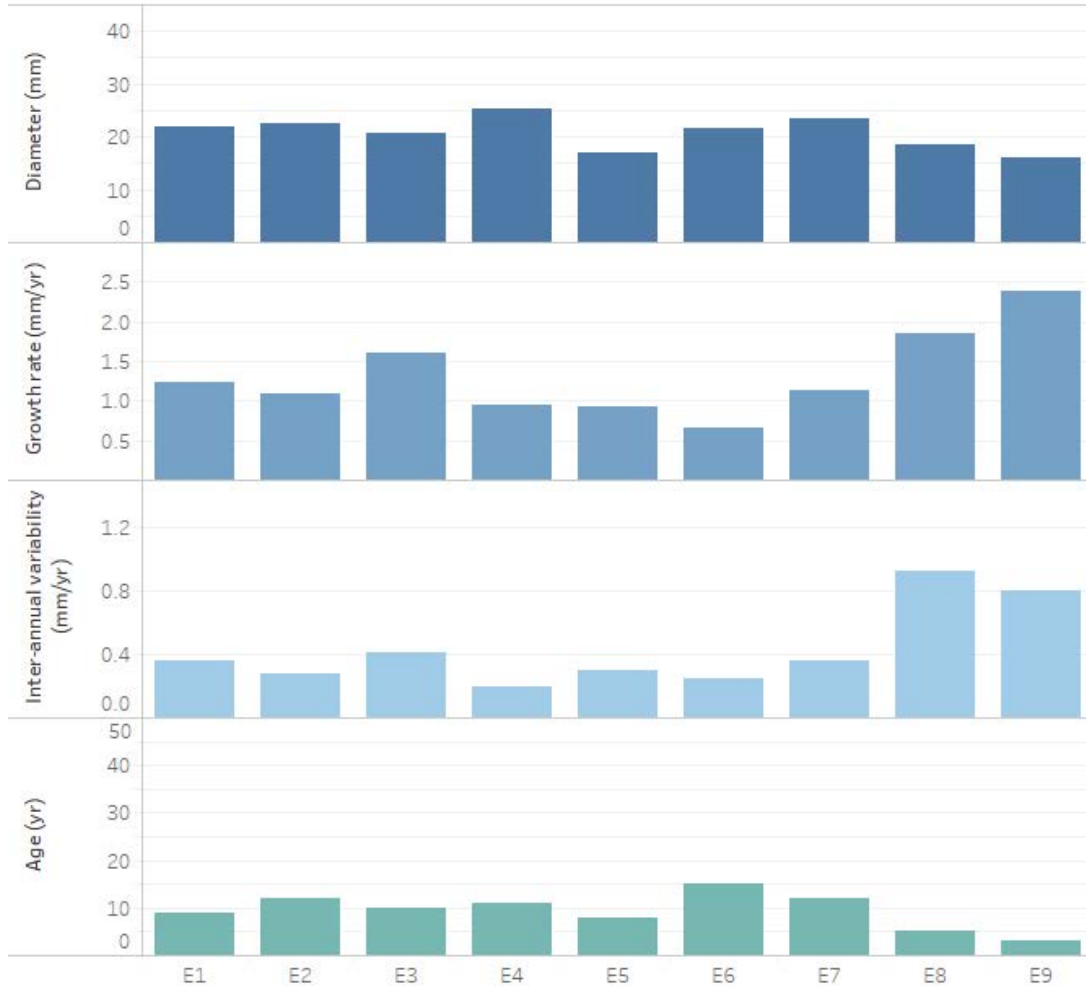


Figure 4-5: Growth ring analysis of *H. trilineatum* at Sani Pass-lower study site.

### 4.2.3 Growth chronologies

#### 4.2.3.1 *Helichrysum* growth chronologies at different elevations

Standardised growth ring chronologies for the three study sites located at different elevations for the period 2004 – 2018 are displayed below (Figure 4-6). *H. trilineatum* from Kotisephola Pass study site had a mean inter-annual shrub growth variability of 0.1 mm/yr (Figure 4-6). Similarly, *H. witbergense* from the same site had a mean inter-annual shrub growth variability of 0.1 mm/yr (Figure 4-6). *H. trilineatum* from Sani Pass-upper study site had a mean inter-annual shrub growth variability of 0.2 mm/yr (Figure 4-6). On the other hand, shrubs sampled from the Sani Pass-lower study site had higher mean inter-annual shrub growth variabilities with *H. trilineatum* having a mean inter-annual shrub growth variability of 0.4 mm/yr. *H. tenuifolium* a mean inter-annual shrub growth variability of 0.6 mm/yr (Figure 4-6).



Figure 4-6: Standardised growth chronologies of *Helichrysum* species at the three study sites.

\*\*Where KHTr: Kotisephola Pass study site *H. trilineatum*, KHW: Kotisephola Pass study site *H. witbergense*, SUHTr: Sani Pass-upper study site *H. trilineatum*, SLHTr: Sani Pass-lower study site *H. trilineatum* and SLHTe: Sani Pass-lower study site *H. tenuifolium*.

A strong mean correlation ( $p < 0.05$ ) exist among the same species at the same elevation. *H. trilineatum* at the Kotisephola Pass study site had a mean correlation between same species samples of  $r = 0.9$  ( $p < 0.05$ ) (Table 4-5). In contrary a weak mean correlation exists between *H. tenuifolium* at the Sani Pass-lower study site ( $r = 0.5$ ,  $p < 0.05$ ). The strongest mean correlation ( $p < 0.05$ ) among the same species at the different elevations existed among the growth ring chronologies of the *H. trilineatum* at the Kotisephola Pass and Sani Pass-upper study site ( $r = 0.4$ ,  $p < 0.05$ ) (Table 4-5), whereas no mean correlation existed between *H. trilineatum* from the Kotisephola Pass and the Sani Pass-lower study sites. Among different species at different

elevations, the strongest mean correlation existed between the growth chronologies of *H. trilineatum* at the Sani Pass-upper study site and *H. tenuifolium* Sani Pass-lower study site ( $r = 0.7$ ,  $p < 0.05$ ) (Table 4-5).

Table 4-5: Mean correlations of shrub growth chronologies of shrub species located at different elevations. Significant level of  $p < 0.05$ .

	KHW	KHTr	SUHTr	SLHTe	SLHTr
KHW	0.7				
KHTr	-0.1	0.9			
SUHTr	0.5	0.4	0.6		
SLHTe	0.5	0.1	0.7	0.5	
SLHTr	-0.2	0.0	0.4	0.5	0.7

\*\*Where KHTr: Kotisephola Pass study site *H. trilineatum*, KHW: Kotisephola Pass study site *H. witbergense*, SUHTr: Sani Pass-upper study site *H. trilineatum*, SLHTr: Sani Pass-lower study site *H. trilineatum* and SLHTe: Sani Pass-lower study site *H. tenuifolium*.

#### 4.2.3.2 *Helichrysum* growth chronologies at different elevations and aspects

Standardised growth ring chronologies for the three study sites located at different elevations and aspects for the 2004 - 2018 period are presented below. Aspects were grouped into four groups: north (incl. north (N), north north west (NNW), north north east (NNE), north east (NE)); east (incl. east north east (ENE), east (E), east south east (ESE) and south east (SE)); south (south (S), south south east (SSE) and south south west (SSW), south west (SW)); and west (incl. west (W), west south west (WSW), west north west (WNW) and north west (NW)).

Mean inter-annual shrub growth variability of *H. trilineatum* sampled at the Kotisephola Pass according to site aspect is as follows: northern aspect: 0.1 mm/yr, eastern aspect 0.2 mm/yr, southern aspect 0.1 mm/yr and western aspect 0.1 mm/yr (Figure 4-7). *H. witbergense* from the same site had a mean inter-annual shrub growth variability of 0.09 mm/yr for shrubs sampled from the southern and less than 0.1 mm/yr for shrubs sampled from the western aspect (Figure 4-8). *H. trilineatum* sampled from the Sani Pass-upper study site had a mean inter-annual shrub growth variability as follows: northern aspect: 0.2 mm/yr, eastern aspect 0.2 mm/yr, southern aspect 0.2 mm/yr and western aspect 0.2 mm/yr (Figure 4-9). *H. trilineatum* sampled from the Sani Pass-lower study site (eastern aspect) had a mean inter-annual variability of 0.4 mm/yr (Figure 4-10) and *H. tenuifolium* a mean inter-annual variability of 0.6 mm/yr (Figure 4-11).

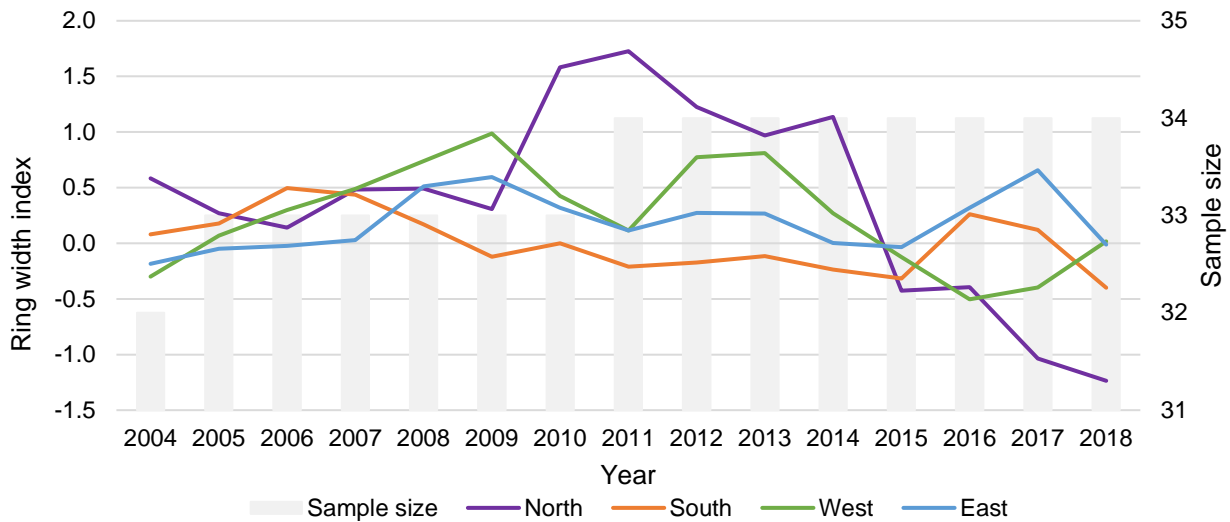


Figure 4-7: Standardised growth chronologies of *H. trilineatum* at different aspects at the Kotisephola Pass study site.

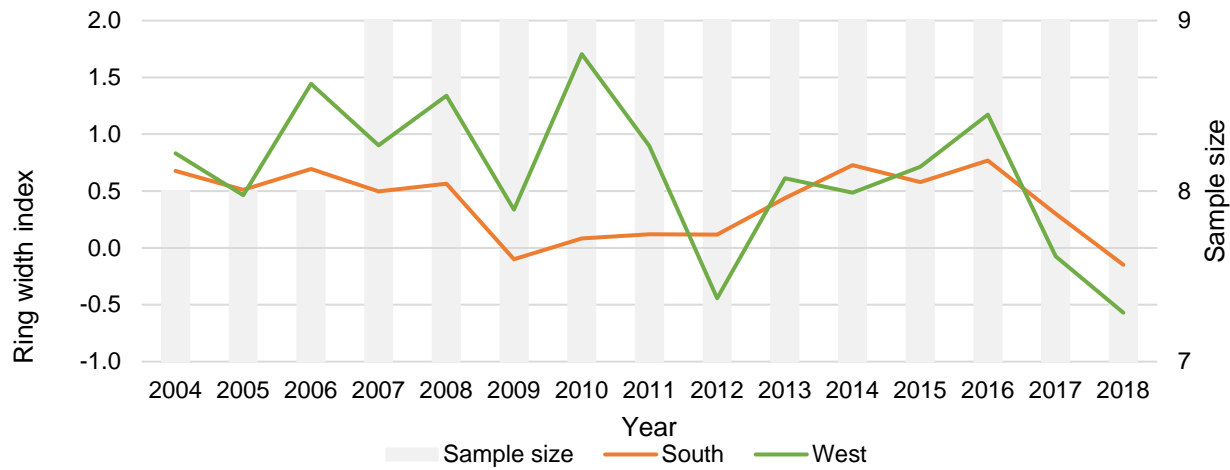


Figure 4-8: Growth chronologies of *H. witbergense* at different aspects at the Kotisephola Pass study site. Ring width index indicates z-scores.

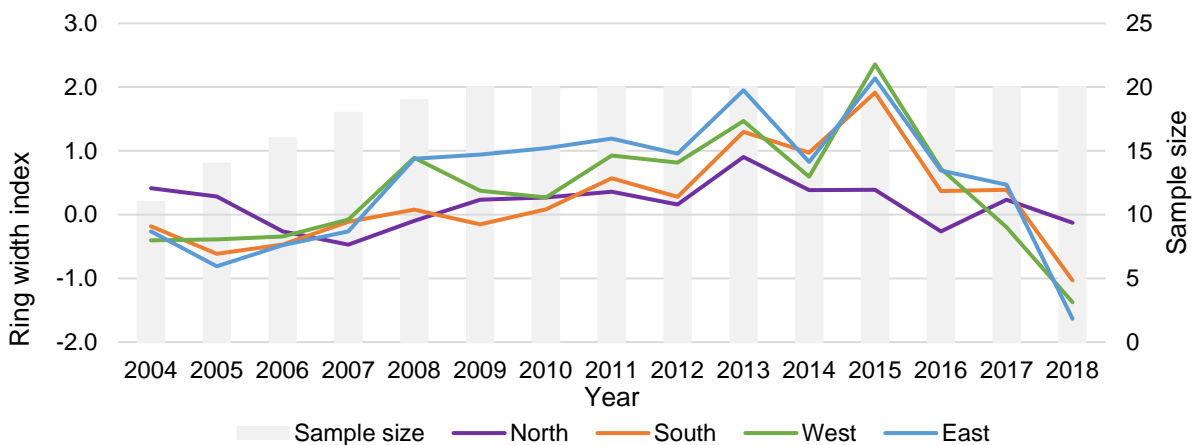


Figure 4-9: Growth chronologies of *H. trilineatum* at the Sani Pass-upper study site.

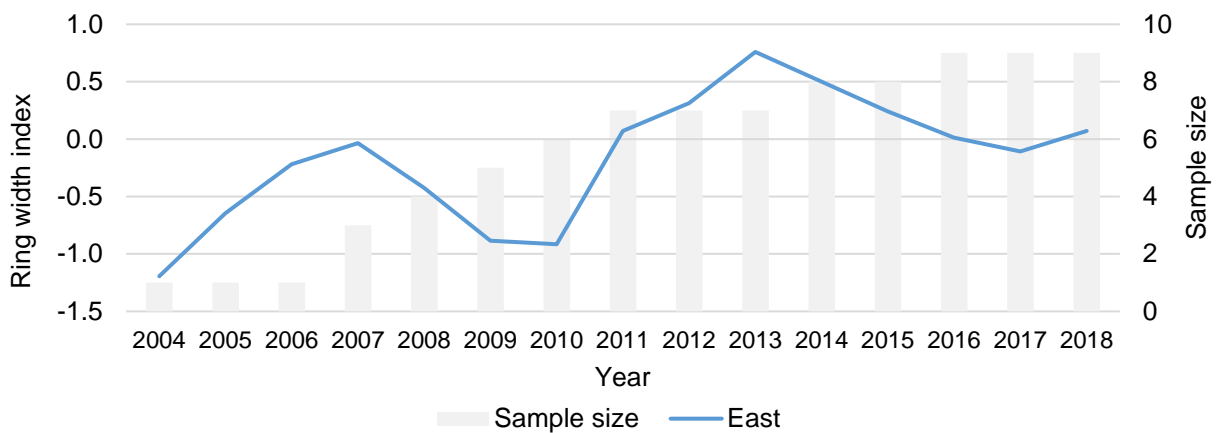


Figure 4-10: Growth chronologies of *H. trilineatum* at the Sani Pass-lower study site.

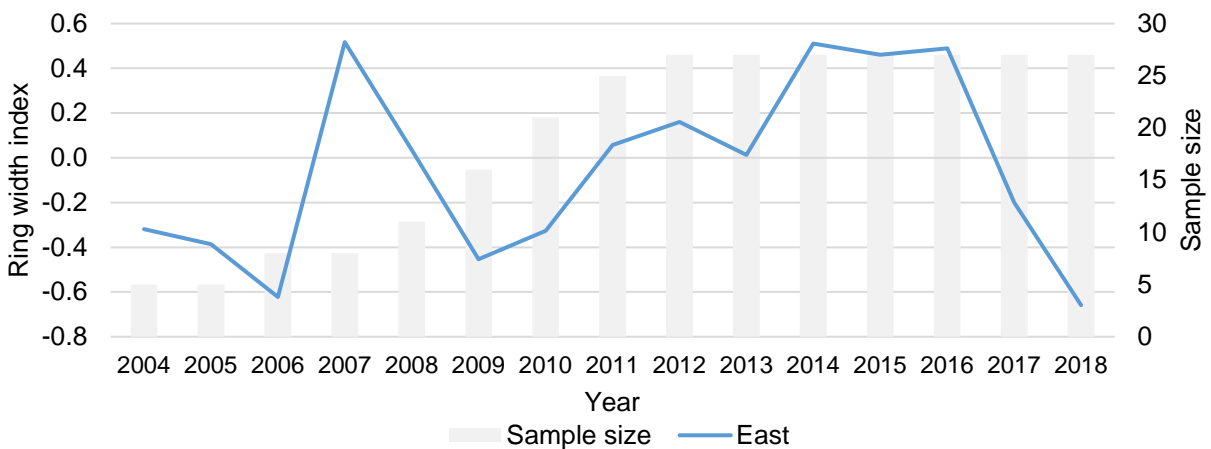


Figure 4-11: Growth chronologies of *H. tenuifolium* at the Sani Pass-lower study site. Ring width index indicates z-scores.

Predominantly positive mean correlations ( $p < 0.05$ ) existed among the growth ring chronologies of different and/ or the same *Helichrysum* species at different elevations and/ or aspects (see Appendix iii). Strong mean correlations exist between two *H. trilineatum* from different aspects (north north west and south south east) at the Kotisephola Pass study site ( $r = 0.7$ ,  $p < 0.05$ ) (see Appendix iii). A strong negative mean correlation existed between same species (*H. trilineatum*) growing on the northern and east south east aspect at different elevations (Sani Pass-upper and Kotisephola Pass study sites) ( $r = -0.8$ ,  $p < 0.05$ ) (see Appendix iii). The greatest mean correlation exists between different species (*H. trilineatum* and *H. witbergense*) that were sampled from different aspects (south west and east) and different elevations (Sani Pass-lower and Kotisephola Pass study sites) ( $r = 0.8$ ,  $p < 0.05$ ) (see Appendix). On the contrary, a negative correlation exists between different species (*H. witbergense* and *H. trilineatum*) sampled from different elevations (Sani Pass-lower and Kotisephola Pass study sites) and different aspects (west south west and east) ( $r = -0.4$ ,  $p < 0.05$ ) (see Appendix iii).

#### 4.2.3.3 Growth correlation coefficients

There was a significant positive correlation ( $p < 0.05$ ) between growth ring widths of same species of *Helichrysum* (different *H. trilineatum* samples, not the same individuals) at the same elevation ( $r = 1.0$ ,  $p < 0.05$ ) (Table 4-6) for all species and elevations. Correlation between growth ring chronologies of different *Helichrysum* at the same elevation shows that *H. trilineatum* and *H. witbergense* (at Kotisephola Pass study site) growth ring widths have an inverse relationship with each other ( $r = -0.2$ ,  $p < 0.05$ ) (Table 4-6). Conversely, at the Sani Pass-lower study site, growth ring chronologies of *H. trilineatum* and *H. tenuifolium* have a positive mean correlation with each other ( $r = 0.7$ ,  $p < 0.05$ ) (Table 4-6).

Table 4-6: Pearson correlation coefficients of *Helichrysum* growth chronologies over a 11-year period from 2007 to 2018. Significant level of  $p < 0.05$ .

	KHW	KHTr	SUHTr	SLHTe	SLHTr
KHW	1.0				
KHTr	-0.2	1.0			
SUHTr	0	-0.4	1.0		
SLHTe	0	-0.1	0.4	1.0	
SLHTr	-0.1	-0.1	0.5	0.7	1.0

\*\*Where KHTr: Kotisephola Pass study site *H. trilineatum*, KHW: Kotisephola Pass study site *H. witbergense*, SUHTr: Sani Pass-upper study site *H. trilineatum*, SLHTr: Sani Pass-lower study site *H. trilineatum* and SLHTe: Sani Pass-lower study site *H. tenuifolium*.

A strong correlation exists between *H. trilineatum* and *H. witbergense* were those sampled at Kotisephola Pass study site from two aspects (east and south south west) ( $r = 0.5$ ,  $p < 0.05$ ) (see Appendix iii). A strong correlation exists between the same species (*H. trilineatum*) were those sampled from different elevations (Sani Pass-upper and Kotisephola Pass study sites), and different aspects (west south west and south south east) ( $r = 0.8$ ,  $p < 0.05$ ) (see Appendix iii). The strongest correlation between the same species (*H. trilineatum*) were those sampled from different elevations (Sani Pass-upper and Kotisephola Pass study sites), and on the same aspect (west) ( $r = 0.6$ ,  $p < 0.05$ ) (see Appendix iii). A significant negative correlation exists between *H. trilineatum* sampled from the east south eastern aspect at Kotisephola Pass and *H. trilineatum* sampled from the northern aspect at Sani Pass-upper study site ( $r = -0.7$ ,  $p < 0.05$ ) (see Appendix iii).



#### 4.2.4 Radiocarbon dating

Calibration with the SH  $^{14}\text{C}$  dataset provided two to seven potential calibrated dates for each sample (Table 4-7). It is possible to eliminate improbable dates by considering that the core of the sample must be relatively older than the outer parts (Robertson *et al.*, 2006). For sample T1, the core sample T1.2 (ring) had a  $^{14}\text{C}$  value of  $129.6 \pm 4.9$  pMC (Percent Modern Carbon), which corresponds to a calibrated radiocarbon date of AD 1962, 1963, 1976, 1982 or 1983 (Table 4-7). Radiocarbon date AD 1976 is consistent with the ring count of 42 years (considering the year it was harvested), the AD 1962, 1963, 1982 and 1983 dates can therefore be eliminated. The date of the half-way ring sample, T1.1 (ring 26), which had a  $^{14}\text{C}$  value of  $110.7 \pm 0.6$  pMC must be younger than the core sample (Table 4-7). For this reason, AD 1958 should be rejected for the Sani Pass-upper sample, and the date chosen for the sample would be AD 1996, 1999 or 2000. Taking into consideration the ring count of 19 and the year it was felled, the AD 1996 and 2000 were eliminated. Within the errors of radiocarbon dating, the rings of the sample appear to be essentially annual in nature and correspond well to the ring counts. The bold dates in Table 4-7 indicate the chosen date that corresponds to the ring count, and the other dates indicate the dates that were rejected as described above. Samples T9, T13 and T14 only had one sample that were radiocarbon dated. A reason for this includes not enough sample were available from the sampled stem disc when it was cut, as rings were too small and could not be cut accurately or insufficient sample remained available after the AMS radiocarbon dating preparation process. Two of the samples (AW7 and E5, marked in red) were the only samples where the ring count (estimated age) did not match the calibrated AMS date, which means that the ring count was 92% accurate in estimating the ages of the samples (Figure 4-12).

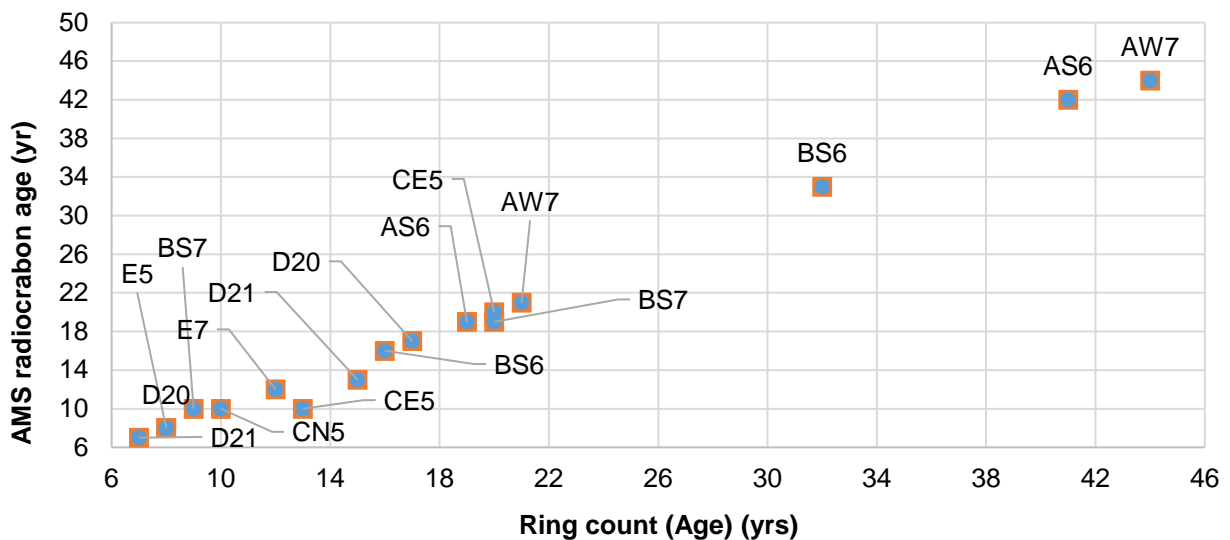


Figure 4-12: AMS radiocarbon age versus ring count of *Helichrysum* samples.

Table 4-7: Radiocarbon dates and deduced mean number of rings formed per year. Where  $\delta^{13}\text{C}$  = a measurement that indicates the source of the C in the sample, pMC (percent Modern Carbon) - the sample age in standard radiocarbon terms.

Sample name	Lab #	$\delta^{13}\text{C}$	pMC	AMS radiocarbon calibrated year (yr AD)	Predicted year	Ring count (Age) (yr)	AMS radiocarbon dated age (yr)
<b>Kotisephola Pass study site</b>							
<i>H. trilineatum</i>							
AS6	T1.1	-27.8	110.7 ± 0.6	1958, 1996, <b>1999</b> , 2000	1999	20	19
AS6	T1.2	-27.8	129.6 ± 4.9	1962, 1963, <b>1976</b> , 1982, 1983	1976	41	42
AW7	T2.1	-28.6	109.8 ± 1.3	1958, 1996, <b>1997</b> , 2003	1997	21	21
AW7	T2.2	-28.6	150.1 ± 1.1	1970, <b>1972</b>	1974	44	44
<i>H. witbergense</i>							
BS6	T3.1	-27.2	109.3 ± 0.6	1958, 1999, <b>2002</b> , 2003	2002	16	16
BS6	T3.2	-27.3	121.9 ± 0.6	1962, 1963, 1983, <b>1985</b>	1985	32	33
BS7	T4.1	-29.2	105.2 ± 0.6	1957, <b>2008</b> , 2011	2008	9	10
BS7	T4.2	-29.2	110.7 ± 0.4	1958, 1996, 1997, <b>1999</b> , 2000	1999	19	19
<b>Sani Pass-upper study site</b>							
<i>H. trilineatum</i>							
CN5	T9.1	-29.2	104.5 ± 0.6	1956, 1957, <b>2008</b> , 2009, 2010, 2011	2008	13	10
CE5	T10.1	-27.0	104.7 ± 0.6	1956, 1957, <b>2008</b> , 2009, 2010, 2011	2008	10	10
CE5	T10.2	-28.1	110.2 ± 0.5	1958, 1997, <b>1998</b> , 2000, 2001	1998	20	20
<b>Sani Pass-lower study site</b>							
<i>H. tenuifolium</i>							
D20	T11.1	-28.6	106.2 ± 0.6	1957, 1958, 2006, <b>2010</b>	2010	8	8
D20	T11.2	-30.0	108.1 ± 0.9	1957, 1958, <b>2001</b> , 2005, 2006	2001	17	17
D21	T12.1	-28.5	105.3 ± 2	1956, 1957, 1958, 2004, 2005, <b>2011</b>	2011	7	7
D21	T12.2	-28.6	108.3 ± 1.1	1957, 1958, 2000, <b>2005</b> , 2006	2005	15	13
<i>H. trilineatum</i>							
E5	T13.2	-29.0	105.7 ± 0.6	1957, 2007, <b>2011</b>	2010	8	8
E7	T14.2	-29.1	107.1 ± 0.4	1957, 1958, 2004, <b>2006</b> , 2007	2006	12	12

### 4.3 Distribution and abundance

#### 4.3.1 Kotisephola Pass study site

*H. trilineatum* and *H. witbergense*, along with other cold-adapted species, were observed at the Kotisephola Pass study site ( $\pm 3\ 282$  to  $3\ 332$  m a.s.l.). *H. witbergense* occur predominantly on the southern aspect, in cool, moist areas close to rock outcrops, 0 - 4 m from rock outcrop (Figure 4-13, Plate 4-3). *H. trilineatum* was observed at the rock outcrop and along the slope, 0 – 10 m and beyond, on the south and western aspects (Figure 4-13, Plate 4-2). Other shrubs, such as *Erica*, *Chrysocoma ciliata*, a variety of grasses, succulents and lichens, were observed on the warmer northern and eastern aspects (Figure 4-13, Plate 4-3). No *H. tenuifolium* was observed at this site. A total of 951 individuals (*Helichrysum* and other plant species) were counted at this site (Appendix vi). As for aerial cover, 69% of the total amount counted were accounted for by *H. trilineatum*, 8% *H. witbergense* and 22% were other shrubs and plant species (including *Erica* and *Chrysocoma ciliata*) (Figure 4-13 and see Appendix vi). *H. trilineatum* (65%) are more abundant on the western aspect, whereas *H. witbergense* are more abundant on the southern aspect (95%) (Appendix vi). Western aspect shrub abundance is the most even (0.6) and diverse (0.7) according to the Shannon-Weiner Diversity and Pielou Index (Appendix vi). Other shrubs and plants that were located on the western aspect had the greatest standard deviation (28.6) of aerial cover among the shrubs and plants located at this site (Appendix vi).

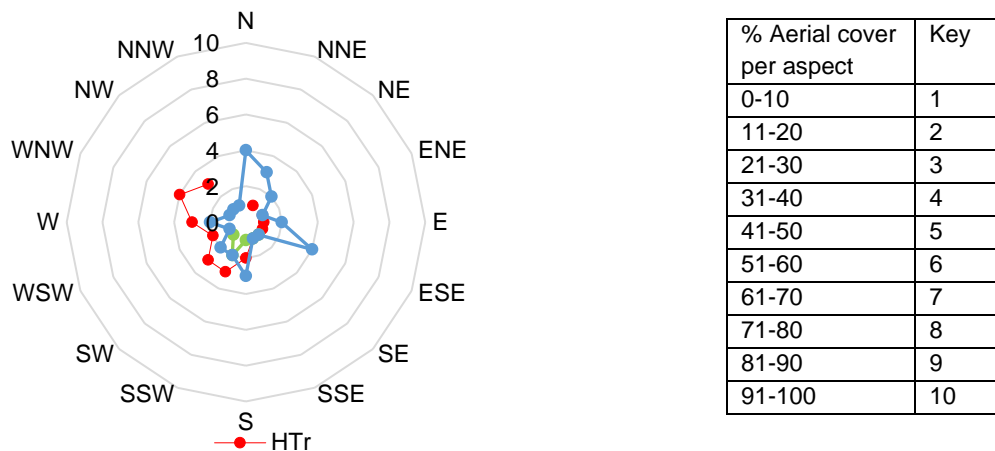


Figure 4-13: Aerial cover percentage and preferred aspect for growth of *Helichrysum* growing at the Kotisephola Pass study site.

\*\*Where 1 refers to less than 10% aerial cover, 2 refers to between than 11-20% aerial cover, 3 to between than 21-30% aerial cover, 4 to between than 31-40% aerial cover, 5 to between than 41-50% aerial cover, 6 to between than 51-60% aerial cover, 7 to between than 61-70% aerial cover, 8 to between than 71-80% aerial cover, 9 to between than 81-90% aerial cover and 10 to between than 91-100% aerial cover.

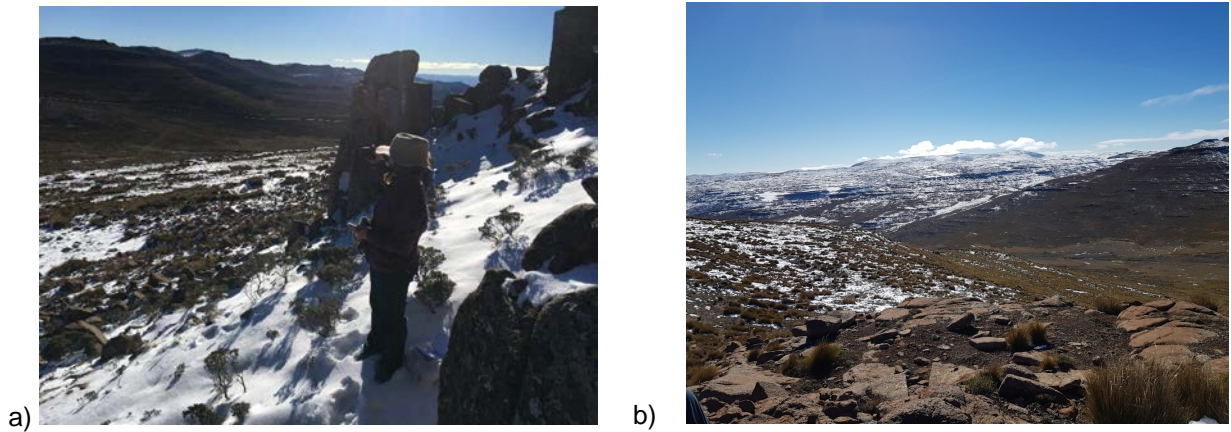


Plate 4-3: a) Photograph of the south-western aspect at the Kotisephola Pass study site, with the rock outcrop on the left and *H. witbergense* and *H. trilineatum* in close vicinity. b) Photograph of the eastern aspect at the Kotisephola Pass study site.

#### 4.3.2 Sani Pass-upper study site

Sani Pass-upper study site ( $\pm 2\ 859$  to  $2\ 916$  m a.s.l.) is sparsely vegetated (Plate 4-4). *H. trilineatum* were observed on all aspects (north, east, south and west), but were most abundant on the western aspect of the mountain (57.5%) (Figure 4-14). No other *Helichrysum* was present. Various other shrubs, such as *Erica* and *C. ciliata* and a variety of grasses were observed on all aspects (Figure 4-14). A total of 1 369 shrubs and other plant individuals were counted at this site (Plate 4-4). As for aerial cover, 38% of the total amount were accounted for by *H. trilineatum*, and 62% were other plant species (including *Erica* and *C. ciliata*) (Figure 4-14 and Appendix vi). The southern aspect's shrub abundance is the most even (0.6) and diverse (0.4) according to the Shannon-Weiner Diversity and Pielou Index (Appendix vi). The combination of shrubs and other plant species, excluding *H. trilineatum*, located on the western aspect have the greatest standard deviation (36.2) among all shrubs and plants located at this site (Appendix vi).



Plate 4-4: Photograph of the southern aspect at the Sani Pass-upper study site.

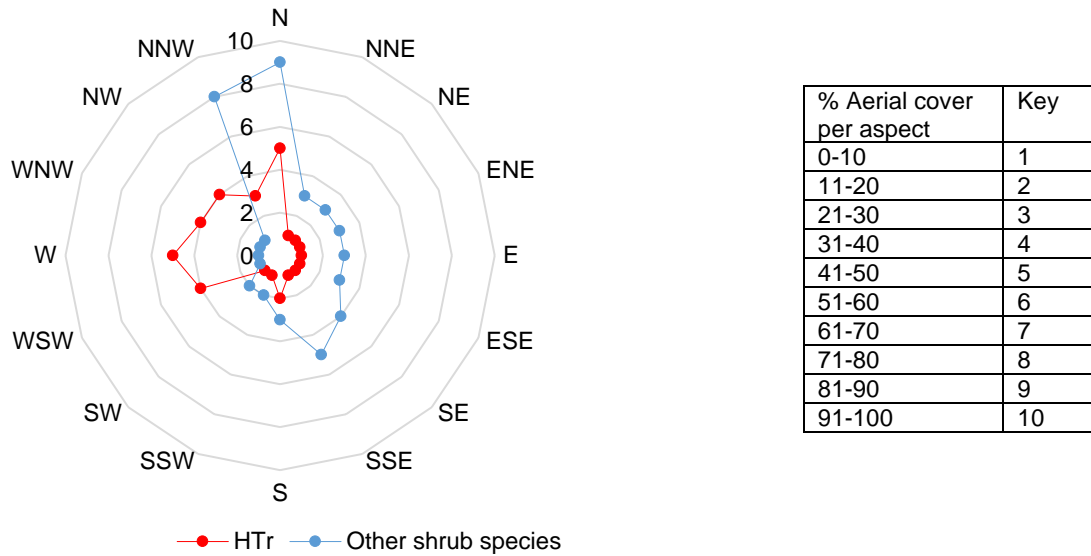


Figure 4-14: Aerial cover percentage and preferred aspect for growth of *Helichrysum* growing at Sani Pass-upper study site.

#### 4.3.3 Sani Pass-lower study site

Sani Pass-lower study site ( $\pm 2\ 514$  to  $2\ 585$  m a.s.l.) is east-facing and located between a gravel road and a gully (Plate 4-5); these features act as protection from fire. *H. trilineatum* and *H. tenuifolium*, a variety of grasses and other shrubs, such as *Euryops tysonii* and *E. evansii* were observed (Plate 4-5). It is mostly rocky and consist of shallow soils. *H. trilineatum* are located throughout the site, while *H. tenuifolium* are only located on the shoulder of the gravel road (Plate 4-5). No *H. witbergense* was observed at this site. A total of 296 individuals and other plant species were counted at this site (Appendix vi). As for aerial cover, 7% of the total amount were accounted for by *H. trilineatum*, 16% by *H. tenuifolium* and 78% by other shrubs and plant species (including *E. tysonii* and *E. evansii*). The site varied in evenness (Pielou Index = 0.3) and had a marginally significant Shannon-Weiner Diversity Index of 0.5 (Appendix vi). The standard deviation among all shrubs and plants at this site was 31.6 (Appendix vi).



a)



b)

Plate 4-5: a) Photograph of the Sani Pass-lower study site located between a gravel road and a gully. b) Photograph of *E. tysonii* and *H. trilineatum* at the Sani Pass-lower study site.

#### 4.4 Climate

##### 4.4.1 Temperature

Past climate simulations are represented by variability in mean, minimum and maximum temperatures. The inconsistency of data accounts for variability in the historical datasets. Mean annual temperature for Sani Top (used for Sani Pass-upper study site) is 6.6°C, for Kotisephola Pass study site 4.8°C and for Sani Pass-lower study site 8.4°C. Figure 4-15 is indicative of cooler and warmer years. Unfortunately, no complete datasets are available for 2002 until 2009 and the incomplete ones cannot be used to accurately represent the mean annual temperatures of the sites and can therefore also not be used as a basis for modelling. Higher mean annual temperatures were recorded in 2011 than in 2010, thereafter a decrease followed for 2012. A gradual increase in mean annual temperatures from 2012 to 2014 indicates that these were possible warmer years. Mean minimum temperature for Sani Top (used for Sani Pass-upper study site) = 0.6°C, for Kotisephola Pass study site = -1.2°C and for Sani Pass-lower study site = 2.4°C (Figure 4-16). As for mean maximum temperature, Sani Top (used for Sani Pass-upper study site) = 11.2°C, for Kotisephola Pass study site = 9.4°C and for Sani Pass-lower study site = 13°C.

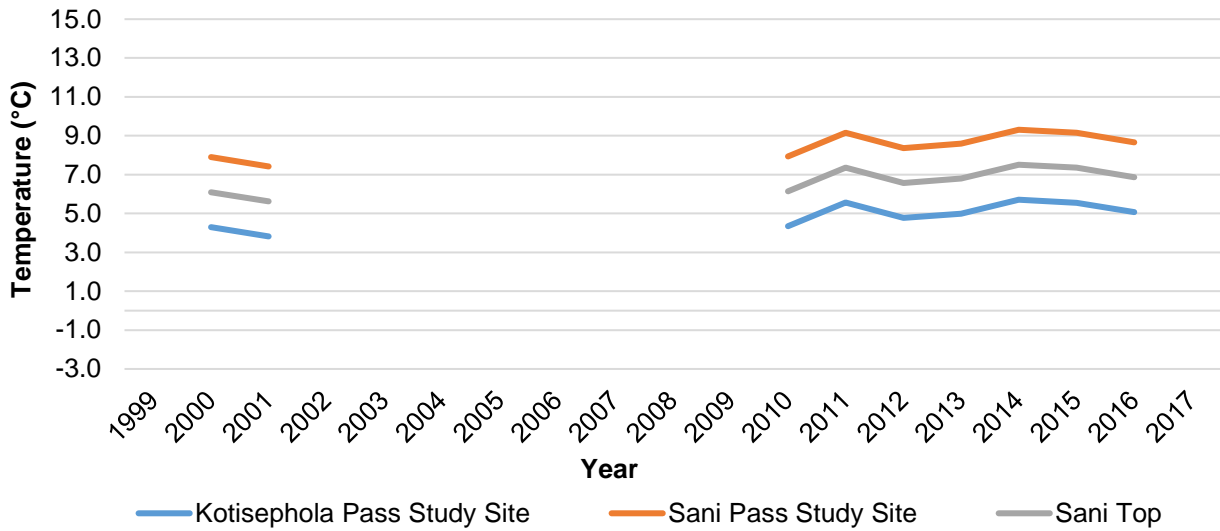


Figure 4-15: Mean annual temperatures for Sani Top, Sani Pass-lower and Kotisephola Pass study site.

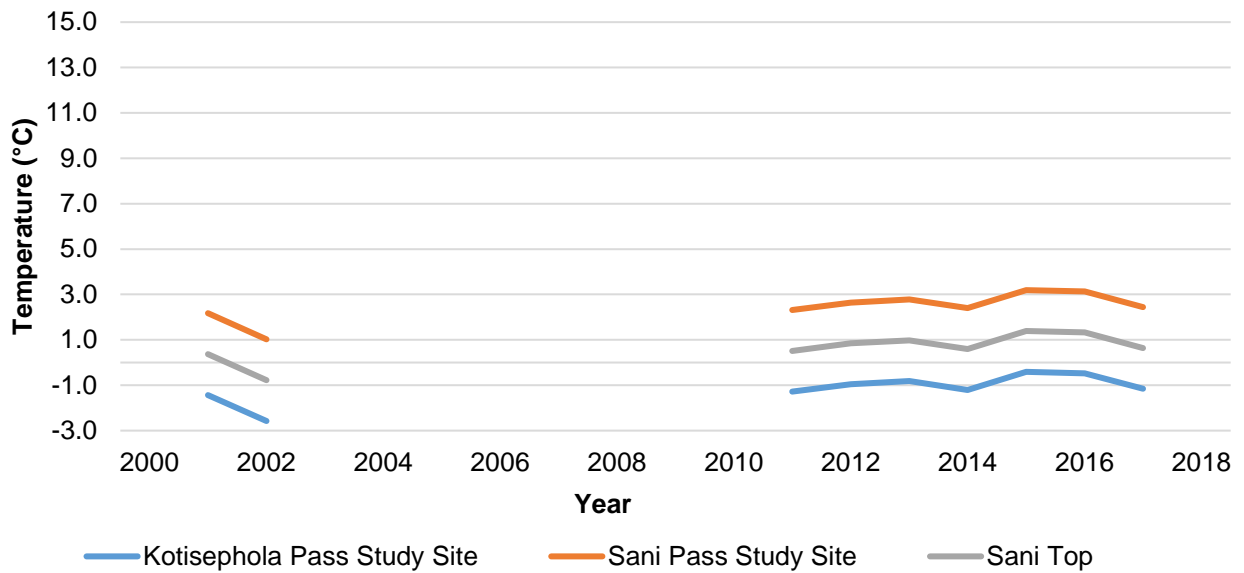


Figure 4-16: Mean minimum temperatures for Sani Top, Sani Pass-lower and Kotisephola Pass study sites.

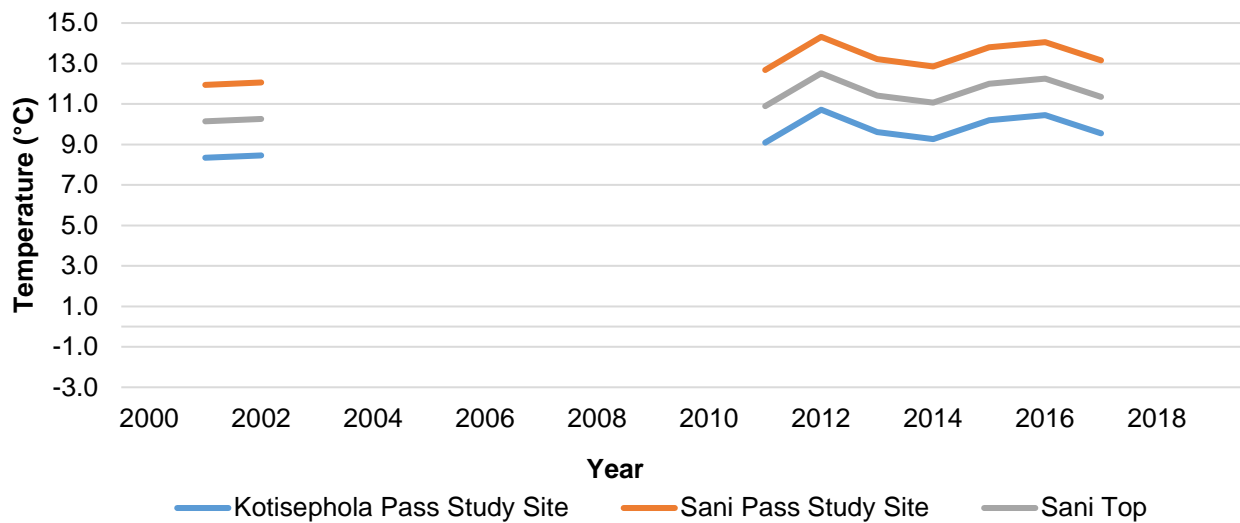


Figure 4-17: Mean maximum temperatures for Sani Top, Sani Pass-lower and Kotisephola Pass study sites.

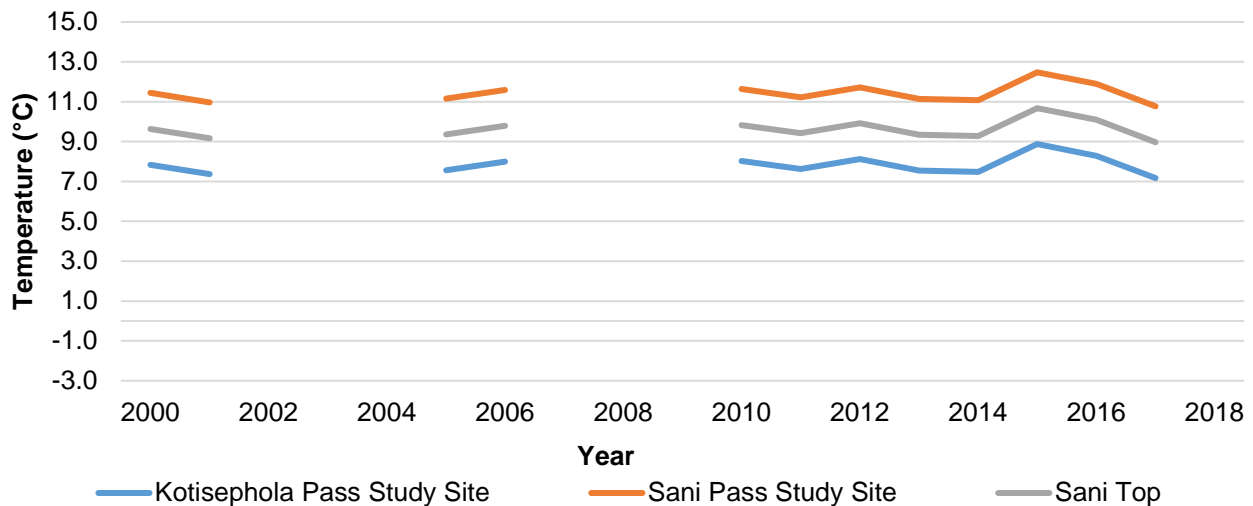


Figure 4-18: Mean annual growing season temperatures for Sani Top, Sani Pass-lower and Kotisephola Pass study site.

The growing season of the *Helichrysum* shrubs may differ in length as a result of air temperature changes and for this reason the period between October and March was studied by comparing combinations of monthly data. Warmer temperatures may create more favorable conditions and increase photosynthesis rate. In contrast, lower temperatures may limit growth and shrubs may enter a dormant state. Mean annual growing season temperature for Sani Top (used for Sani Pass-upper study site) is 9.6°C, for Kotisephola Pass study site 7.8°C and for Sani Pass-lower study site 11.4°C. Figure 4-15 is indicative of cooler and warmer growing seasons. There was a decrease in mean annual temperatures from 2000 to 2001. Unfortunately, no complete datasets are available for 2002 to 2004 and 2007 to 2009, and the incomplete ones cannot be used to accurately represent the mean annual growing season temperatures of the sites. The continuous data between 2010



and 2017 indicates that 2012 and 2015 had warmer growing seasons. This means that the October to December months of 2011 and 2014 significantly contributed to the high growing season temperatures of the 2012 and 2015 growing seasons.

#### 4.4.2 Rainfall

Mean annual precipitation at the three weather stations in the vicinity of the study sites are as follow: Giant’s Castle - 658 mm, Mokhotlong - 567 mm and Shaleburn - 1027 mm. Unfortunately, the datasets from the weather stations has incomplete data and for this reason a composite dataset was created. Figure 4-19 indicates wetter and drier years between 1992 and 2019. From this, it is evident that 1992 was particularly dry (488 mm), compared to the following years when annual rainfall was between 690 mm and 940 mm. A wettest year was in 2000 (1118 mm), followed by drier years in 2002 (666 mm) and 2003 (685 mm). The most recent years (2017 to 2019) seem to have been notably dry (Figure 4-19).

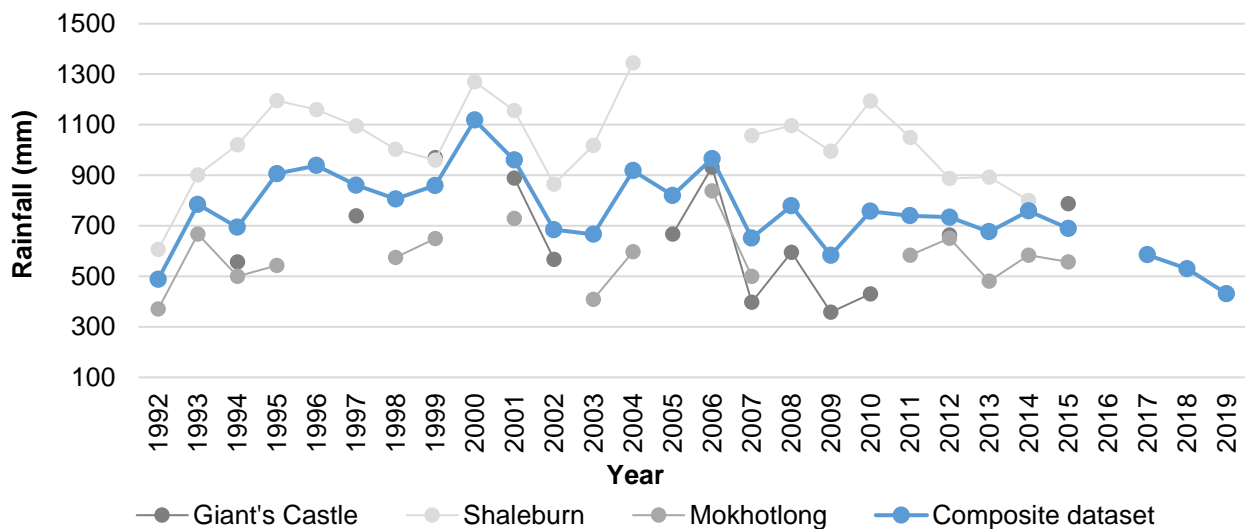


Figure 4-19: Total annual rainfall for Giant's Castle, Shaleburn, Mokhotlong and a composite of these three sites.

The mean total growing season precipitation at Giant’s Castle is 560 mm, at Mokhotlong is 487 mm and at Shaleburn is 878 mm (Figure 4-20). Unfortunately, the datasets from the weather stations has incomplete data and for this reason a composite dataset was created from available data. Figure 4-20 indicates wetter and drier growing seasons between 1992 and 2018, with the 1991-1992 growing season being particularly dry (446 mm) and well below the mean growing season rainfall (661 mm) calculated for the composite dataset. In contrast the following growing season, 1992-

1993, was much wetter (865 mm). The growing season of 1989-1999 was wetter (1023 mm), while that for 2017-2018 was drier (307 mm) (Figure 4-20).

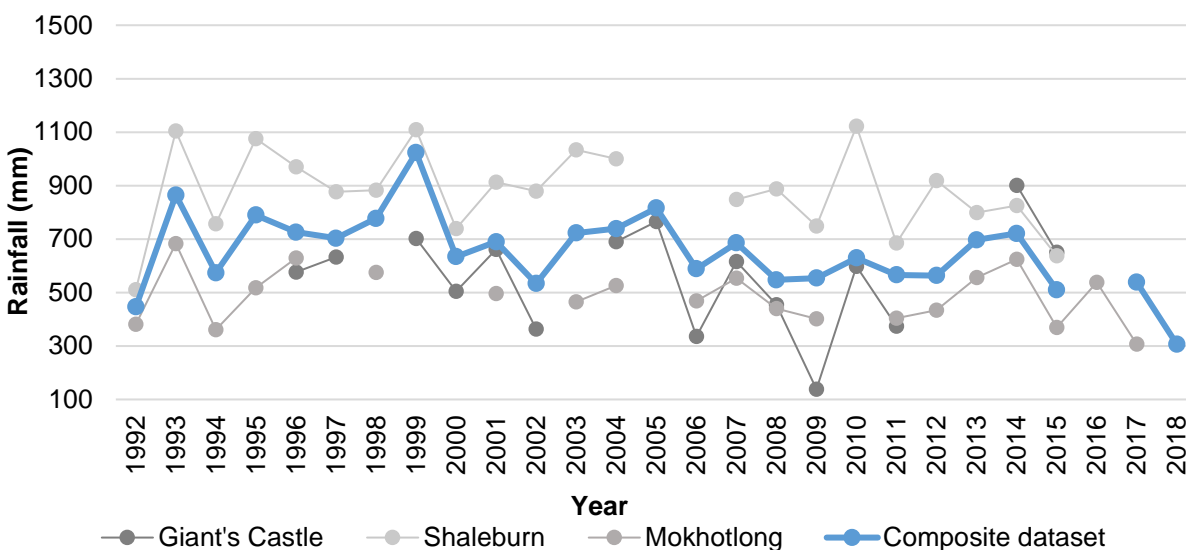


Figure 4-20: Total growing season rainfall for Giant’s Castle, Shaleburn, Mokhotlong and a composite of these three sites.

#### 4.5 Climate-growth relationship

##### 4.5.1 Pearson correlation coefficients of *Helichrysum* growth and temperature

Table 4-8: Pearson correlation analysis results of *Helichrysum* growth and seasonal temperature.

	KHTr	KHW	SUHTr	SLHTe	SLHTr
November – December Mean Temperature	-0.4	0.4	0.5	0.5	-0.1
December – January Mean Temperature	-0.2	0.4	0.4	0.6	0.4
November – January Mean Temperature	-0.2	0.4	0.4	0.6	0.1
October – March Mean Temperature	-0.2	0.5	0.5	0.5	0.0
November – February Mean Temperature	-0.2	0.5	0.5	0.6	0.2
December – March Mean Temperature	0.0	0.6	0.7	0.6	0.4
January – February Mean Temperature	0.4	0.7	0.6	0.5	0.6

*Helichrysum* shrub ring width was positively correlated with the growing season mean temperatures (Table 4-8). A positive correlation exist between *H. witbergense* (from the Kotisephola Pass study site) growth and January - February mean temperature ( $r = 0.7$ ,  $p < 0.05$ ) (Table 4-8). *H. trilineatum* (from the Kotisephola study site) growth also had a positive correlation with January and February’s mean temperature ( $r = 0.6$ ,  $p < 0.05$ ) (Table 4-8). Growth of *H. trilineatum* (from the Kotisephola study site) was, however, negatively correlated with the mean temperatures for the October to March period ( $r = -0.4$ ,  $p < 0.05$ ) (Table 4-8). The shrub ring width of the sampled *H. trilineatum* at the

Middle study site was positively correlated with all the growing season monthly temperatures (Table 4-8), with the correlation between shrub ring width and December to March's mean temperature being the strongest ( $r = 0.7$ ,  $p < 0.05$ ). The growth of the sampled *H. trilineatum* at the Sani Pass-lower study site was positively correlated with most of the growing season month's mean temperatures, except for the November to December period weak negative correlation ( $r = -0.1$ ,  $p < 0.05$ ) (Table 4-8). *H. tenuifolium* growth and growing season mean temperature are all positively correlated ( $p < 0.05$ ) (Table 4-8).

#### 4.5.2 Pearson correlation coefficients of *Helichrysum* growth and rainfall

Table 4-9: Pearson correlation analysis results of *Helichrysum* growth and seasonal rainfall.

	KHTr	KHW	SUHTr	SLHTe	SLHTr
November - December	-0.3	-0.1	-0.4	-0.3	-0.3
December - January	0.3	-0.1	-0.2	-0.3	-0.2
November - January	0.2	0.0	0.2	0.2	0.0
October - March	0.1	-0.1	0.0	-0.1	-0.2
November - February	-0.2	-0.2	-0.3	0.2	-0.2
December - March	0.0	-0.2	-0.2	0.0	-0.3
January - February	-0.1	-0.3	-0.2	0.3	-0.1

No significant correlation exists between any of the *Helichrysum* species and any combination of the growing season monthly total rainfall.

#### 4.5.3 Multiple regression analysis

Multiple correlation tests indicated significant results, with high coefficients of determination ( $R^2$ ) for the following combinations of variables for the 1999 to 2018 period (see Appendix v): mean November and December temperature and total November and December rainfall for the *H. trilineatum* at the Kotisephola Pass study site at all aspects ( $R^2 = 0.66$ ); mean January and February temperature and total January and February rainfall for the *H. witbergense* at the Kotisephola Pass study site at the SW, SSW and WSW aspects ( $R^2 = 0.51$ ); mean December to March as well as November to February temperature and total December to March and November to February rainfall for the *H. trilineatum* at the Sani Pass-upper study site at all aspects ( $R^2 = 0.77$ ); mean December to March temperature and total December to March rainfall for the *H. tenuifolium* at the Sani Pass-lower study site eastern aspect ( $R^2 = 0.68$ ); January and February temperature and total January and February rainfall for *H. trilineatum* at the Sani Pass-lower study site eastern

aspect ( $R^2 = 0.82$ ). All the other combinations of variables resulted in non-significant regressions (see Appendix v).

#### 4.6 Summary

In conclusion, age determination was conducted for 55 *H. trilineatum*, nine *H. witbergense* and 27 *H. tenuifolium*, with annual growth rings detected and measured on samples with shrubs ranging in age from three to 45 years old. Cross-dating and standardisation was attempted, and master chronologies were produced for each site and species. However, the weak correlations of the site indicate that the shrubs are not responding to environmental conditions and may call into question the reliability of the cross-dating results and master chronology produced. Correlation analysis and multiple regression analysis was conducted between the master chronology, local climate variables, elevation, and aspect. Correlation analyses revealed a lack of significant relationships between the growth of *Helichrysum* and rainfall data.

# CHAPTER FIVE

## Discussion

The primary aim of this study is to investigate the growth patterns of *Helichrysum tenuifolium*, *H. trilineatum* and *H. witbergense* along an elevation gradient in the DAC, and their potential response to climate. The need for such research is highlighted through the knowledge gaps identified in Chapter 2 (Literature Review). The results of the growth pattern analyses of shrubs sampled from three study sites at Kotisephola Pass and Sani Pass-upper and lower are presented in Chapter 4 (Results). Chapter 4 develops growth ring chronologies for each species and site, and explores growth patterns between species located at the same and different elevations. This is followed by a regional synthesis in which the growth ring chronologies for the three sites are compared to explore the influence of seasonality, possible microclimates, elevation, and topographical differences. Shrub distribution and abundance is compared between sites to understand the occurrence of possible microclimatic conditions. The outcomes from this study are also compared with the climatological, dendrochronological, and ecological information for Lesotho, as outlined in Chapter 2, and with growth ring chronologies from other shrubs and trees from elsewhere in southern Africa and further afield. Finally, the prospects for future work are explored, based on the successes and limitations experienced in this study.

### 5.1 Growth patterns

An anatomical description of microscopic features of the growth rings of three *Helichrysum* species was undertaken. Cross-dating was successful for all three species across all sites and between individuals at the same elevation and aspects resulting in similar growth trends. Thus, growth of *Helichrysum* species can be linked to the annual calendar dates and seasonality. This was confirmed by the AMS radiocarbon dating results, since most of the expected ages corresponded to the same calendar dates, while some differed by a year or two, which can be attributed to human error in terms of ring count or cutting. Hilliard (1977) confirmed that the *Helichrysum* shrub species are perennial and, therefore, accurate dating and measuring of the shrub species' growth rings could be performed. Similar growth patterns between *Helichrysum* species in a region that have definite inter-annual climate variation, may indicate that *Helichrysum* species prefer certain microclimatic conditions (Hughes, 2002; Carrer and Urbinati, 2004).

The annual increments of *Helichrysum tenuifolium*, *H. trilineatum* and *H. witbergense* are comparable to those of other species growing in high alpine and arctic environments (Hallinger *et al.*, 2010; Owczarek, 2010; Lu *et al.*, 2016). In general, *Helichrysum* are slow-growing species. For *Helichrysum*, shrub age of more than 50 years is significant for slow-growing species and for sites

where overgrazing and fuelwood harvesting is frequent. The average age of all the sampled *Helichrysum* is 18 years, with the minimum age of three years and the maximum of 54 years. Growth ring widths vary between 0.3 mm and 2.4 mm, with an average shrub growth ring width of 0.9 mm. At higher elevations, there was a greater abundance of older shrubs than at lower elevations. Older shrubs tend to have smaller growth ring widths than younger shrubs. Contributing factors to these growth patterns are the low temperatures and a shorter growing season at high elevations which may lead to shrubs showing low growth rates as a way to adapt to their environment (Gao *et al.*, 2013). Furthermore, environmental differences that are associated with elevation gradients may affect shrub growth. For instance, rocky and barren (shallow) soil at these high elevation sites (Gao *et al.*, 2013) may contribute to unfavourable growing conditions and result in the observed differences in radial growth between the sampled *Helichrysum*. Another factor that may influence the different growth patterns is aspect and the role of solar inclination which may influence the growing season as some regions may receive sun for longer periods than other. In order to account for this standardised ring width chronologies were created.

The stem discs of the sampled *Helichrysum tenuifolium*, *H. trilineatum* and *H. witbergense* have an average diameter of 21.6 mm. The greatest average diameter (40.2 mm) was measured from a *H. tenuifolium*, and the smallest average diameter (11.6 mm) from a *H. trilineatum*. It is interesting to note that age and diameter is positively correlated for all studied *Helichrysum* at all three study sites. Therefore, an older shrub will have a greater diameter.

## 5.2 Growth chronologies

The establishment of the growth ring chronologies was carried out with relatively high inter-series correlations. The success of cross dating between individuals of the same species proves that a similar variation in their growth pattern is not a coincidence (Stahle, 1999), and that an external factor influences in the same way, tree growth corresponding to a periodical wood formation (Eckstein *et al.*, 1981; Worbes, 1995). Correlation analyses ( $p < 0.05$ ) among the same *Helichrysum* at the same elevation confirmed that growth changes in one *Helichrysum* may reflect growth changes of another individual of the same species at the same elevation. The mean correlation analysis between the growth ring chronologies of different *Helichrysum* at the same elevation concludes that the relationship is different for different shrub species and different elevations. An inverse relationship existed between *H. trilineatum* and *H. witbergense* growths located at the Kotisephola Pass study site, whereas *H. trilineatum* and *H. tenuifolium* growths at the Sani Pass study site had a positive mean correlation. Positive mean correlations existed among the growth ring chronologies of the same *Helichrysum* species at different elevations suggesting that growth changes in one *H. trilineatum* reflects growth changes in other *H. trilineatum* at different elevations.

The annual nature of growth rings in *H. tenuifolium*, *H. trilineatum* and *H. witbergense* and the precision of using radiocarbon dating as cross-dating method implies potential for shrub dendrochronological studies in mountain environments in southern Africa.

Correlation analyses among different species, aspects and elevations indicated that growth changes in one shrub species may also reflect growth changes in different species located at different elevations, but on the same aspects. Strong positive mean correlations suggest that growth changes in a specific species located at a certain elevation may also be reflected by the same species located at the same aspect and different elevations. Furthermore, growth changes in a specific species located at a certain elevation may also be reflected by the same species shrubs located at different aspects at the same elevation.

#### 5.4 Distribution and abundance

*H. witbergense* grow predominantly on the southern aspect, in cool, moist areas close to rock outcrops (0 – 4 m from rocks) at Kotisephola Pass mountain ( $\pm$  3 282 to 3 332 m a.s.l.). *H. trilineatum* can be found on the southern and western aspects of Kotisephola Pass ( $\pm$  3 282 to 3 332 m a.s.l.), covering the area from the rock outcrop up to 10 m and beyond downslope. The cool, moist regions closest to the rock outcrop can be regarded as a possible microhabitat, as it consists of site-specific conditions, in terms of soil type, soil moisture, wind, and other specific microclimatic conditions due to the protection the rock outcrop may offer. Shrubs, a variety of grasses, succulents and lichens were found on the warmer northern and eastern aspects. The presence of these types of plants indicate a warmer and less moist environment, and the presence of karroid shrubs and sparse vegetation on the eastern aspect may be indicative of overgrazing practices and extensive harvesting. At the Sani Pass-upper study site ( $\pm$  2 859 to 2 916 m a.s.l.), *H. trilineatum* were found on all aspects (north, east, south, and west), but were most abundant on the western aspect of the slope, below the rock outcrop. This study site was sparsely vegetated. The DAC is located within the Grassland Biome, therefore a high number of grass species and grassland forbs such as *Merxmuellera*, *Festuca*, *Danthonia* and *Pentaschistis* species was observed.

*H. trilineatum* and *H. tenuifolium*, a variety of *Merxmuellera*, *Festuca*, *Danthonia* and *Pentaschistis* species and other shrubs such as *E. tysonii* and *E. evansii* were found on the east-facing aspect at the Sani Pass-lower study site ( $\pm$  2 514 to 2 585 m a.s.l.). The *H. trilineatum* were observed in all quadrants, while *H. tenuifolium* was only on the one edge (the side of the gravel road). This site can be regarded as a possible microhabitat, as it consists of site-specific conditions, in terms of soil,

vegetation, wind, and other specific climatic conditions that may be the result of the protective barrier the road and gully forms around the study site. This site is an obvious fire refugium.

A recommendation would be to incorporate temperature buttons, microclimate analyses, soil analyses and diversity indices to develop an in-depth study in terms of abundance and distribution of the three *Helichrysum* shrubs.

## 5.5 Climate

Temperature data were only available for Sani Top (Sani Pass-upper study site). This dataset was used as a baseline and the international lapse rate ( $0.6^{\circ}\text{C}$  per  $100\text{m}^{-1}$ ) was used to extrapolate temperature datasets for both the Kotisephola Pass and Sani Pass-lower study sites. Sani Top data were used as an indication of the climate at the Sani Pass-lower study site as it is located at the same elevation. Mean monthly temperature graphs representing monthly temperature ranges show that air temperature is cool to mild in summer, but cold in winter. Temperatures for the Sani Top and Sani Pass-lower study site is similar to the measured mean daily temperature of  $9.7^{\circ}\text{C}$  by Nel and Sumner (2008).

Precipitation data for three weather stations were obtained for the 20-year period (1994 - 2014). The weather stations are located at Shaleburn (1614 m a.s.l.) and Giants Castle (1759 m a.s.l.) in South Africa, and Mokhotlong (2209 m a.s.l.) in Lesotho. Shaleburn and Giants Castle are both within the lower-montane thermal zone, while Mokhotlong is in the upper-montane thermal zone. These weather station datasets were chosen as they are representative of two thermal zones. The higher-based station (i.e. Mokhotlong) has the lowest mean total annual precipitation. This is a well-known phenomenon of mountain climates. The drought years (1992/3, 2003/4 and 2006/7) correspond to the findings by Malherbe *et al.* (2015). Malherbe *et al.* (2015) documented the dry periods as follow: 1926–1933, 1946–1952, 1965–1973, 1983–1994 and 2003–2007.

The total annual precipitation and total annual growing season precipitation composite datasets show a decreasing trend between 1992 – 2019 (Figure 4-19 and Figure 4-20). The 2016 Vulnerability Assessment of Lesotho report confirmed that there is going to be increased precipitation during autumn and winter seasons, while summer and spring seasons will experience decreased precipitation. According to Archer *et al.* (2018), there is uncertainty in the minority projections indicating rainfall increases over specific regions or insignificant decreases. However, the largest rainfall decreases are projected for the southern parts of South Africa, which includes Lesotho (Archer *et al.*, 2018). These trends correspond to projections of future climate change for the months of December, January and February (Engelbrecht *et al.* 2009; Engelbrecht *et al.*; 2011).



Although a detailed analysis of observed and simulated trends in climate over eastern Lesotho falls beyond the scope of this study, it was possible to correlate the wet and dry periods with shrub growth.

## 5.6 Climate-growth relationship

Correlation analyses indicated strong relationships between shrub growth and a range of local climate variables. The phenology of *H. trilineatum*, *H. tenuifolium* and *H. witbergense* is assumed to be firmly synchronized with seasonality. Flowering began to occur during the spring (October to November). This seasonality in growth suggests that radial growth is restricted to the summer rainfall season and would support the annual nature of growth rings. Results indicated a positive correlation between shrub growth and precipitation during the rainy season, suggesting that both temperature and rainfall may influence shrub growth. Significant correlation with growth and rainfall during the November to December may be attributed to the start of the rainy season.

In this study all *Helichrysum* individuals at all study sites were positively correlated with one if not all, summer month (December to February) temperatures (Table 4-8). High summer temperatures are often described as vital for plant growth as it enhances photosynthetic rate (Chen *et al.*, 2011). However, increased summer temperatures do not necessarily initiate wider ring widths. Wielgolaski (1966) noted that transpiration increases when temperature rises, however, the plants' stomata may close if the plant lacks water. This lowers plant assimilation during the day, consequently affecting both growth and respiration. Weak correlations exist between growth and rainfall from October to November (Table 4-9). Ring widths of most of the sampled *Helichrysum* were positively correlated with mean growing season temperatures (Table 4-8). The strongest correlation between shrub growth and temperature existed between *H. witbergense* growth and mean temperature in January-February and for *H. trilineatum* from the Sani Pass-upper study site and mean December to March temperatures (Table 4-8).

An early and warm spring onset can prolong the growing season by activating the cambium earlier and it may lead to increased earlywood formation (Chen *et al.*, 2011; Lehejček, 2015). In dry areas, shrub growth is mostly dependent on the balance between drought stress and the early onset of cambial activity by warm temperatures (Gao *et al.*, 2013). The negative correlation between *Helichrysum* growth and November / December temperatures (Table 4-8) may indicate that these shrubs possibly suffered moisture stress in the early growing season. This phenomenon was noted in other studies where different species had a negative correlation between shrub growth and November (May equivalent in the Northern Hemisphere) temperature (Blok *et al.*, 2011; Liang *et al.*, 2011; Gao *et al.*, 2013; Lu *et al.*, 2016). For the reasons discussed above, it can be concluded that *Helichrysum* growth is limited by relatively low summer temperature and low precipitation during

early growing seasons. A suggestion would be to study specifically earlywood and latewood growing patterns for *Helichrysum*.

Significant multiple regression results identified the combination of months during which different shrubs at different elevations prefer specific climatic conditions. *H. trilineatum* from the three different elevations do not prefer the same growing months. At the Kotisephola Pass study site these shrubs prefer the November to December mean temperature and total rainfall, whereas shrubs at the Sani Pass-upper study site prefer a longer period, from December to March, and the shrubs at the Sani Pass-lower study site prefer the January to February mean temperature and total rainfall. Similarly, *H. witbergense* prefer the January to February mean temperature and total rainfall. *H. tenuifolium*, such as the *H. trilineatum* at the Sani Pass-upper study site, prefer December to March mean temperatures and total rainfall.

Along an elevation gradient, the shrub-ring parameter statistics varied between the growth chronologies from different species and different elevations. Despite the differences in elevations, *Helichrysum* shared a similar climate–growth pattern, which was characterised by significant responses to low growing season temperatures and drought periods in the early growing season (November and December). However, climate record limitations have made it difficult to understand decadal changes. For this reason, these results and possible climate reconstructions based on growth rings should be interpreted with caution. In-depth investigations on *Helichrysum* species' response to seasonal climate variability and the role of specific microclimatic conditions on growth required in an effort to improve our understanding of the climate–growth relationships of *Helichrysum* in the Drakensberg Alpine Centre.

## 5.7 Key findings

### **Question 1: Does climate influence the growth patterns of three *Helichrysum* species growing in the DAC?**

Despite the differences in elevations, *Helichrysum* shared similar climate–growth patterns, which were characterised by significant responses to low growing season temperatures and drought stress in the early growing season. *Helichrysum* species exhibit the potential for dendroclimatological work as these shrubs show positive correlations between growth and climate variables. The influence of microclimatic conditions cannot be set apart from local climate influences and further research is necessary to determine what climatic conditions contribute the most.

**Question 2: Does aspect and elevation zonation impact the growth rates of *Helichrysum tenuifolium*, *H. trilineatum* and *H. witbergense*?**

By comparing *Helichrysum* species from three different study sites, it was determined that ring width differences between *Helichrysum* species and study sites differ. These differences may be explained by varied resource availability and differing local and microclimatic conditions between sites. Shrub growth exhibits differences among shrubs that grow at different aspects and elevations. Shrubs located at higher elevation were mostly older and had narrower growth ring widths, whereas at lower elevations shrubs were mostly younger with wider growth rings. This may be indicative of the site-specific conditions linked to elevation and climate controlling shrub growth. Overall, shrubs located on the eastern aspects exhibited greater average growth rates than *Helichrysum* located on other aspects.

**Question 3: Do *Helichrysum tenuifolium*, *H. trilineatum* and *H. witbergense* favour particular microhabitats in mountain environments?**

Shrub abundance analyses confirmed that *H. witbergense* were to be found at high elevations (i.e. Kotisephola Pass study site) and are more abundant on south-facing slopes. In contrast, *H. tenuifolium* were only found at lower elevations (i.e. Sani Pass study site) on the eastern aspect. *H. trilineatum* were found at all elevations (Kotisephola Pass study site, Sani Pass-upper study site and Sani Pass-lower study site) and are more abundant on south- and west-facing slopes, except for the Sani Pass-lower study site that is only east-facing. Microhabitats were identified during this study. *Helichrysum* generally favoured the cool, moist regions closest to rock outcrops, representing site-specific niches in terms of soil type, soil moisture, protection from wind and fire, and other specific microclimatic conditions (such as partial shading).

# CHAPTER SIX

## Conclusions and recommendations

Site and species selection are essential, while greater sample size may contribute to a more accurate representation of the data. This research has demonstrated the potential to develop annual chronologies for different sites using *H. trilineatum*, *H. tenuifolium* and *H. witbergense* growth ring. The development of accurate chronologies is important for understanding growth response to climate variability of the recent past. In addition, other longer-lived woody shrub species in the DAC, should be analysed for their dendrochronological potential. Geochemistry, specifically isotopic analysis, may further strengthen the chronology and possibly allow for climate reconstruction. It would be beneficial to compile an alpine shrub growth ring database and growth index for all the possible alpine shrub species in Sub-Saharan Africa. This research confirms that climate, elevation, and aspect all influence growth patterns and that the species have habitat preferences in terms of microhabitats and ecological niches.

Dendrochronology and dendroclimatology have been successfully studied in the northern hemisphere but remains underdeveloped in lower latitudes alpine environments. The attempt at cross-dating of *H. trilineatum*, *H. tenuifolium* and *H. witbergense* adds to the body of palaeodendrochronological work available for southern Africa, particularly Lesotho, contributing to the existing global network of shrub growth ring studies. Due to a variety of data that primarily focus on northern hemisphere dendrochronological work, those from the southern hemisphere, particularly at lower latitudes in Africa, such as in the DAC, are particularly useful.

Attempts at cross-dating and the subsequent development of a 54-year growth ring width chronology may support the dendrochronological potential of *Helichrysum* species. The dendroclimatological potential of *H. trilineatum*, *H. tenuifolium* and *H. witbergense* should be further investigated, possibly through isotopic analysis so that specific climatic conditions could be inferred. This study contributes to shrub and tree ring research in southern Africa and adds to palaeoecological information available for southern Africa.

Further knowledge and predictions of future high mountain climatic change, and microclimates, are necessary as changes in these systems will impact the endemic alpine biodiversity. Comprehensive climate data are required, and further analysis of the Sani Pass-lower and Kotisephola Pass study areas' temperature and precipitation data are needed for improved comparisons between sites. The data used in this research assessed only  $\pm 20$  years of climatic changes, further analyses of long-

term data are needed to better understand the long-term temperature and precipitation trends in the DAC and the implications on specifically *Helichrysum* species.

This research opens the possibility for further use of dendrochronology in the DAC. Future research directions should focus on assessing the dendroclimatological and -geomorphological potential of other *Helichrysum* species. Comparisons between the same species at different locations are more likely to provide a more developed regional chronology, providing a clearer assessment of climate sensitivity. This would allow for stable isotopic analysis to be applied, possibly providing stronger climate signals, with a high level of precision. Geomorphic and other ecological disturbances, such as fire, should be investigated. This may lead to an increased understanding of local and regional climate change in the DAC. Such work would thus be of tremendous value and would assist in understanding plant adaptations to climate change in this important alpine region.

# REFERENCE LIST

- Alberto, F.J., Aitken, S.N., Alía, R., González-Martínez, S.C., Hänninen, H., Kremer, A., Lefèvre, F., Lenormand, T., Yeaman, S., Whetten, R. and Savolainen, O. (2013). Potential for evolutionary responses to climate change—evidence from tree populations. *Global Change Biology*, 19(6): 1645-1661. <https://doi.org/10.1111/gcb.12181>
- Allen, K.J., Cook, E.R., Evans, R., Francey, R., Buckley, B.M., Palmer, J.G., Peterson, M.J. and Baker, P.J. (2018). Lack of cool, not warm, extremes distinguishes late 20th Century climate in 979-year Tasmanian summer temperature reconstruction. *Environmental Research Letters*, 13(3): 034041. <https://doi.org/10.1088/1748-9326/aaafd7>
- Allen, K.J., Anchukaitis, K.J., Grose, M.G., Lee, G., Cook, E.R., Risbey, J.S., O’Kane, T.J., Monselesan, D., O’Grady, A., Larsen, S. and Baker, P.J. (2019). Tree-ring reconstructions of cool season temperature for far southeastern Australia, 1731–2007. *Climate Dynamics*, 1-15. <https://doi.org/10.1007/s00382-018-04602-2>
- Andreu-Hayles, L., Gaglioti, B.V., D’Arrigo, R., Anchukaitis, K.J. and Goetz, S. (2017). Shrub sensitivity to recent warming across Arctic Alaska from dendrochronological and remote sensing records. *19th EGU General Assembly, EGU 2017, proceedings from the conference held 23-28 April 2017 in Vienna, Austria.*, 16398.
- Archer, E., Engelbrecht, F., Hänsler, A., Landman, W., Tadross, M. and Helmschrot, J. (2018) Seasonal prediction and regional climate projections for southern Africa. In: Revermann, R., Krewenka, K.M., Schmiedel, U., Olwoch, J.M., Helmschrot, J. and Jürgens, N.(eds.), *Climate change and adaptive land management in southern Africa – assessments, changes, challenges, and solutions, Biodiversity & Ecology*, 6, Klaus Hess Publishers: Göttingen and Windhoek, 14-21.
- Arnold, J.R. and Libby, W.F. (1951). Radiocarbon dates. *Science*, 113(2927): 111-120.
- Arzhannikov, S.G., Ivanov, A.V., Arzhannikova, A.V., Demonterova, E.I., Jolivet, M., Voronin, V.I., Buyantuev, V.A. and Oskolkov, V.A. (2017). Age of the Jombolok lava field (East Sayan): evidence from dendrochronology and radiocarbon dating. *Russian Geology and Geophysics*, 58(1): 20-36. <https://doi.org/10.1016/j.rgg.2016.07.001>

- Au, R. and Tardif, J.C. (2007). Allometric relationships and dendroecology of the dwarf shrub *Dryas integrifolia* near Churchill, subarctic Manitoba. *Botany*, 85(6): 585-597.  
<https://doi.org/10.1139/B07-055>
- Bär, A., Bräuning, A. and Löffler, J. (2006). Dendroecology of dwarf shrubs in the high mountains of Norway—A methodological approach. *Dendrochronologia*, 24(1): 17-27.  
<https://doi.org/10.1016/j.dendro.2006.05.001>
- Barros, V.R., Boninsegna, J.A., Camilloni, I.A., Chidiak, M., Magrín, G.O. and Rusticucci, M. (2015). Climate change in Argentina: trends, projections, impacts and adaptation. *Wiley Interdisciplinary Reviews: Climate Change*, 6(2): 151-169. <https://doi.org/10.1002/wcc.316>
- Bayer, R.J., Breitwieser, I., Ward, J. and Puttock, C. 2007. Tribe Gnaphalieae (Cass.) *Lecoq.* and *Juillet.* (1831). In: Kadereit, J.W., Jeffrey, C. (eds.), *The families and genera of vascular plants, Volume 8*. Springer, Berlin, pp. 246-284.
- Benedict, J.B., Benedict, R.J., Lee, C.M. and Staley, D.M. (2008). Spruce trees from a melting ice patch: Evidence for Holocene climatic change in the Colorado Rocky Mountains, USA. *The Holocene*, 18(7): 1067-1076. <https://doi.org/10.1177/0959683608095578>
- Beniston, M. (2003). Climatic change in mountain regions: a review of possible impacts. In: Diaz, H.F., Grosjean, M and Graumlich, L. (eds.), *Climate variability and change in high elevation regions: Past, present & future*. Springer, Dordrecht, pp. 5-31.
- Bentley, L.K. (2016). Assessing the potential impact of climate change in the South-Eastern Great Escarpment, Southern Africa. Unpublished M.Sc. Thesis, Rhodes University, Grahamstown.
- Bentley, L.K., Robertson, M.P. and Barker, N.P. (2019). Range contraction to a higher elevation: the likely future of the montane vegetation in South Africa and Lesotho. *Biodiversity and Conservation*, 28(1):131-153. <https://doi.org/10.1007/s10531-018-1643-6>
- Bentley, L.K. and O'Connor, T.G. (2018). Temperature control of the distributional range of five C<sub>3</sub> grass species in the uKhahlamba-Drakensberg Park, KwaZulu-Natal, South Africa. *African Journal of Range & Forage Science*, 35(1): 45-54.  
<https://doi.org/10.2989/10220119.2018.1459841>
- Billings, W. D. (1974). Adaptations and origins of alpine plants. *Arctic and alpine research*, 6(2), 129-142. <https://doi.org/10.1080/00040851.1974.12003769>

- Bhattarai, K.R. and Vetaas, O.R. (2003). Climatic change in mountain regions: a review of possible impacts. *Global Ecology and Biogeography*, 12(4): 327-340. [https://doi.org/10.1007/978-94-015-1252-7\\_2](https://doi.org/10.1007/978-94-015-1252-7_2)
- Bi, Y., Xu, J., Yang, J., Li, Z., Gebrekirstos, A., Liang, E. and Yang, X. (2017). Ring-widths of the above tree-line shrub *Rhododendron* reveal the change of minimum winter temperature over the past 211 years in Southwestern China. *Climate Dynamics*, 48(11-12): 3919-3933. <https://doi.org/10.1007/s00382-016-3311-4>
- Biondi, F., Strachan, S.D., Mensing, S. and Piovesan, G. (2007). Radiocarbon analysis confirms the annual nature of sagebrush growth rings. *Radiocarbon*, 49(3): 1231-1240.
- Blok, D., Sass-Klaassen, U., Schaepman-Strub, G., Heijmans, M.M.P.D., Sauren, P. and Berendse, F. (2011). What are the main climate drivers for shrub growth in Northeastern Siberian tundra? *Biogeosciences*, 8(5): 1169-1179. <https://doi.org/10.5194/bg-8-1169-2011>
- Bordy, E.M., Hancox, P.J. and Rubidge, B.S. (2005). The contact of the Molteno and Elliot formations through the main Karoo Basin, South Africa: a second-order sequence boundary. *South African Journal of Geology*, 108(3): 351-364. DOI: 10.2113/108.3.351
- Boscutti, F., Casolo, V., Beraldo, P., Braidot, E., Zancani, M. and Rixen, C. (2018). Shrub growth and plant diversity along an elevation gradient: Evidence of indirect effects of climate on alpine ecosystems. *PloS one*, 13(4): e0196653. <https://doi.org/10.1371/journal.pone.0196653>
- Brand, R.F., Brown, L.R. and du Preez, P.J. (2010). A floristic analysis of the vegetation of Platberg, eastern Free State, South Africa. *Koedoe*, 2(1): Art. #710. DOI:10.4102/koedoe.v52i1.710.
- Brand, R.F., Scott-Shaw, C.R. and O'Connor, T.G. (2019). The alpine flora on inselberg summits in the Maloti–Drakensberg Park, KwaZulu-Natal, South Africa. *Bothalia-African Biodiversity & Conservation*, 49(1): 1-15. <http://dx.doi.org/10.4102/abc.v49i1.2386>
- Britten, L., Breuckner, A., Christian, H.B., Dyer, R.A., Henderson, M.D., Killick, D.J.B., Story, R., Verdoorn, I.C., Wild, H. (1954). Newly Described Species. *Bothalia*, 6(2): 415-451. <https://doi.org/10.4102/abc.v6i2.1699>



- Bryan, E., Deressa, T.T., Gbetibouo, G.A. and Ringler, C. (2009). Adaptation to climate change in Ethiopia and South Africa: options and constraints. *Environmental science & policy*, 12(4): 413-426. <https://doi.org/10.1016/j.envsci.2008.11.002>
- Buchwal, A., Weijers, S., Blok, D. and Elberling, B. (2019). Temperature sensitivity of willow dwarf shrub growth from two distinct High Arctic sites. *International journal of biometeorology*, 63(2): 167-181. <https://doi.org/10.1007/s00484-018-1648-6>
- Buckley, B.M., Ummenhofer, C.C., D'Arrigo, R.D., Hansen, K.G., Truong, L.H., Le, C.N. and Stahle, D.K. (2019). Interdecadal Pacific Oscillation reconstructed from trans-Pacific tree rings: 1350–2004 CE. *Climate Dynamics*, 1-16. <https://doi.org/10.1007/s00382-019-04694-4>
- Caran, S.C. (1998). Quaternary paleoenvironmental and paleoclimatic reconstruction: A discussion and critique, with examples from the southern High Plains. *The Plains Anthropologist*, 43(164): 111-124. <https://doi.org/10.1080/2052546.1998.11931894>
- Carbutt, C. and Edwards, T.J. (2004). The flora of the Drakensberg alpine centre. *Edinburgh Journal of Botany*, 60(3), 581-607. <https://doi.org/10.1017/S0960428603000428>
- Carbutt, C. and Edwards, T.J. (2006). The endemic and near-endemic angiosperms of the Drakensberg Alpine Centre. *South African Journal of Botany*, 72(1), 105-132. <https://doi.org/10.1016/j.sajb.2005.06.001>
- Carbutt, C. (2012). The emerging invasive alien plants of the Drakensberg Alpine Centre, southern Africa. *Bothalia*, 42(2): 71-85. <https://doi.org/10.4102/abc.v42i2.10>
- Carbutt, C. and Edwards, T.J. (2015a). Plant–soil interactions in lower–upper montane systems and their implications in a warming world: a case study from the Maloti-Drakensberg Park, southern Africa. *Biodiversity*, 16(4), 262–277. <https://doi.org/10.1080/14888386.2015.1116409>
- Carbutt, C. and Edwards, T.J. (2015b). Reconciling ecological and phytogeographical spatial boundaries to clarify the limits of the montane and alpine regions of sub-Saharan Africa. *South African Journal of Botany*, 98, 64-75. <https://doi.org/10.1016/j.sajb.2015.01.014>
- Carbutt, C., Henwood, W.D. and Gilfedder, L.A. (2017). Global plight of native temperate grasslands: going, going, gone? *Biodiversity and Conservation*, 26(12): 2911-2932. <https://doi.org/10.1007/s10531-017-1398-5>

- Carrer, M. and Urbinati, C. (2004). Age-dependent tree-ring growth responses to climate in *Larix Decidua* and *Pinus Cembra*. *Ecology*, 85(3): 730-740. <https://doi.org/10.1890/02-0478>
- Carrer, M., Pellizzari, E., Prendin, A.L., Pividori, M. and Brunetti, M. (2019). Winter precipitation-not summer temperature-is still the main driver for Alpine shrub growth. *Science of The Total Environment*, 682: 171-179. <https://doi.org/10.1016/j.scitotenv.2019.05.152>
- Chen, L., Wu, S. and Pan, T. (2011). Variability of climate-growth relationships along an elevation gradient in the Changbai Mountain, northeastern China. *Trees*, 25(6): 1133-1139. <https://doi.org/10.1007/s00468-011-0588-0>
- Cingo, P. (2015). Plant diversity and morphology in seasonally snow-abundant niches of the Drakensberg Alpine Centre, Lesotho. Unpublished MSc Thesis, University of the Witwatersrand, Johannesburg.
- Clifton, C.F., Day, K.T., Luce, C.H., Grant, G.E., Safeeq, M., Halofsky, J.E. and Staab, B.P. (2018). Effects of climate change on hydrology and water resources in the Blue Mountains, Oregon, USA. *Climate Services*, 10: 9-19. <https://doi.org/10.1016/j.cliser.2018.03.001>
- Connolly, R., Connolly, M., Soon, W., Legates, D.R., Cionco, R.G. and Velasco Herrera, V. (2019). Northern Hemisphere Snow-Cover Trends (1967–2018): A Comparison between Climate Models and Observations. *Geosciences*, 9(3):135. <https://doi.org/10.3390/geosciences9030135>
- Cook, E.R. and Kairiukstis, L.A. (1990) *Methods of Dendrochronology. Applications in the Environmental Sciences*. International Institute for Applied Systems Analysis. Kluwer Academic Publishers, Dordrecht, pp. 98-102. <http://dx.doi.org/10.1007/978-94-015-7879-0>
- Curtis, B.A., Tyson, P.D. and Dyer, T.G.J. (1978). Dendrochronological age determination of *podocarpus falactus*. *South African Journal of Science*, 74: 92-95.
- Czimczik, C.I. and Welker, J.M. (2010). Radiocarbon content of CO<sub>2</sub> respired from high arctic tundra in Northwest Greenland. *Arctic, Antarctic, and Alpine Research*, 42(3): 342-350. <https://doi.org/10.1657/1938-4246-42.3.342>
- Dearborn, K.D. and Danby, R.K. (2017). Aspect and slope influence plant community composition more than elevation across forest-tundra ecotones in subarctic Canada. *Journal of Vegetation Science*, 28(3): 595-604. <https://doi.org/10.1111/jvs.12521>

- Drees, B.M., Jackman, J.A. and Merchant, M.E. (1994). Wood-Boring Insects of Trees and Shrubs. *Bulletin/Texas Agricultural Extension Service*; no. 5086.
- Diaz, H.F., Grosjean, M. and Graumlich, L. (2003). Climate variability and change in high elevation regions: past, present and future. *Climatic change*, 59(1-2), 1-4.  
<https://doi.org/10.1023/A:1024416227887>
- Donat, M.G., Lowry, A.L., Alexander, L.V., O’Gorman, P.A. and Maher, N. (2016). More extreme precipitation in the world’s dry and wet regions. *Nature Climate Change*, 6(5): 508-513.  
<https://doi.org/10.1038/nclimate2941>
- Dong, Z., Driscoll, C.T., Campbell, J.L., Pourmokhtarian, A., Stoner, A.M. and Hayhoe, K. (2019). Projections of water, carbon, and nitrogen dynamics under future climate change in an alpine tundra ecosystem in the southern Rocky Mountains using a biogeochemical model. *Science of the Total Environment*, 650, 1451-1464. <https://doi.org/10.1016/j.scitotenv.2018.09.151>
- Dullinger, S., Gatttringer, A., Thuiller, W., Moser, D., Zimmermann, N.E., Guisan, A., Willner, W., Plutzer, C., Leitner, M., Mang, T. and Caccianiga, M. (2012). Extinction debt of high-mountain plants under twenty-first-century climate change. *Nature Climate Change*, 2(8): 619.  
<https://doi.org/10.1038/nclimate1514>
- Dunwiddie, P.W. and LaMarche, V.C. (1980). A climatically responsive tree-ring record from *Widdringtonia cedarbergensis*, Cape Province, South Africa. *Nature*, 286(5775): 796-797.  
<https://doi.org/10.1038/286796a0>
- Archer, E., Engelbrecht, F., Hänsler, A., Landman, W., Tadross, M. and Helmschrot, J. (2018) Seasonal prediction and regional climate projections for southern Africa. In: Revermann, R., Krewenka, K.M., Schmiedel, U., Olwoch, J.M., Helmschrot, J. and Jürgens, N.(eds.), *Climate change and adaptive land management in southern Africa – assessments, changes, challenges, and solutions*, *Biodiversity & Ecology*, 6, Klaus Hess Publishers: Göttingen and Windhoek, 14-21.
- Eckstein, D., Ogden, J., Jacoby, G.C., and Ash, J. (1981). Age and growth rate determination in tropical trees: The application of dendrochronological methods. In: Bormann, F.H. and Berlyn, G. (eds.), *Age and growth rate of tropical trees: New directions for research*. Yale School of Forestry & Environmental Studies Bulletin Series. 6 nr. 84: Connecticut, 83-106.  
[https://elischolar.library.yale.edu/yale\\_fes\\_bulletin/6](https://elischolar.library.yale.edu/yale_fes_bulletin/6)

- Edmond, J.B., Senn, T.L., Andrews, F.S. and Halfacre, R.G. (1957). *Fundamentals of horticulture* (4th ed.). McGraw-Hill, Inc., New York, U.S.A., pp. 55-131.
- Elsen, P.R. and Tingley, M.W. (2015). Global mountain topography and the fate of montane species under climate change. *Nature Climate Change*, 5(8): 772.  
<https://doi.org/10.1038/nclimate2656>
- Engelbrecht, F.A., McGregor, J.L. and Engelbrecht, C.J. (2009). Dynamics of the Conformal-Cubic Atmospheric Model projected climate-change signal over southern Africa. *International Journal of Climatology: A Journal of the Royal Meteorological Society*, 29(7): 1013-1033.  
<https://doi.org/10.1002/joc.1742>
- Engelbrecht, F.A., Landman, W.A., Engelbrecht, C.J., Landman, S., Bopape, M.M., Roux, B., McGregor, J.L. and Thatcher, M. (2011). Multi-scale climate modelling over Southern Africa using a variable-resolution global model. *Water SA*, 37(5): 647-658.  
<http://dx.doi.org/10.4314/wsa.v37i5.2>
- Engelbrecht, F., Adegoke, J., Bopape, M.J., Naidoo, M., Garland, R., Thatcher, M., McGregor, J., Katzfey, J., Werner, M., Ichoku, C. and Gatebe, C. (2015). Projections of rapidly rising surface temperatures over Africa under low mitigation. *Environmental Research Letters*, 10(8): 085004. DOI:10.1088/1748-9326/10/8/085004
- Engler, R., Randin, C.F., Thuiller, W., Dullinger, S., Zimmermann, N.E., Araújo, M.B., Pearman, P.B., Le Lay, G., Piedallu, C., Albert, C.H. and Choler, P. (2011). 21st century climate change threatens mountain flora unequally across Europe. *Global Change Biology*, 17(7): 2330-2341.  
<https://doi.org/10.1111/j.1365-2486.2010.02393.x>
- Esper, J., Shiyatov, S.G., Mazepa, V.S., Wilson, R.J.S., Graybill, D.A., and Funkhouser, G. (2003). Temperature-sensitive Tien Shan tree ring chronologies show multi-centennial growth trends. *Climate Dynamics*, 21(7-8): 699-706. <https://doi.org/10.1007/s00382-003-0356-y>
- Fay, N. and de Berker, N. (2018). A review of the theory and practice of tree coring on live ancient and veteran trees. Scottish Natural Heritage Research Report No. 789, 1-58.
- February, E.C. (1994). Rainfall reconstruction using wood charcoal from two archaeological sites in South Africa. *Quaternary Research*, 42(1): 100-107. <https://doi.org/10.1006/qres.1994.1057>

- February, E.C., and Stock, W.D. (1998). The relationship between ring width measures and precipitation for *Widdringtonia cedarbergensis*. *South African Journal of Botany*, 64(3): 213-216. [https://doi.org/10.1016/S0254-6299\(15\)30870-X](https://doi.org/10.1016/S0254-6299(15)30870-X)
- February, E.C. and Stock, W.D. (1999). Declining trend in the  $^{13}\text{C}/^{12}\text{C}$  ratio of atmospheric carbon dioxide from tree rings of South African *Widdringtonia cedarbergensis*. *Quaternary Research*, 52(2): 229-236. <https://doi.org/10.1006/qres.1999.2057>
- February, E.C., Mader, A.D. and Bond, W.J. (2006). Age determination of two South African *Acacia* species using ring counts and radiocarbon dating. *African Journal of Ecology*, 44(3):417-419. <https://doi.org/10.1111/j.1365-2028.2006.00651.x>
- Fedrigo, M., Stewart, S.B., Kasel, S., Levchenko, V., Trouvé, R. and Nitschke, C.R. (2019). Radiocarbon dating informs tree fern population dynamics and disturbance history of temperate forests in southeast Australia. *Radiocarbon*, 61(2), 445-460. <https://doi.org/10.1017/RDC.2018.119>
- Fitchett, J.M. (2015). Towards a multi-proxy holocene palaeoenvironmental and palaeoclimatic reconstruction for Eastern Lesotho (Doctoral dissertation). University of the Witwatersrand, Johannesburg.
- Fitchett, J.M., Grab, S.W., Bamford, M.K. and Mackay, A.W. (2016). A multi-proxy analysis of late Quaternary palaeoenvironments, Sekhokong Range, eastern Lesotho. *Journal of Quaternary Science*, 31(7): 788-798. <https://doi.org/10.1002/jqs.2902>
- Fitchett, J.M., Bamford, M.K., Mackay, A.W. and Grab, S.W. (2017). *Chrysocoma ciliata* L. (Asteraceae) in the Lesotho Highlands: an anthropogenically introduced invasive or a niche coloniser? *Biological Invasions*, 19(9): 2711-2728. <https://doi.org/10.1007/s10530-017-1478-1>
- Fichtler, E., Trouet, V., Beeckman, H., Coppin, P. and Worbes, M. (2004). Climatic signals in tree rings of *Burkea africana* and *Pterocarpus angolensis* from semiarid forests in Namibia. *Trees*, 18(4): 442-451. <https://doi.org/10.1007/s00468-004-0324-0>
- Foden, W.B., Young, B.E., Akçakaya, H.R., Garcia, R.A., Hoffmann, A.A., Stein, B.A., Thomas, C.D., Wheatley, C.J., Bickford, D., Carr, J.A. and Hole, D.G. (2018). Climate change vulnerability assessment of species. *Wiley Interdisciplinary Reviews: Climate Change*, 10(1): e551. <https://doi.org/10.1002/wcc.551>

- Franklin, R.S. (2013). Growth response of the alpine shrub, *Linanthus pungens*, to snowpack and temperature at a rock glacier site in the eastern Sierra Nevada of California, USA. *Quaternary International*, 310: 20-33. <https://doi.org/10.1016/j.quaint.2012.07.018>
- Fritts, H.C. (1976). *Tree rings and climate*. Academic Press: London, New York, San Francisco, 14-28.
- Gaire, N.P., Bhujju, D.R. and Koirala, M. (2013). Dendrochronological studies in Nepal: Current status and future prospects. *FUUAST Journal of Biology*, 3(1): 1-9.
- Gamm, C.M. (2015). Declining growth of arctic shrubs in a warming climate: Species specific effects of drought and herbivory in west Greenland (Doctoral dissertation). University of Alaska, Anchorage.
- Gamm, C.M., Sullivan, P.F., Buchwal, A., Dial, R.J., Young, A.B., Watts, D.A., Cahoon, S.M., Welker, J.M. and Post, E. (2018). Declining growth of deciduous shrubs in the warming climate of continental western Greenland. *Journal of Ecology*, 106(2): 640-654. <https://doi.org/10.1111/1365-2745.12882>
- Gao, L., Gou, X., Deng, Y., Liu, W., Yang, M. and Zhao, Z. (2013). Climate–growth analysis of *Qilian juniper* across an altitudinal gradient in the central Qilian Mountains, northwest China. *Trees*, 27(2), 379-388. <https://doi.org/10.1007/s00468-012-0776-6>
- Gardiner, B., Berry, P. and Moulia, B. (2016). Wind impacts on plant growth, mechanics and damage. *Plant Science*, 245: 94-118. <https://doi.org/10.1016/j.plantsci.2016.01.006>
- Gebrekirstos, A., Bräuning, A., Sass-Klassen, U. and Mbow, C. (2014). Opportunities and applications of dendrochronology in Africa. *Current Opinion in Environmental Sustainability*, 6: 48-53. <https://doi.org/10.1016/j.cosust.2013.10.011>
- Gentili, R., Badola, H.K. and Birks, H.J.B. (2015). Alpine biodiversity and refugia in a changing climate. *Biodiversity*, 16(4): 193–195. <https://doi.org/10.1080/14888386.2015.1117023>
- Gilbert, A. and Vincent, C. 2013. Atmospheric temperature changes over the 20th century at very high elevations in the European Alps from englacial temperatures. *Geophysical Research Letters*, 40(10): 2102-2108. <https://doi.org/10.1002/grl.50401>

- Glennon, K.L. and Cron, G.V. (2015). Climate and leaf shape relationships in four *Helichrysum* species from the Eastern Mountain Region of South Africa. *Evolution Ecology*, 29: 657–678. <https://doi.org/10.1007/s10682-015-9782-7>
- Godwin, H. (1962). Half-life of radiocarbon. *Nature*, 195(4845): 984-984.
- Gottfried, M., Pauli, H., Futschik, A., Akhalkatsi, M., Barančok, P., Alonso, J.L.B., Coldea, G., Dick, J., Erschbamer, B., Kazakis, G. and Krajčič, J. 2012. Continent-wide response of mountain vegetation to climate change. *Nature climate change*, 2(2): 111-115. <https://doi.org/10.1038/nclimate1329>
- Google Maps (2019). Map of Lesotho. Accessed on 10 May 2019 from <https://www.google.co.za/maps/place/Sani+Pass/@-29.5856552,29.2851563,18.25z/data=!4m5!3m4!1s0x1ef4827516d5bab3:0xb4a0e56c87edeef2!8m2!3d-29.5879785!4d29.2921966>
- Gourlay, I.D. and Kanowski, P.J. (1991). Marginal parenchyma bands and crystalliferous chains as indicators of age in African *Acacia* species. *IAWA Journal*, 12(2): 187-194. <https://doi.org/10.1163/22941932-90001236>
- Gourlay, I.D. (1995). Growth ring characteristics of some African *Acacia* species. *Journal of tropical ecology*, 11(1):121-140. <https://doi.org/10.1017/S0266467400008488>
- Grab, S.W. (2000). Stone-banked lobes and environmental implications, high Drakensberg, southern Africa. *Permafrost and Periglacial Processes*, 11(3): 177-187. [https://doi.org/10.1002/1099-1530\(200007/09\)11:3<177::AID-PPP349>3.0.CO;2-R](https://doi.org/10.1002/1099-1530(200007/09)11:3<177::AID-PPP349>3.0.CO;2-R)
- Grab, S.W. (2010). Alpine turf exfoliation pans in Lesotho, southern Africa: Climate–process–morphological linkages. *Geomorphology*, 114(3): 261-275. <https://doi.org/10.1016/j.geomorph.2009.07.007>
- Grab, S.W. (2013). Fine-scale variations of near-surface-temperature lapse rates in the high Drakensberg Escarpment, South Africa: environmental implications. *Arctic, Antarctic, and Alpine Research*, 45(4): 500-514. <https://doi.org/10.1657/1938-4246-45.4.500>
- Grab, S.W., Linde, J. and De Lemos, H. (2017). Some attributes of snow occurrence and snowmelt/sublimation rates in the Lesotho Highlands: environmental implications. *Water SA*, 43(2): 333-342. <http://dx.doi.org/10.4314/wsa.v43i2.16>

- Grab, S.W. and Mills, S.C. (2011). Quaternary slope processes and morphologies in the upper Sehonghong Valley, eastern Lesotho. *Proceedings of the Geologists' Association*, 122(1), 179-186. <https://doi.org/10.1016/j.pgeola.2010.02.001>
- Grabowski, M.M. (2015). Interspecific boreal shrub growth response to climate, fertilization and herbivory (Doctoral dissertation). University of British Columbia, Vancouver.
- Granato-Souza, D., Stahle, D.W., Barbosa, A.C., Feng, S., Torbenson, M.C., de Assis Pereira, G., Schöngart, J., Barbosa, J.P. and Griffin, D. (2019). Tree rings and rainfall in the equatorial Amazon. *Climate Dynamics*, 52(3-4): 1857-1869. <https://doi.org/10.1007/s00382-018-4227-y>
- Groffman, P.M., Rustad, L.E., Templer, P.H., Campbell, J.L., Christenson, L.M., Lany, N.K., Soggi, A.M., Vadeboncoeur, M.A., Schaberg, P.G., Wilson, G.F. and Driscoll, C.T. (2012). Long-term integrated studies show complex and surprising effects of climate change in the northern hardwood forest. *BioScience*, 62(12): 1056-1066. <https://doi.org/10.1525/bio.2012.62.12.7>
- Grundy, I.M. (2006). Age determination of miombo species *Brachystegia spiciformis* (Leguminosae–Caesalpinoideae) in Zimbabwe using growth rings. *Southern African Forestry Journal*, 206(1): 5-12. <https://doi.org/10.2989/10295920609505238>
- Hall, M. (1976). Dendroclimatology, rainfall and human adaptation in the later Iron Age of Natal and Zululand. *Annals of the Natal Museum*, 22(3): 693-703. [https://hdl.handle.net/10520/AJA03040798\\_617](https://hdl.handle.net/10520/AJA03040798_617)
- Hall, G., Woodborne, S. and Scholes, M. (2008). Stable carbon isotope ratios from archaeological charcoal as palaeoenvironmental indicators. *Chemical Geology*, 247(3-4): 384-400. <https://doi.org/10.1016/j.chemgeo.2007.11.001>
- Hall, G., Woodborne, S. and Pienaar, M. (2009). Rainfall control of the  $\delta^{13}\text{C}$  ratios of *Mimusops caffra* from KwaZulu-Natal, South Africa. *The Holocene*, 19(2): 251-260. <https://doi.org/10.1177/09596836083608100569>
- Hallinger, M., Manthey, M. and Wilmking, M. (2010). Establishing a missing link: warm summers and winter snow cover promote shrub expansion into alpine tundra in Scandinavia. *New Phytologist*, 186(4): 890-899. <https://doi.org/10.1111/j.1469-8137.2010.03223.x>



- Hatfield, J.L. and Prueger, J.H. (2015). Temperature extremes: Effect on plant growth and development. *Weather and climate extremes*, 10: 4-10.  
<https://doi.org/10.1016/j.wace.2015.08.001>
- Heaton, T.J., Blackwell, P.G. and Buck, C.E. (2009). A Bayesian approach to the estimation of radiocarbon calibration curves: the IntCal09 methodology. *Radiocarbon*, 51(4): 1151-1164.
- Heinrich, I. and Allen, K. (2013). Current Issues and Recent Advances in Australian Dendrochronology: Where to Next? *Geographical Research*, 51(2): 180-191.  
<https://doi.org/10.1111/j.1745-5871.2012.00786.x>
- Helama, S., Timonen, M., Holopainen, J., Ogurtsov, M.G., Mielikäinen, K., Eronen, M., and Meriläinen, J. (2009). Summer temperature variations in Lapland during the Medieval Warm Period and the Little Ice Age relative to natural instability of thermohaline circulation on multi-decadal and multi-centennial scales. *Journal of Quaternary Science*, 24(5): 450-456.  
<https://doi.org/10.1002/jqs.1291>
- Hilliard, O.M. (1963). Asteraceae (Compositae). In: de Winter, B., Killick, D.J.B. and Leitsner, O.A. (eds.) *Flora of Southern Africa 33 Asteraceae, Part 7 Inuleae, Fascicle 2. Pretoria: National Botanical Institute*, pp. 219-221.
- Hilliard, O.M. (1977). *Compositae in Natal*. University of Natal Press, Pietermaritzburg.
- Hoffman, M.T., Rohde, R.F. and Gillson, L. (2019). Rethinking catastrophe? Historical trajectories and modelled future vegetation change in southern Africa. *Anthropocene*, 25: 100189.  
<https://doi.org/10.1016/j.ancene.2018.12.003>
- Hogg, A.G., Hua, Q., Blackwell, P.G., Niu, M., Buck, C.E., Guilderson, T.P., Heaton, T.J., Palmer, J.G., Reimer, P.J., Reimer, R.W. and Turney, C.S. (2013). SHCal13 Southern Hemisphere calibration, 0–50,000 years cal BP. *Radiocarbon*, 55(4): 1889-1903.  
[https://doi.org/10.2458/azu\\_js\\_rc.55.16783](https://doi.org/10.2458/azu_js_rc.55.16783)
- Holmgren, K., Norström, E. and Morth, C.M. (2005). Rainfall-driven variations in  $\delta^{13}\text{C}$  composition and wood anatomy of *Breonadia salicina* trees from South Africa between AD 1375 and 1995. *South African Journal of Science*, 101(3): 162-168.
- Hua, Q., Barbetti, M. and Rakowski, A.Z. (2013). Atmospheric radiocarbon for the period 1950–2010. *Radiocarbon*, 55(4): 2059-2072. [https://doi.org/10.2458/azu\\_js\\_rc.v55i2.16177](https://doi.org/10.2458/azu_js_rc.v55i2.16177)

- Hughes, M.K. (2002). Dendrochronology in climatology – the state of the art. *Dendrochronologia*, 20(1-2): 95-116. <https://doi.org/10.1078/1125-7865-00011>
- IPCC. (2018). Summary for Policymakers. In: V. Masson-Delmotte, P. Zhai, H. O. Pörtner, D. Roberts, J. Skea, P. R. Shukla, A. Pirani, W. Moufouma-Okia, C. Péan, R. Pidcock, S. Connors, J. B. R. Matthews, Y. Chen, X. Zhou, M. I. Gomis, E. Lonnoy, T. Maycock, M. Tignor, T. Waterfield (eds.). *Global warming of 1.5°C. An IPCC Special Report on the impacts of global warming of 1.5°C above pre-industrial levels and related global greenhouse gas emission pathways, in the context of strengthening the global response to the threat of climate change, sustainable development, and efforts to eradicate poverty*. World Meteorological Organization, Geneva, Switzerland, 32 pp.
- Iturrate-Garcia, M., Heijmans, M.M., Schweingruber, F.H., Maximov, T.C., Niklaus, P.A. and Schaepman-Strub, G. (2017). Shrub growth rate and bark responses to soil warming and nutrient addition—A dendroecological approach in a field experiment. *Dendrochronologia*, 45:12-22. <https://doi.org/10.1016/j.dendro.2017.07.001>
- Jacobsen, A.L., Agenbag, L., Esler, K.J., Pratt, R.B., Ewers, F.W. and Davis, S.D. (2007). Xylem density, biomechanics and anatomical traits correlate with water stress in 17 evergreen shrub species of the Mediterranean-type climate region of South Africa. *Journal of Ecology*, 95(1): 171-183. <https://doi.org/10.1111/j.1365-2745.2006.01186.x>
- Jiang, L., Jiapaer, G., Bao, A., Guo, H. and Ndayisaba, F. (2017). Vegetation dynamics and responses to climate change and human activities in Central Asia. *Science of the Total Environment*, 599: 967-980. <https://doi.org/10.1016/j.scitotenv.2017.05.012>
- Kerns, B.K., Powell, D.C., Mellmann-Brown, S., Carnwath, G. and Kim, J.B. (2018). Effects of projected climate change on vegetation in the Blue Mountains ecoregion, USA. *Climate Services*, 10: 33-43. <https://doi.org/10.1016/j.cliser.2017.07.002>
- Killick, D.J.B. (1963). An account of the plant ecology of the Cathedral Peak area of the Natal Drakensberg. *Memoirs of the Botanical Survey of South Africa*, 34:178.
- Killick, D.J.B. (1978). Notes on the vegetation of the Sani Pass area of the southern Drakensberg. *Bothalia*, 12(3): 537–542. <https://doi.org/10.4102/abc.v12i3.1812>
- Killick, D.J.B. (1990). *A Field Guide: The Flora of the Natal Drakensberg*. Jonathan Ball and Ad. Donker Publishers, Johannesburg, South Africa.

- Kitching, J. and Raath, M. (1984). Fossils from the Elliot and Clarens formation (Karoo sequence) of the Northeastern Cape, Orange free state and Lesotho, and a suggested biozonation based on tetrapods. *Palaeontologia Africana*, 25: 111-125.
- Knight, J., Grab, S.W. and Carbutt, C. (2018). Influence of mountain geomorphology on alpine ecosystems in the Drakensberg Alpine Centre, Southern Africa. *Geografiska Annaler: Series A, Physical Geography*, 1-23. <https://doi.org/10.1080/04353676.2017.1418628>
- Köhler, T., Giger, M., Hurni, H., Ott, C., Wiesmann, U., von Dach, S.W. and Maselli, D. (2010). Mountains and climate change: a global concern. *Mountain Research and Development*, 30(1): 53-56. <https://doi.org/10.1659/MRD-JOURNAL-D-09-00086.1>
- Kolusu, S.R., Shamsudduha, M., Todd, M.C., Taylor, R.G., Seddon, D., Kashaigili, J.J., Ebrahim, G.Y., Cuthbert, M.O., Sorensen, J.P., Villholth, K.G. and MacDonald, A.M. (2019). The El Niño event of 2015-2016: climate anomalies and their impact on groundwater resources in East and Southern Africa. *Hydrology and Earth System Sciences*, 23(3): 1751-1762. <https://doi.org/10.5194/hess-23-1751-2019>
- Körner C, Ohsawa M, Spehn E, Berge E, Bugmann H, Groombridge B, Hamilton L, Hofer T, Ives J, Jodha N, Messerli B, Pratt J, Price M, Reasoner M, Rodgers A, Thonell J and Yoshino M. (2005). Mountain systems. In: Hassan R, Scholes R, Ash N (eds.), *Ecosystems and human well-being: current state and trends (Volume 1)*. Island Press, Washington DC, pp. 683 – 716.
- Körner, C., Paulsen, J. and Spehn, E.M. (2011). A definition of mountains and their bioclimatic belts for global comparisons of biodiversity data. *Alpine Botany*, 121(2): 73. <https://doi.org/10.1007/s00035-011-0094-4>
- Körner, C., Jetz, W., Paulsen, J., Payne, D., Rudmann-Maurer, K. and Spehn, E.M. (2017). A global inventory of mountains for bio-geographical applications. *Alpine Botany*, 127(1): 1-15. <https://doi.org/10.1007/s00035-016-0182-6>
- Kromer, B. (2009). Radiocarbon and dendrochronology. *Dendrochronologia*, 27(1): 15-19. <https://doi.org/10.1016/j.dendro.2009.03.001>
- Kyncl, T., Suda, J., Wild, J., Wildová, R. and Herben, T. (2006). Population dynamics and clonal growth of *Spartocytisus supranubius* (Fabaceae), a dominant shrub in the alpine zone of Tenerife, Canary Islands. *Plant Ecology*, 186(1): 97-108. <https://doi.org/10.1007/s11258-006-9115-6>

- Lavergne, A., Daux, V., Pierre, M., Stievenard, M., Srur, A.M. and Villalba, R. (2017). Past summer temperatures inferred from dendrochronological records of *Fitzroya cupressoides* on the eastern slope of the northern Patagonian Andes. *Journal of Geophysical Research: Biogeosciences*, 123(1): 32-45. <https://doi.org/10.1002/2017JG003989>
- Le Moullec, M., Buchwal, A., van der Wal, R., Sandal, L. and Hansen, B.B. (2019). Annual ring growth of a widespread high arctic shrub reflects past fluctuations in community-level plant biomass. *Journal of Ecology*, 107(1): 436-451. <https://doi.org/10.1111/1365-2745.13036>
- Lehejček, J., (2015). Dwarf tundra shrubs growth as a proxy for late Holocene climate change. *Czech Polar Reports*, 5(2):185-199. DOI: 10.5817/CPR2015-2-16
- Letšela, T., Witkowski, E.T.F. and Balkwill, K. (2003). Plant resources used for subsistence in Tsehlanyane and Bokong in Lesotho. *Economic Botany*, 57(4): 619-639. [https://doi.org/10.1663/0013-0001\(2003\)057\[0619:PRUFSI\]2.0.CO;2](https://doi.org/10.1663/0013-0001(2003)057[0619:PRUFSI]2.0.CO;2)
- Lewis, F. and Oosthuizen, S. (2014). *Adapting to a Changing Climate – Integrating Ecosystem and Community Based Adaptation for a Resilient Future. A Study in the Highlands of Lesotho*. Institute of Natural Resources NPC. Pietermaritzburg.
- Lézine, A.M., Izumi, K., Kageyama, M. and Achoundong, G. (2019). A 90 000-year record of Afromontane forest responses to climate change. *Science*, 363(6423): 177-181. DOI: 10.1126/science.aav6821
- Li, Z., Liu, G., Fu, B., Zhang, Q., Ma, K. and Pederson, N. (2013). The growth-ring variations of alpine shrub *Rhododendron przewalskii* reflect regional climate signals in the alpine environment of Miyaluo Town in Western Sichuan Province, China. *Acta Ecologica Sinica*, 33(1): 23-31. <https://doi.org/10.1016/j.chnaes.2012.12.004>
- Liang, E., Lu, X., Ren, P., Li, X., Zhu, L. and Eckstein, D. (2011). Annual increments of juniper dwarf shrubs above the tree line on the central Tibetan Plateau: a useful climatic proxy. *Annals of Botany*, 109(4): 721-728. <https://doi.org/10.1093/aob/mcr315>
- Lindholm, M., Lehtonen, H., Kolström, T., Meriläinen, J., Eronen, M., and Timonen, M. (2000). Climatic signals extracted from ring-width chronologies of Scots pines from the northern, Sani Pass-upper and southern parts of the boreal forest belt in Finland. *Silva Fennica*, 34(4): 317-330.

- Loader, N.J., Robertson, I., Barker, A.C., Switsur, V.R. and Waterhouse, J.S. (1997). An improved technique for the batch processing of small wholewood samples to  $\alpha$ -cellulose. *Chemical Geology*, 136(3-4): 313-317. [https://doi.org/10.1016/S0009-2541\(96\)00133-7](https://doi.org/10.1016/S0009-2541(96)00133-7)
- Lodder, J., Hill, T.R. and Finch, J.M. (2018). A 5000-yr record of Afromontane vegetation dynamics from the Drakensberg Escarpment, South Africa. *Quaternary International*, 470: 119-129. <https://doi.org/10.1016/j.quaint.2017.08.019>
- Loftus, E., Sealy, J. and Lee-Thorp, J. (2016). New radiocarbon dates and Bayesian models for Nelson Bay Cave and Byneskranskop 1: Implications for the South African later Stone Age sequence. *Radiocarbon*, 58(2): 365-381. <https://doi.org/10.1017/RDC.2016.12>
- Lopez, L., Stahle, D., Villalba, R., Torbenson, M., Feng, S. and Cook, E. (2017). Tree ring reconstructed rainfall over the southern Amazon Basin. *Geophysical Research Letters*, 44(14): 7410-7418. <https://doi.org/10.1002/2017GL073363>
- Lorrey, A.M., Brookman, T.H., Evans, M.N., Fauchereau, N.C., Macinnis-Ng, C., Barbour, M.M., Criscitiello, A., Eischeid, G., Fowler, A.M., Horton, T.W. and Schrag, D.P. (2016). Stable oxygen isotope signatures of early season wood in New Zealand kauri (*Agathis australis*) tree rings: Prospects for palaeoclimate reconstruction. *Dendrochronologia*, 40: 50-63. <https://doi.org/10.1016/j.dendro.2016.03.012>
- Lourens, A.C.U., Viljoen, A.M. and van Heerden, F.R. (2008). South African *Helichrysum* species: A review of the traditional uses, biological activity and phytochemistry. *Journal of Ethnopharmacology*, 119: 630-652. <https://doi.org/10.1016/j.jep.2008.06.011>
- Lu, X., Camarero, J.J., Wang, Y., Liang, E. and Eckstein, D. (2015). Up to 400-year-old *Rhododendron* shrubs on the southeastern Tibetan Plateau: prospects for shrub-based dendrochronology. *Boreas*, 44(4): 760-768. <https://doi.org/10.1111/bor.12122>
- Lu, X., Huang, R., Wang, Y., Sigdel, S.R., Dawadi, B., Liang, E. and Camarero, J.J. (2016). Summer temperature drives radial growth of alpine shrub willows on the northeastern Tibetan Plateau. *Arctic, Antarctic and Alpine Research*, 48(3): 461-468. <https://doi.org/10.1657/AAAR0015-069>
- Luo, L., Ma, W., Zhang, Z., Zhuang, Y., Zhang, Y., Yang, J., Cao, X., Liang, S. and Mu, Y. (2017). Freeze/ Thaw-induced deformation monitoring and assessment of the slope in permafrost

- based on terrestrial laser scanner and GNSS. *Remote Sensing*, 9(3): 198.  
<https://doi.org/10.3390/rs9030198>
- Luomaranta, A., Aalto, J. and Jylhä, K. (2019). Snow cover trends in Finland over 1961–2014 based on gridded snow depth observations. *International Journal of Climatology*, 39(7): 3147-3159. <https://doi.org/10.1002/joc.6007>
- Malherbe, J., Dieppois, B., Maluleke, P., Van Staden, M. and Pillay, D.L. (2016). South African droughts and decadal variability. *Natural Hazards*, 80(1): 657-681.  
<https://doi.org/10.1007/s11069-015-1989-y>
- Marsh, P. (2017). Regional temperature and precipitation trends in the Drakensberg alpine and montane zones: implications for endemic plant species. Unpublished MSc Thesis, University of the Witwatersrand, Johannesburg.
- Mata-González, R., Pieper, R.D. and Cárdenas, M.M. (2002). Vegetation patterns as affected by aspect and elevation in small desert mountains. *The Southwestern Naturalist*, 47(3): 440-448. DOI: 10.2307/3672501.
- McCarroll, D. and Loader, N.J. (2004). Stable isotopes in tree rings. *Quaternary Science Reviews*, 23(7): 771-801. <https://doi.org/10.1016/j.quascirev.2003.06.017>
- McDonald, L., Chivall, D., Miles, D. and Ramsey, C.B. (2019). Seasonal variations in the <sup>14</sup>C Content of Tree Rings: Influences on Radiocarbon Calibration and Single-Year Curve Construction. *Radiocarbon*, 61(1): 185-194. <https://doi.org/10.1017/RDC.2018.64>
- McGrath, J.M. and Lobell, D.B. (2013). Regional disparities in the CO<sub>2</sub> fertilization effect and implications for crop yields. *Environmental Research Letters*, 8(1): 014054.  
DOI:10.1088/1748-9326/8/1/014054
- McNaughton, J. and Tyson, P.O. (1979). A preliminary assessment of *Podocarpus falcatus* in dendrochronological and dendroclimatological studies in the Witelsbos Forest Reserve. *South African Forestry Journal*, 111(1): 29-33. <https://doi.org/10.1080/00382167.1979.9630201>
- Mills, S.C., Grab, S.W. and Carr, S.J. (2009). Recognition and palaeoclimatic implications of late Quaternary niche glaciation in eastern Lesotho. *Journal of Quaternary Science*, 24(7): 647-663. <https://doi.org/10.1002/jqs.1247>

- Mills, S.C., Barrows, T.T., Telfer, M.W. and Fifield, L.K. (2017). The cold climate geomorphology of the Eastern Cape Drakensberg: A re-evaluation of past climatic conditions during the last glacial cycle in Southern Africa. *Geomorphology*, 278: 184-194.  
<https://doi.org/10.1016/j.geomorph.2016.11.011>
- Mina, M., Bugmann, H., Cordonnier, T., Irauschek, F., Klopčič, M., Pardos, M. and Cailleret, M. (2017). Future ecosystem services from European mountain forests under climate change. *Journal of Applied Ecology*, 54(2): 389-401. <https://doi.org/10.1111/1365-2664.12772>
- Morris, C.D., Taintoi, N.M. and Boleme, S. (1993). Classification of the eastern alpine vegetation of Lesotho. *African Journal of Range and Forage Science*, 10(1): 47-53.  
<https://doi.org/10.1080/10220119.1993.9638321>
- Morris, C. (2017a). Historical vegetation–environment patterns for assessing the impact of climatic change in the mountains of Lesotho. *African Journal of Range and Forage Science*, 34(1): 45-51. <https://doi.org/10.2989/10220119.2017.1333150>
- Morris, C. (2017b). Vegetation gradients around cattleposts in the eastern mountains of Lesotho. *African Journal of Range and Forage Science*, 34(4): 219-225.  
<https://doi.org/10.2989/10220119.2017.1406404>
- Morrisette-Boileau, C., Boudreau, S., Tremblay, J.P. and Côté, S.D. (2018). Revisiting the role of migratory caribou in the control of shrub expansion in northern Nunavik (Québec, Canada). *Polar Biology*, 41(9):1845-1853. <https://doi.org/10.1007/s00300-018-2325-2>
- Moshoeshe, S. and Sekantsi, M. (2013). Lesotho: Desertification Control Program. In: Heshmati, G.A and Squires, V.R. (eds.), *Combating Desertification in Asia, Africa and the Sani Pass-upper East*. Springer, Dordrecht, pp. 153-167.
- Mucina, L, Rutherford, M.C. (2006). The vegetation of South Africa, Lesotho and Swaziland. *Strelitzia* 19: Pretoria: South African National Biodiversity Institute, South Africa. pp. 2-748.
- Mukwada, G. and Manatsa, D. (2018). Spatiotemporal analysis of the effect of climate change on vegetation health in the Drakensberg Mountain Region of South Africa. *Environmental Monitoring and Assessment*, 190(6): 358. <https://doi.org/10.1007/s10661-018-6660-0>

- Munalula, F., Seifert, T. and Meincken, M. (2016). The Expected Effects of Climate Change on Tree Growth and Wood Quality in Southern Africa. *Springer Science Reviews*, 4(2): 99-111. <https://doi.org/10.1007/s40362-017-0042-9>
- Myers-Smith, I.H., Hallinger, M., Blok, D., Sass-Klaassen, U., Rayback, S.A., Weijers, S., Trant, A.J., Tape, K.D., Naito, A.T., Wipf, S., Rixen, C., Dawes, M.A., Wheeler, J.A., Buchwal, A., Baittinger, C., Macias-Fauria, M., Forbes, B.C., Lévesque, E., Boulanger-Lapointe, N., Beil, I., Ravolainen, V. and Wilmking, M. (2015). Methods for measuring arctic and alpine shrub growth: a review. *Earth-Science Reviews*, 140:1-3. <https://doi.org/10.1016/j.earscirev.2014.10.004>
- Naidoo, S., Zbonák, A. and Ahmed, F. (2006). The effect of moisture availability on wood density and vessel characteristics of *Eucalyptus grandis* in the warm temperate region of South Africa. In: Kurjatko, S., Kúdela, J. and Lagaña, R. (eds.). *Wood Structure and Properties '06*. Arbora Publishers, Zvolen, Slovakia, pp. 117-122.
- Nash, D.J. and Adamson, G.C. (2014). Recent advances in the historical climatology of the tropics and subtropics. *Bulletin of the American Meteorological Society*, 95(1): 131-146. <https://doi.org/10.1175/BAMS-D-12-00030.1>
- Nash, D. (2017). Changes in precipitation over southern Africa during recent centuries. Oxford University Press, Oxford Research Encyclopedia of Climate Science. <https://doi.org/10.1007/s10584-018-2352-6>
- Nel, W. and Sumner, P. (2008). Rainfall and temperature attributes on the Lesotho–Drakensberg escarpment edge, southern Africa. *Geografiska Annaler: Series A, Physical Geography*, 90(1): 97-108. <https://doi.org/10.1111/j.1468-0459.2008.00337.x>
- Ngwenya, S.J., Torquebiau, E. and Ferguson, J.W.H. (2018). Mountains as a critical source of ecosystem services: the case of the Drakensberg, South Africa. *Environment, Development and Sustainability*, 1-18. <https://doi.org/10.1007/s10668-017-0071-1>
- Norström, E., Holmgren, K. and Mörth, C.M. (2008). A 600-year-long  $\delta^{18}\text{O}$  record from cellulose of *Breonadia salicina* trees, South Africa. *Dendrochronologia*, 26(1): 21-33. <https://doi.org/10.1016/j.dendro.2007.08.001>



- Norström, E., Bringensparr, C., Fitchett, J.M., Grab, S.W., Rydberg, J. and Kylander, M. (2018). Late-Holocene climate and vegetation dynamics in eastern Lesotho highlands. *The Holocene*, 28(9): 1483-1494. DOI: 10.1177/0959683618777054
- Nsengiyumva, P. (2019). African Mountains in a Changing Climate: Trends, Impacts, and Adaptation Solutions. *Mountain Research and Development*, 39(2): 1-8. <https://doi.org/10.1659/MRD-JOURNAL-D-19-00062.1>
- Nüsser, M. (2002). Maloti-Drakensberg: Naturraum und Nutzungsmuster im Hochgebirge des südlichen Africa, *Petermanns Geographische Mitteilungen*, 146(4): 60-69.
- Nüsser, M. and Grab, S. (2002). Land degradation and soil erosion in the eastern Highlands of Lesotho, Southern Africa. *Die Erde*, 133(3): 291-311.
- Olsson, I.U. 1986. Radiometric Methods. In: Berglung, B. (ed), *Handbook of Holocene Palaeoecology and Palaeohydrology*. John Wiley and Sons, United Kingdom, pp. 273 – 312.
- Opała-Owczarek, M., Błaś, M., Owczarek, P., Sobik, M. and Godek, M. (2019). A dendroclimatological study of east-and west-facing slopes in mountainous areas subjected to strong air pollution (the Sudetes, Central Europe). *Physical Geography*, 40(2): 186-208. <https://doi.org/10.1080/02723646.2018.1547872>
- Owczarek, P. (2010). Dendrochronological dating of geomorphic processes in the High Arctic. *Landform Analysis*, 14: 45-56.
- Owczarek, P., Latocha, A., Wistuba, M. and Malik, I. (2013). Reconstruction of modern debris flow activity in the arctic environment with the use of dwarf shrubs (south-western Spitsbergen) – (south-western Spitsbergen) a new dendrochronological approach. *Zeitschrift für Geomorphologie, Supplementary Issue*, 57(3): 75-95. <https://doi.org/10.1127/0372-8854/2013/S-00145>
- Owczarek, P. and Opała, M. (2016). Dendrochronology and extreme pointer years in the tree-ring record (AD 1951–2011) of polar willow from southwestern Spitsbergen (Svalbard, Norway). *Geochronometria*, 43(1): 84-95. DOI 10.1515/geochr-2015-0035
- Panthi, S., Bräuning, A., Zhou, Z.K. and Fan, Z.X. (2018). Growth response of *Abies georgei* to climate increases with elevation in the central Hengduan Mountains, southwestern China. *Dendrochronologia*, 47: 1-9. <https://doi.org/10.1016/j.dendro.2017.11.001>

- Patrut, A., Von Reden, K.F., Lowy, D.A., Alberts, A.H., Pohlman, J.W., Wittmann, R., Gerlach, D., Xu, L. and Mitchell, C.S., (2007). Radiocarbon dating of a very large African baobab. *Tree Physiology*, 27(11):1569-1574. <https://doi.org/10.1093/treephys/27.11.1569>
- Patrut, A., Karl, F., Danthu, P., Pock-Tsy, J.M.L., Patrut, R.T. and Lowy, D.A. (2015). Searching for the oldest baobab of Madagascar: Radiocarbon investigation of large *Adansonia rubrostipa* trees. *PLOS One*, 10(3): e0121170. <https://doi.org/10.1371/journal.pone.0121170>
- Patrut, A., Woodborne, S., Patrut, R.T., Hall, G., Rakosy, L., Winterbach, C., and Von Reden, K.F. (2019). Age, Growth and Death of a National Icon: The Historic Chapman Baobab of Botswana. *Forests*, 10(11): 983. <https://doi.org/10.3390/f10110983>
- Patton, A.I., Rathburn, S.L. and Capps, D.M. (2019). Landslide response to climate change in permafrost regions. *Geomorphology*, 340: 116-128. <https://doi.org/10.1016/j.geomorph.2019.04.029>
- Pauchard, A., Milbau, A., Albiñ, A., Alexander, J., Burgess, T., Daehler, C. and Haider, S. (2015). Non-native and native organisms moving into high elevation and high latitude ecosystems in an era of climate change: new challenges for ecology and conservation. *Biological Invasions*, 18(2): 345-353. <https://doi.org/10.1007/s10530-015-1025-x>
- Pauli, H., Gottfried, M., Dullinger, S., Abdaladze, O., Akhalkatsi, M., Alonso, J.L.B., Coldea, G., Dick, J., Erschbamer, B., Calzado, R.F., Ghosn, D., Holten, J.I., Kanka, R., Kazakis, G., Kollar, J., Larsson, P., Moiseev, P., Moiseev, D., Molau, U., Mesa, J.M., Nagy, L., Pelino, G., Puşcaş, M., Rossi, G., Stanisci, A., Syverhuset, A.O., Theurillat, J.P., Tomaselli, M., Unterluggauer, P., Villar, L., Vittoz, P. and Grabherr, G. (2012). Recent Plant Diversity Changes on Europe's Mountain Summits. *Science*, 336(6079): 353-355. DOI: 10.1126/science.1219033
- Pauli, H., Gottfried, M., Dirnböck, T., Dullinger, S. and Grabherr, G. (2003). Assessing the long-term dynamics of endemic plants at summit habitats. In: Nagy, L., Grabherr, G., Körner, C. and Thompson, D.B.A. (eds.), *Alpine Biodiversity in Europe (ECOLSTUD, volume 167)*. Springer, Berlin, Heidelberg, pp. 195-207. [https://doi.org/10.1007/978-3-642-18967-8\\_9](https://doi.org/10.1007/978-3-642-18967-8_9)
- Pignatelli, O. (2010). Dendrochronology. In: Kasal, B. and Tannert, T. (eds.) *In Situ Assessment of Structural Timber*, Springer: Dordrecht, 109-114. [https://doi.org/10.1007/978-94-007-0560-9\\_13](https://doi.org/10.1007/978-94-007-0560-9_13)

- Prävălie, R. (2014). Nuclear weapons tests and environmental consequences: a global perspective. *Ambio*, 43(6): 729-744. <https://dx.doi.org/10.1007%2Fs13280-014-0491-1>
- Pooley, E. (2003). *Mountain flowers: A field guide to the flora of the Drakensberg and Lesotho*. Flora Publication Trust, Durban North, South Africa. pp.1-320.
- Quarta, G., d'Elia, M., Valzano, D. and Calcagnile, L. (2005). New bomb pulse radiocarbon records from annual tree rings in the northern hemisphere temperate region. *Radiocarbon*, 47(1): 27-30. <https://doi.org/10.1017/S0033822200052164>
- Ramsey, C.B. (2001). Development of the radiocarbon calibration program. *Radiocarbon*, 43(2A): 355-363.
- Ramsey, C. (2008). Radiocarbon dating: revolutions in understanding. *Archaeometry*, 50(2), 249-275. <https://doi.org/10.1111/j.1475-4754.2008.00394.x>
- Ramsey, C. (2009). Bayesian analysis of radiocarbon dates. *Radiocarbon*, 51(1): 337-360. <https://doi.org/10.1017/S0033822200033865>
- Rathgeber, C.B., Cuny, H.E. and Fonti, P. (2016). Biological basis of tree-ring formation: a crash course. *Frontiers in Plant Science*, 7: 734. <https://doi.org/10.3389/fpls.2016.00734>
- Rayback, S.A., Shrestha, K.B. and Hofgaard, A. (2017). Growth variable-specific moisture and temperature limitations in co-occurring alpine tree and shrub species, central Himalayas, Nepal. *Dendrochronologia*, 44: 193-202. <https://doi.org/10.1016/j.dendro.2017.06.001>
- Reimer, P.J., Brown, T.A. and Reimer, R.W. (2004). Discussion: reporting and calibration of post-bomb <sup>14</sup>C data. *Radiocarbon*, 46(3): 1299-1304. <https://doi.org/10.1017/S0033822200033154>
- Robertson, I., Loader, N.J., Froyd, C.A., Zambatis, N., Whyte, I. and Woodborne, S. (2006). The potential of the baobab (*Adansonia digitata* L.) as a proxy climate archive. *Applied Geochemistry*, 21(10), 1674-1680. <https://doi.org/10.1016/j.apgeochem.2006.07.005>
- Rogora, M., Frate, L., Carranza, M.L., Freppaz, M., Stanisci, A., Bertani, I., Bottarin, R., Brambilla, A., Canullo, R., Carbognani, M. and Cerrato, C. (2018). Assessment of climate change effects on mountain ecosystems through a cross-site analysis in the Alps and Apennines. *Science of the Total Environment*, 624: 1429-1442. <https://doi.org/10.1016/j.scitotenv.2017.12.155>

- Röpke, A., Stobbe, A., Oeggl, K., Kalis, A.J. and Tinner, W. (2011). Late-Holocene land-use history and environmental changes at the high altitudes of St Antönien (Switzerland, Northern Alps): Combined evidence from pollen, soil and tree-ring analyses. *The Holocene*, 21(3): 485-498. <https://doi.org/10.1177%2F0959683610385727>
- Schweingruber, F.H., Poschlod, P. (2005). Growth rings in herbs and shrubs: life span, age determination and stem anatomy. In: Innes, J.L. and Hogan, D.L. (eds.), *Forest Snow and Landscape Research (Volume 79)*. Birmensdorf: Swiss Federal Research Institute WSL, pp. 246
- Schweingruber, F.H. and Börner, A. (2018). Evolution of stems. In: Schweingruber, F.H. and Börner, A. *The Plant Stem*. Springer, Cham, pp. 121-132.
- Schwinning, S., Sala, O.E., Loik, M.E. and Ehleringer, J.R. (2004). Thresholds, memory, and seasonality: understanding pulse dynamics in arid/ semi-arid ecosystems. *Oecologia*, 141, 191-193. <https://doi.org/10.1007/s00442-004-1683-3>
- Scott, L., Holmgren, K., Talma, A.S., Woodborne, S. and Vogel, J.C. (2003). Age interpretation of the Wonderkrater spring sediments and vegetation change in the Savanna Biome, Limpopo province, South Africa. *South African Journal of Science*, 99(9-10): 484-488. <https://hdl.handle.net/10520/EJC97686>
- Sene, K.J., Jones, D.A., Meigh, J.R. and Farquharson, F.A.K. (1998). Rainfall and flow variations in the Lesotho Highlands. *International Journal of Climatology: A Journal of the Royal Meteorological Society*, 18(3): 329-345. [https://doi.org/10.1002/\(SICI\)1097-0088\(19980315\)18:3%3C329::AID-JOC251%3E3.0.CO;2-5](https://doi.org/10.1002/(SICI)1097-0088(19980315)18:3%3C329::AID-JOC251%3E3.0.CO;2-5)
- Serdeczny, O., Adams, S., Baarsch, F., Coumou, D., Robinson, A., Hare, W., Schaeffer, M., Perrette, M. and Reinhardt, J. (2017). Climate change impacts in Sub-Saharan Africa: from physical changes to their social repercussions. *Regional Environmental Change*, 17(6):1585-1600. <https://doi.org/10.1007/s10113-015-0910-2>
- Shetti, R., Buras, A., Smiljanic, M. and Wilmking, M. (2018). Climate sensitivity is affected by growth differentiation along the length of *Juniperus communis* L. shrub stems in the Ural Mountains. *Dendrochronologia*, 49: 29-35. <https://doi.org/10.1016/j.dendro.2018.02.006>

- Shi, J., Lu, H., Li, J., Shi, S., Wu, S., Hou, X. and Li, L. (2015). Tree-ring based February–April precipitation reconstruction for the lower reaches of the Yangtze River, southeastern China. *Global and Planetary Change*, 131: 82-88. <https://doi.org/10.1016/j.gloplacha.2015.05.006>
- Shroder Jr., J.F. (1980). Dendrogeomorphology: review and new techniques of tree-ring dating. *Progress in Physical geography*, 4(2): 161-188. <https://doi.org/10.1177/030913338000400202>
- Sithole, A. and Murewi, C.T. (2009). Climate variability and change over southern Africa: impacts and challenges. *African Journal of Ecology*, 47, 17-20. <https://doi.org/10.1111/j.1365-2028.2008.01045.x>
- Slota, F., Helle, G., Heussner, K.U., Shemang, E., Riedel, F. and Heußner, K.U. (2017). Baobabs on Kubu Island, Botswana, - A dendrochronological multiparameter study using ring width and stable isotopes ( $\delta^{13}\text{C}$ ,  $\delta^{18}\text{O}$ ). *Erdkunde*, 71(1): 23-43. <https://www.jstor.org/stable/44280264>
- Spehn, E.M., Rudmann-Maurer, K. and Körner, C. (2011). Mountain biodiversity. *Plant Ecology and Diversity*, 4(4): 301-302. <https://doi.org/10.1080/17550874.2012.698660>
- Stewart, B.A. and Mitchell, P.J. (2018). Late Quaternary palaeoclimates and human-environment dynamics of the Maloti-Drakensberg region, southern Africa. *Quaternary Science Reviews*, 196: 1-20. <https://doi.org/10.1016/j.quascirev.2018.07.014>
- Sofer, Z. (1980). Preparation of carbon dioxide for stable carbon isotope analysis of petroleum fractions. *Analytical Chemistry*, 52(8): 1389-1391. <https://doi.org/10.1021/ac50058a063>
- Stahle, D.W. (1999). Useful strategies for the development of tropical tree-ring chronologies. *IAWA Journal*, 20(3): 249-253. <https://doi.org/10.1163/22941932-90000688>
- Stoffel, M. and Bollschweiler, M. (2008). Tree-ring analysis in natural hazards research? an overview. *Natural Hazards and Earth System Science*, 8(2): 187-202.
- Strachan, K.L., Finch, J.M., Hill, T. and Barnett, R.L. (2014). A late Holocene sea-level curve for the east coast of South Africa. *South African Journal of Science*, 110(1-2): 1-9.
- Steenkamp, C.J., Vogel, J.C., Fuls, A., Van Rooyen, N. and Van Rooyen, M.W. (2008). Age determination of *Acacia erioloba* trees in the Kalahari. *Journal of Arid Environments*, 72(4): 302-313. <https://doi.org/10.1016/j.jaridenv.2007.07.015>

- Stock, W.D., Chuba, D.K. and Verboom, G.A. (2004). Distribution of South African C<sub>3</sub> and C<sub>4</sub> species of Cyperaceae in relation to climate and phylogeny. *Austral Ecology*, 29(3): 313-319. <https://doi.org/10.1111/j.1442-9993.2004.01368.x>
- Stuiver, M. (1961). Variations in radiocarbon concentration and sunspot activity. *Journal of Geophysical Research*, 66(1): 273-276.
- Stuiver, M. and Polach, H.A. (1977). Discussion reporting of <sup>14</sup>C data. *Radiocarbon*, 19(3): 355-363.
- Stuiver, M. and Reimer, P.J. (1993). Extended <sup>14</sup>C data base and revised CALIB 3.0 <sup>14</sup>C age calibration program. *Radiocarbon*, 35(1): 215-230. <https://doi.org/10.1017/S0033822200013904>
- Suess, H.E. (1955). Radiocarbon concentration in modern wood. *Science*, 122(3166): 415-417.
- Suess, H.E. (1980). The radiocarbon record in tree rings of the last 8 000 years. *Radiocarbon*, 22(2): 200-209. <https://doi.org/10.1017/S0033822200009462>
- Syampungani, S., Geldenhuys, C.J. and Chirwa, P.W. (2010). Age and growth rate determination using growth rings of selected miombo woodland species in charcoal and, slash and burn regrowth stands in Zambia. *Journal of Ecology and the Natural Environment*, 2: 167–174.
- Therrell, M.D., Stahle, D.W., Ries, L.P. and Shugart, H.H. (2006). Tree-ring reconstructed rainfall variability in Zimbabwe. *Climate Dynamics*, 26(7-8): 677. <https://doi.org/10.1007/s00382-005-0108-2>
- Therrell, M.D., Stahle, D.W., Mukelabai, M.M. and Shugart, H.H. (2007). Age, and radial growth dynamics of *Pterocarpus angolensis* in southern Africa. *Forest Ecology and Management*, 244(1-3): 24-31. <https://doi.org/10.1016/j.foreco.2007.03.023>
- Thomas, C.D. (2010). Climate, climate change and range boundaries. *Diversity and Distributions*, 16(3): 488-495. <https://doi.org/10.1111/j.1472-4642.2010.00642.x>
- Torbenson, M.C.A. (2015). Section 4.2.8: Dendrochronology. In: British Society for Geomorphology, *Geomorphological Techniques (Chapter 4 Section 2.8)*. (Online edition, ISSN 2047-0371).

- Trouet, V., Haneca, K., Coppin, P. and Beeckman, H. (2001). Tree ring analysis of *Brachystegia spiciformis* and *Isoberlinia tomentosa*: evaluation of the enso-signal in the Miombo woodland of eastern Africa. *IAWA Journal*, 22(4), 385-399. <https://doi.org/10.1163/22941932-90000384>
- Trouet, V., Coppin, P. and Beeckman, H. (2006). Annual growth ring patterns in *Brachystegia spiciformis* reveal influence of precipitation on tree growth. *Biotropica: The Journal of Biology and Conservation*, 38(3): 375-382. <https://doi.org/10.1111/j.1744-7429.2006.00155.x>
- Trouet, V., Esper, J. and Beeckman, H. (2010). Climate/ growth relationships of *Brachystegia spiciformis* from the miombo woodland in south central Africa. *Dendrochronologia*, 28(3): 161-171. <https://doi.org/10.1016/j.dendro.2009.10.002>
- Twine, W.C. and Holdo, R.M. (2016). Fuelwood sustainability revisited: integrating size structure and resprouting into a spatially realistic fuelshed model. *Journal of Applied Ecology*, 53(6): 1766-1776. DOI: 10.1111/1365-2664.12713
- Tyson, P.D., Cooper, G.R.J. and McCarthy, T.S. (2002). Millennial to multi-decadal variability in the climate of southern Africa. *International Journal of Climatology: A Journal of the Royal Meteorological Society*, 22(9): 1105-1117. <https://doi.org/10.1002/joc.787>
- United Nations Environmental Programme (UNEP). (2016). Vulnerability Assessment Report - UNEP/GEF Climate change study in Lesotho, Project Number GF/2200-96-16. 38-39.
- Vandeputte, K., Moens, L. and Dams, R. (1996). Improved sealed-tube combustion of organic samples to CO<sub>2</sub> for stable carbon isotope analysis, radiocarbon dating and percent carbon determinations. *Analytical Letters*, 29(15): 2761-2773. <https://doi.org/10.1080/00032719608002279>
- Van Strydonck, M. (2016). Radiocarbon Dating. *Topics in Current Chemistry*, 374(13): 1-18. DOI: 10.1007/s41061-016-0011-9.
- Van Wyk, A.E. and Smith, G.F. (2001). Regions of floristic endemism in southern Africa: a review with emphasis on succulents. Umdaus Press, Pretoria, pp. 110-116.
- Vogel, J.S., Southon, J.R., Nelson, D.E. and Brown, T.A. (1984). Performance of catalytically condensed carbon for use in accelerator mass spectrometry. *Nuclear Instruments and Methods in Physics Research Section B: Beam Interactions with Materials and Atoms*, 5(2): 289-293. [https://doi.org/10.1016/0168-583X\(84\)90529-9](https://doi.org/10.1016/0168-583X(84)90529-9)

- Vogel, J.C., Fuls, A. and Visser, E. (2001). Radiocarbon adjustments to the dendrochronology of a yellowwood tree. *South African Journal of Science*, 97(3-4): 164-166.  
<https://hdl.handle.net/10520/EJC97292>
- Walther, G.R., Post, E., Convey, P., Menzel, A., Parmesan, C., Beebee, T.J., Fromentin, J.M., Hoegh-Guldberg, O. and Bairlein, F. (2002). Ecological responses to recent climate change. *Nature*, 416(6879): 389-395. <https://doi.org/10.1038/416389a>
- Weijers, S., Broekman, R. and Rozema, J. (2010). Dendrochronology in the High Arctic: July air temperatures reconstructed from annual shoot length growth of the circumarctic dwarf shrub *Cassiope tetragona*. *Quaternary Science Reviews*, 29(27-28): 3831-3842.  
<https://doi.org/10.1016/j.quascirev.2010.09.003>
- Wielgolaski, F.E. (1966). The influence of air temperature on plant growth and development during the period of maximal stem elongation. *Oikos*, 17(2): 121-141. DOI: 0.2307/3564937
- Wikle, T.A. (2015). Subsistence Farming and Economic Hardship in Lesotho, Africa's Mountain Kingdom. *Focus on Geography*, 58(2): 79-90. <https://doi.org/10.1111/foge.12051>
- Wilkening, J., Pearson-Prestera, W., Mungi, N.A. and Bhattacharyya, S. (2019). Endangered species management and climate change: When habitat conservation becomes a moving target. *Wildlife Society Bulletin*, 43(1): 11-20. <https://doi.org/10.1002/wsb.944>
- Wimmer, R. (2002). Wood anatomical features in tree-rings as indicators of environmental change. *Dendrochronologia*, 20(1-2): 21-36. <https://doi.org/10.1078/1125-7865-00005>
- Woodborne, S., Mélice, J.L. and Scholes, R.J. (2008). Long-term sunspot forcing of savanna structure inferred from carbon and oxygen isotopes. *Geophysical Research Letters*, 35(2):1-4.  
<https://doi.org/10.1029/2007GL032019>
- Woodborne, S., Hall, G., Robertson, I., Patrut, A., Rouault, M., Loader, N. J. and Hofmeyr, M. (2015). A 1000-year carbon isotope rainfall proxy record from South African baobab trees (*Adansonia digitata* L.). *PLOS One*, 10(5): e0124202.  
<https://doi.org/10.1371/journal.pone.0124202>
- Woodborne, S., Gandiwa, P., Hall, G., Patrut, A. and Finch, J. (2016). A Regional Stable Carbon Isotope Dendro-Climatology from the South African Summer Rainfall Area. *PLOS One*, 11(7): e0159361. <https://doi.org/10.1371/journal.pone.0159361>



- Worbes, M. (1995). How to measure growth dynamics in tropical trees a review. *IAWA journal*: 16(4), 337-351. <https://doi.org/10.1163/22941932-90001424>
- Young, A.B., Watts, D.A., Taylor, A.H. and Post, E. (2016). Species and site differences influence climate-shrub growth responses in West Greenland. *Dendrochronologia*, 37: 69-78. <https://doi.org/10.1016/j.dendro.2015.12.007>
- Zhang, X., Bai, X., Hou, M., Chen, Z. and Manzanedo, R.D. (2019). Warmer winter ground temperatures trigger rapid growth of *Dahurian larch* in the permafrost forests of northeast China. *Journal of Geophysical Research: Biogeosciences*. 124: 1-10. <https://doi.org/10.1029/2018JG004882>
- Ziervogel, G., New, M., Archer van Garderen, E., Midgley, G., Taylor, A., Hamann, R., Stuart-Hill, S., Myers, J. and Warburton, M. (2014). Climate change impacts and adaptation in South Africa. *Wiley Interdisciplinary Reviews: Climate Change*, 5(5):605-620. <https://doi.org/10.1002/wcc.295>
- Zimowski, M., Leuschner, H. H., Gärtner, H. and Bergmeier, E. (2014). Age and diversity of Mediterranean dwarf shrublands: a dendrochronological approach along an altitudinal gradient on Crete. *Journal of Vegetation Science*, 25(1): 122-134. <https://doi.org/10.1111/jvs.12067>
- Zoppi, U. (2010). Radiocarbon AMS Data Analysis: From Measured Isotopic Ratios to  $^{14}\text{C}$  Concentrations. *Radiocarbon*, 52(1): 165-170. <https://doi.org/10.1017/S0033822200045112>

# APPENDIXES

## Appendix i: Sample information

Kotisephola Pass study site

Sample name	Shrub species	Slope	Slope angle (degrees)	Coordinates	Elevation (m a.s.l)
AS1	<i>Helichrysum trilineatum</i>	S	182	29°31'4.8"S 29°11'57.3"E	3325
AS2	<i>Helichrysum trilineatum</i>	SSW	199	29°31'5.17"S 29°11'57.19"E	3324
AS3	<i>Helichrysum trilineatum</i>	SSW	202	29°31'4.48"S 29°11'56.43"E	3323
AS4	<i>Helichrysum trilineatum</i>	SW	222	29°31'4.38"S 29°11'56.65"E	3324
AS5	<i>Helichrysum trilineatum</i>	SW	230	29°31'4.42"S 29°11'56.49"E	3323
AS6	<i>Helichrysum trilineatum</i>	SW	221	29°31'4.46"S 29°11'56.38"E	3322
AS7	<i>Helichrysum trilineatum</i>	SSW	200	29°31'5.14"S 29°11'56.51"E	3322
AS8	<i>Helichrysum trilineatum</i>	S	183	29°31'5.01"S 29°11'57.62"E	3325
AS9	<i>Helichrysum trilineatum</i>	S	178	29°31'12.59"S 29°11'55.81"E	3294
AS10	<i>Helichrysum trilineatum</i>	SW	223	29°31'14.33"S 29°11'54.16"E	3285
AS11	<i>Helichrysum trilineatum</i>	SSW	202	29°31'15.98"S 29°11'55.82"E	3282
AS12	<i>Helichrysum trilineatum</i>	SSW	200	29°31'11.83"S 29°11'58.88"E	3298
AS13	<i>Helichrysum trilineatum</i>	SW	225	29°31'7.11"S 29°12'4.75"E	3303
AW1	<i>Helichrysum trilineatum</i>	WSW	244	29°31'10"S 29°11'52.54"E	3290
AW2	<i>Helichrysum trilineatum</i>	WSW	249	29°31'9.9"S 29°11'52.56"E	3290
AW3	<i>Helichrysum trilineatum</i>	W	265	29°31'9.35"S 29°11'52.92"E	3294
AW4	<i>Helichrysum trilineatum</i>	W	268	29°31'8.42"S 29°11'53.77"E	3301
AW5	<i>Helichrysum trilineatum</i>	W	273	29°31'8.41"S 29°11'54.56"E	3305

AW6	<i>Helichrysum trilineatum</i>	WSW	253	29°31'3.77"S 29°11'50.25"E	3291
AW7	<i>Helichrysum trilineatum</i>	WSW	248	29°31'3.10"S 29°11'51.72"E	3301
AW8	<i>Helichrysum trilineatum</i>	W	271	29°30'58.74"S 29°11'55.52"E	3327
AW9	<i>Helichrysum trilineatum</i>	W	269	29°30'57.01"S 29°11'55.86"E	3328
AW10	<i>Helichrysum trilineatum</i>	WNW	289	29°30'57.15"S 29°11'56.29"E	3332
AN1	<i>Helichrysum trilineatum</i>	NNW	333	29°31'0.45"S 29°11'57.33"E	3327
AN2	<i>Helichrysum trilineatum</i>	NNW	339	29°31'0.39"S 29°11'57.32"E	3327
AE1	<i>Helichrysum trilineatum</i>	E	93	29°31'3.2"S 29°11'58.89"E	3328
AE2	<i>Helichrysum trilineatum</i>	ESE	113	29°31'3.39"S 29°12'0.62"E	3325
AE3	<i>Helichrysum trilineatum</i>	ESE	111	29°31'3.16"S 29°11'59.55"E	3329
AE4	<i>Helichrysum trilineatum</i>	SSE	158	29°31'2.64"S 29°12'2.08"E	3317
AE5	<i>Helichrysum trilineatum</i>	SSE	160	29°31'3.29"S 29°12'3.11"E	3311
AE6	<i>Helichrysum trilineatum</i>	SE	133	29°31'4.60"S 29°12'2.11"E	3318
AE7	<i>Helichrysum trilineatum</i>	E	89	29°31'5.69"S 29°12'4.25"E	3306
AE8	<i>Helichrysum trilineatum</i>	SSE	155	29°31'5.7"S 29°12'4.14"E	3306
AE9	<i>Helichrysum trilineatum</i>	SE	135	29°31'6.57"S 29°12'5.04"E	3302
BS1	<i>Helichrysum witbergense</i>	SSW	195	29°31'3.01"S 29°11'57.62"E	3329
BS2	<i>Helichrysum witbergense</i>	SSW	198	29°31'5.22"S 29°11'57.31"E	3324
BS3	<i>Helichrysum witbergense</i>	SSW	188	29°31'4.81"S 29°11'57.3"E	3325
BS4	<i>Helichrysum witbergense</i>	SW	224	29°31'5.25"S 29°11'57.77"E	3325
BS5	<i>Helichrysum witbergense</i>	SW	219	29°31'4.82"S 29°11'58.39"E	3327
BS6	<i>Helichrysum witbergense</i>	SSW	199	29°31'9.61"S 29°11'56.36"E	3309

BS7	<i>Helichrysum witbergense</i>	SSW	187	29°31'9.61"S 29°11'56.36"E	3309
BS8	<i>Helichrysum witbergense</i>	WSW	239	29°31'9.99"S 29°11'55.97"E	3306
BW1	<i>Helichrysum witbergense</i>	WSW	245	29°31'8.25"S 29°11'55.02"E	3308

### Sani Pass-upper study site

Sample name	Shrub species	Slope	Slope angle (degrees)	Coordinates	Elevation (m a.s.l)
CW1	<i>Helichrysum trilineatum</i>	W	272	29°34'43.99"S 29°15'46.94"E	2904
CW2	<i>Helichrysum trilineatum</i>	WSW	246	29°34'43.87"S 29°15'46.84"E	2902
CW3	<i>Helichrysum trilineatum</i>	W	269	29°34'42.82"S 29°15'46.42"E	2912
CW4	<i>Helichrysum trilineatum</i>	W	290	29°34'42.92"S 29°15'46.14"E	2916
CS1	<i>Helichrysum trilineatum</i>	WSW	223	29°34'39.48"S 29°16'16.41"E	2883
CS2	<i>Helichrysum trilineatum</i>	SSW	202	29°34'39.15"S 29°16'16.24"E	2884
CS3	<i>Helichrysum trilineatum</i>	S	182	29°34'38.32"S 29°16'14.74"E	2896
CS4	<i>Helichrysum trilineatum</i>	S	179	29°34'37.13"S 29°16'14.79"E	2901
CS5	<i>Helichrysum trilineatum</i>	SSW	201	29°34'40.30"S 29°16'17.25"E	2883
CN1	<i>Helichrysum trilineatum</i>	N	336	29°34'18.91"S 29°15'58.45"E	2870
CN2	<i>Helichrysum trilineatum</i>	N	358	29°34'19.07"S 29°15'58.72"E	2869
CN3	<i>Helichrysum trilineatum</i>	NNE	24	29°34'18.88"S 29°15'58.86"E	2871
CN4	<i>Helichrysum trilineatum</i>	N	3	29°34'20.05"S 29°15'59.49"E	2879
CN5	<i>Helichrysum trilineatum</i>	NNE	22	29°34'20.08"S 29°15'59.50"E	2877
CN6	<i>Helichrysum trilineatum</i>	N	5	29°34'20.30"S 29°15'59.55"E	2877
CE1	<i>Helichrysum trilineatum</i>	E	89	29°34'16.41"S 29°16'7.86"E	2859
CE2	<i>Helichrysum trilineatum</i>	E	66	29°34'16.62"S 29°16'8.06"E	2864
CE3	<i>Helichrysum trilineatum</i>	ESE	110	29°34'16.99"S 29°16'7.80"E	2867
CE4	<i>Helichrysum trilineatum</i>	E	92	29°34'17.32"S 29°16'6.41"E	2871

CE5	<i>Helichrysum trilineatum</i>	ESE	112	29°34'17.18"S 29°16'6.52"E	2870
-----	--------------------------------	-----	-----	-------------------------------	------

### Sani Pass-lower study site

Sample name	Shrub species	Slope	Slope angle (degrees)	Coordinates	Elevation (m a.s.l)
D1	<i>Helichrysum tenuifolium</i>	E	89	29°35'28.63"S 29°17'43.5"E	2568
D2	<i>Helichrysum tenuifolium</i>	E	86	29°35'28.63"S 29°17'43.5"E	2568
D3	<i>Helichrysum tenuifolium</i>	E	91	29°35'28.63"S 29°17'43.5"E	2568
D4	<i>Helichrysum tenuifolium</i>	E	90	29°35'28.63"S 29°17'43.5"E	2568
D5	<i>Helichrysum tenuifolium</i>	E	91	29°35'28.63"S 29°17'43.5"E	2568
D6	<i>Helichrysum tenuifolium</i>	E	89	29°35'28.63"S 29°17'43.5"E	2568
D7	<i>Helichrysum tenuifolium</i>	E	88	29°35'28.63"S 29°17'43.5"E	2568
D8	<i>Helichrysum tenuifolium</i>	E	91	29°35'28.63"S 29°17'43.5"E	2568
D9	<i>Helichrysum tenuifolium</i>	E	92	29°35'28.63"S 29°17'43.5"E	2568
D10	<i>Helichrysum tenuifolium</i>	E	94	29°35'28.63"S 29°17'43.5"E	2568
D11	<i>Helichrysum tenuifolium</i>	E	90	29°35'28.63"S 29°17'43.5"E	2568
D12	<i>Helichrysum tenuifolium</i>	E	87	29°35'28.63"S 29°17'43.5"E	2568
D13	<i>Helichrysum tenuifolium</i>	E	89	29°35'28.63"S 29°17'43.5"E	2568
D14	<i>Helichrysum tenuifolium</i>	E	90	29°35'28.83"S 29°17'44.85"E	2514
D15	<i>Helichrysum tenuifolium</i>	E	92	29°35'28.66"S 29°17'45.08"E	2560
D16	<i>Helichrysum tenuifolium</i>	E	90	29°35'28.66"S 29°17'45.08"E	2560
D17	<i>Helichrysum tenuifolium</i>	E	91	29°35'28.66"S 29°17'45.08"E	2560
D18	<i>Helichrysum tenuifolium</i>	E	93	29°35'28.66"S 29°17'45.08"E	2560
D19	<i>Helichrysum tenuifolium</i>	E	88	29°35'28.66"S 29°17'45.08"E	2560
D20	<i>Helichrysum tenuifolium</i>	E	89	29°35'28.66"S 29°17'45.08"E	2560
D21	<i>Helichrysum tenuifolium</i>	E	90	29°35'28.66"S 29°17'45.08"E	2560

D22	<i>Helichrysum tenuifolium</i>	E	90	29°35'28.66"S 29°17'45.08"E	2560
D23	<i>Helichrysum tenuifolium</i>	E	89	29°35'28.66"S 29°17'45.08"E	2560
D24	<i>Helichrysum tenuifolium</i>	E	88	29°35'28.66"S 29°17'45.08"E	2560
D25	<i>Helichrysum tenuifolium</i>	E	90	29°35'29.17"S 29°17'44.95"E	2556
D26	<i>Helichrysum tenuifolium</i>	E	92	29°35'29.17"S 29°17'44.95"E	2556
D27	<i>Helichrysum tenuifolium</i>	E	91	29°35'29.17"S 29°17'44.95"E	2556
E1	<i>Helichrysum trilineatum</i>	E	87	29°35'27.58"S 29°17'43.82"E	2585
E2	<i>Helichrysum trilineatum</i>	E	93	29°35'27.58"S 29°17'43.82"E	2585
E3	<i>Helichrysum trilineatum</i>	E	92	29°35'27.58"S 29°17'43.82"E	2585
E4	<i>Helichrysum trilineatum</i>	E	91	29°35'27.58"S 29°17'43.82"E	2585
E5	<i>Helichrysum trilineatum</i>	E	88	29°35'27.04"S 29°17'44.06"E	2564
E6	<i>Helichrysum trilineatum</i>	E	92	29°35'27.04"S 29°17'44.06"E	2564
E7	<i>Helichrysum trilineatum</i>	E	90	29°35'27.04"S 29°17'44.06"E	2564
E8	<i>Helichrysum trilineatum</i>	E	89	29°35'27.04"S 29°17'44.06"E	2564
E9	<i>Helichrysum trilineatum</i>	E	91	29°35'27.04"S 29°17'44.06"E	2564

Appendix ii: AMS Radiocarbon dating results

Sample	Lab	$\delta^{13}\text{C}$	pMC	pMC_err	Age	Age err
T1.1	IT-C-1734	-27.8	110.7	0.6	-820	40
T1.2	IT-C-1740	-27.8	122.2	0.9	-1610	60
T1.2	IT-C-1903	-27.8	129.6	4.9	-2080	300
T2.1	IT-C-1739	-28.6	109.8	1.3	-750	90
T2.2	IT-C-1722	-28.6	148.2	1.8	-3160	100
T2.2	IT-C-1895	-28.6	150.1	1.1	-3260	60
T3.1	IT-C-1729	-27.2	107.6	1	-590	80
T3.1	IT-C-1896	-27.2	109.3	0.6	-710	40
T3.2	IT-C-1732	-27.3	118.6	1.8	-1370	120
T3.2	IT-C-1901	-27.3	121.9	0.6	-1590	40
T4.1	IT-C-1770	-29.2	105.2	0.6	-410	40
T4.2	IT-C-1721	-29.2	110.7	0.4	-820	30
T5.1	IT-C-1735	-28.3	105	0.6	-390	50
T5.2	IT-C-1731	-27	107.9	2.7	-610	200
T5.2	IT-C-1900	-27	112.3	0.5	-930	40
T6.1	IT-C-1726	-27.5	106.8	0.9	-530	60
T6.1	IT-C-1894	-27.5	108.1	0.9	-630	70
T6.2	IT-C-1736	-27.1	118.1	0.5	-1340	30
T7.2	IT-C-1724	-29.3	106.6	1	-510	80
T7.2	IT-C-1904	-29.3	109.6	0.6	-740	40
T8.1	IT-C-1718	-28.2	105	0.6	-390	40
T8.2	IT-C-1737	-28.8	110.7	0.6	-820	40
T9.1	IT-C-1741	-29.2	104.5	0.6	-350	40
T9.2	IT-C-1742	-27.9	107.6	1	-590	80
T9.2	IT-C-1898	-27.9	108.9	0.6	-680	40
T10.1	IT-C-1730	-27	104.7	0.6	-370	40
T10.2	IT-C-1727	-28.6	99.9	1.2	10	100
T10.2	IT-C-1899	-28.1	110.2	0.5	-780	40
T11.1	IT-C-1751	-28.6	106.2	0.6	-480	40
T11.2	IT-C-1738	-30	108.1	0.9	-630	70
T12.1	IT-C-1733	-28.5	105.3	2	-410	150
T12.2	IT-C-1725	-28.6	105.3	1.2	-410	90
T12.2	IT-C-1897	-28.6	108.3	1.1	-640	80
T13.2	IT-C-1723	-29	105.7	0.6	-450	50
T14.2	IT-C-1720	-29.1	107.1	0.4	-550	30

Lab # : Laboratory analysis number  $\delta^{13}\text{C}$  : A measurement that indicates the source of the C in the sample and is used in the production of the final date

pMC : An acronym for the “percent modern carbon”. A standard radiocarbon term indicating sampling age

pMC err : The error on the measurement of pMC

Age : The age of the sample expressed in “radiocarbon years” before present (1950)

Age err : The error estimate on the radiocarbon age

### Appendix iii: Mean correlation results

Mean correlations of shrub growth chronologies of shrub species located at different elevations and aspects. Significant level of  $p < 0.05$ .

	KHTr - E	KHTr - ESE	KHTr - SE	KHTr - SSE	KHTr - S	KHTr - SSW	KHTr - SW	KHTr - WSW	KHTr - W	KHTr - WNW	KHTr - NNW	KHW - WSW	KHW - SSW	KHW - SW	SUTr - N	SUTr - NNE	SUTr - E	SUTr - ESE	SUTr - S	SUTr - SSW	SUTr - WSW	SUTr - W	SLHTe - E	SLHTr - E
KHTr - E	0.27																							
KHTr - ESE	-0.20	0.71																						
KHTr - SE	-0.27	0.27	0.69																					
KHTr - SSE	-0.13	0.05	-0.47	0.75																				
KHTr - S	0.04	0.37	-0.02	0.65	0.82																			
KHTr - SSW	0.01	-0.02	-0.22	0.70	0.77	0.72																		
KHTr - SW	-0.29	-0.15	-0.19	0.11	0.27	0.45	0.83																	
KHTr - WSW	0.42	0.01	-0.52	0.48	0.37	0.48	0.17	0.71																
KHTr - W	0.05	0.00	-0.08	0.23	0.40	0.40	0.10	0.18	0.13															
KHTr - WNW	-0.28	0.19	0.44	-0.01	-0.06	0.07	0.22	0.13	-0.20	0.67														
KHTr - NNW	0.12	0.21	-0.03	0.71	0.70	0.60	0.00	0.24	0.25	0.08	0.82													
KHW - WSW	0.10	0.47	-0.07	0.24	0.34	0.32	-0.31	0.20	0.01	0.26	0.30	0.54												
KHW - SSW	0.60	0.03	-0.22	0.36	0.41	0.24	-0.48	0.46	0.14	-0.04	0.45	0.42	0.74											
KHW - SW	0.43	-0.18	-0.40	0.41	0.45	0.44	-0.02	0.68	0.17	-0.39	0.32	0.22	0.58	0.68										
SUTr - N	0.37	-0.75	-0.57	0.45	0.07	0.36	0.15	0.39	0.09	-0.16	0.39	-0.10	0.42	0.51	0.50									
SUTr - NNE	-0.06	0.13	-0.27	0.58	0.48	0.31	-0.25	0.30	0.18	0.09	0.57	0.15	0.49	0.17	0.16	0.55								
SUTr - E	0.53	-0.41	-0.08	0.19	-0.07	0.23	-0.11	0.69	-0.17	0.00	0.13	0.03	0.46	0.81	0.52	-0.28	0.64							
SUTr - ESE	0.11	-0.41	-0.26	0.49	-0.07	0.24	0.02	0.25	-0.30	0.00	0.16	0.06	0.15	0.46	0.51	-0.03	0.46	0.28						
SUTr - S	0.27	0.23	-0.26	0.28	0.47	0.33	0.03	0.57	0.08	-0.17	0.11	0.44	0.36	0.48	-0.13	-0.10	0.53	-0.06	0.39					
SUTr - SSW	-0.10	-0.02	-0.50	0.55	0.48	0.52	0.37	0.40	-0.17	-0.01	0.55	0.25	0.14	0.16	0.35	0.25	0.08	0.28	0.23	0.33				
SUTr - WSW	0.28	-0.27	-0.56	0.70	0.50	0.67	0.38	0.74	-0.14	0.02	0.67	0.28	0.31	0.67	0.60	0.29	0.61	0.46	0.27	0.57	0.83			
SUTr - W	0.44	-0.07	0.09	-0.16	-0.18	-0.07	-0.48	0.19	0.01	0.15	0.03	0.13	0.29	-0.07	0.34	0.22	0.13	-0.07	-0.28	-0.06	0.14	0.14		
SLHTe - E	0.45	-0.40	-0.01	0.16	-0.18	0.09	-0.18	0.52	-0.15	-0.16	0.22	-0.15	0.34	0.77	0.50	-0.35	0.84	0.51	0.45	0.08	0.55	0.08	0.51	
SLHTr - E	0.09	-0.56	-0.01	0.46	-0.32	0.19	0.16	0.02	0.03	-0.14	-0.02	-0.44	-0.23	0.29	0.48	-0.31	0.36	0.59	-0.19	0.05	0.11	-0.22	0.54	0.71



Appendix iv: Correlation coefficients of *Helichrysum* shrubs growing at different elevations and aspects

Pearson correlation coefficients of *H. trilineatum* shrubs at different elevations and on different aspects. Significant level of  $p < 0.05$ . Where KHTr: Kotisephola Pass study site *H. trilineatum*, KHW: Kotisephola Pass study site *H. witbergense*, MHTr: Sani Pass-upper study site *H. trilineatum*, SHTr: Sani Pass-lower study site *H. trilineatum* and SHTe: Sani Pass-lower study site *H. tenuifolium*, and N = North, E = East, E = South and W = West refers to the aspect of the slope.

	KHTr - E	KHTr - ESE	KHTr - SE	KHTr - SSE	KHTr - S	KHTr - SSW	KHTr - SW	KHTr - WS W	KHTr - W	KHTr - WN W	KHTr - NN W	KHTr - WS W	KHTr - SSW	KHTr - SW	SUHTr - N	SUHTr - NNE	SUHTr - E	SUHTr - ESE	SUHTr - S	SUHTr - SSW	SUHTr - WS W	SUHTr - W	SLHTe - E	SLHTr - E
KHTr - E	1.00																							
KHTr - ESE	0.10	1.00																						
KHTr - SE	0.23	0.08	1.00																					
KHTr - SSE	-0.37	-0.14	-0.23	1.00																				
KHTr - S	-0.25	0.75	-0.19	0.32	1.00																			
KHTr - SSW	-0.35	0.13	-0.25	0.65	0.61	1.00																		
KHTr - SW	-0.39	0.19	-0.44	0.61	0.73	0.90	1.00																	
KHTr - WSW	-0.02	0.24	0.28	0.44	0.35	0.55	0.45	1.00																
KHTr - W	0.00	-0.05	-0.10	-0.11	0.06	0.22	0.23	0.19	1.00															
KHTr - WNW	-0.07	-0.19	0.12	0.01	-0.22	0.23	0.04	0.53	-0.09	1.00														
KHTr - NNW	-0.08	0.19	-0.38	0.56	0.40	0.44	0.39	0.07	-0.28	-0.01	1.00													
KHW - WSW	0.19	0.49	-0.16	-0.09	0.31	0.26	0.10	0.14	-0.22	0.27	0.44	1.00												
KHW - SSW	0.54	-0.04	0.28	-0.43	-0.43	-0.76	-0.69	-0.32	-0.28	-0.21	-0.14	-0.11	1.00											
KHW - SW	0.10	0.20	0.41	0.31	0.09	0.03	-0.16	0.18	-0.16	-0.30	0.07	0.10	-0.15	1.00										
SUHTr - N	0.01	-0.70	-0.28	0.48	-0.34	0.10	0.09	-0.06	0.02	0.05	0.32	-0.14	-0.06	0.04	1.00									
SUHTr - NNE	-0.33	-0.10	-0.09	0.19	0.14	0.10	0.11	0.04	0.09	-0.07	0.21	-0.04	-0.04	-0.14	0.10	1.00								
SUHTr - E	0.21	-0.19	0.47	0.29	-0.34	-0.01	-0.27	0.43	-0.31	0.39	0.02	0.07	0.02	0.63	0.28	-0.38	1.00							
SUHTr - ESE	-0.10	-0.40	0.00	0.45	-0.32	0.11	-0.03	-0.06	-0.29	0.06	0.08	-0.02	-0.22	0.33	0.46	-0.19	0.39	1.00						
SUHTr - S	0.04	0.54	0.44	0.04	0.32	0.05	-0.01	0.53	-0.34	0.21	-0.13	0.24	-0.02	0.50	-0.41	-0.39	0.57	-0.14	1.00					
SUHTr - SSW	-0.30	0.00	-0.54	0.55	0.33	0.46	0.57	0.27	-0.43	0.30	0.54	0.34	-0.30	-0.21	0.28	0.20	-0.04	0.22	0.04	1.00				
SUHTr - WSW	-0.24	0.06	-0.21	0.84	0.38	0.69	0.52	0.52	-0.19	0.27	0.74	0.35	-0.43	0.30	0.38	0.28	0.36	0.30	0.14	0.58	1.00			
SUHTr - W	0.21	-0.29	-0.03	-0.33	-0.30	0.02	-0.09	0.06	0.64	0.41	-0.13	0.06	0.02	-0.50	0.21	0.13	-0.18	-0.21	-0.48	-0.32	-0.13	1.00		
SLHTe - E	-0.05	-0.24	0.39	0.40	-0.28	0.00	-0.19	0.11	-0.42	0.15	0.20	-0.11	-0.09	0.59	0.34	-0.42	0.79	0.62	0.31	-0.01	0.31	-0.35	1.00	
SLHTr - E	0.09	-0.56	-0.01	0.46	-0.32	0.19	0.16	0.02	0.03	-0.14	-0.02	-0.44	-0.23	0.29	0.48	-0.31	0.36	0.59	-0.19	0.05	0.11	-0.22	0.54	1.00

Appendix v: Multiple regression of climate-growth relationships.

Where the dependent variable (Y) is average shrub ring width and independent variables are: Xa = Temperature, Xb = Rainfall, Xc = Elevation, Xd = Aspect

Site and shrub species	Independent Parameters	Equation	P	F-value	R <sup>2</sup>
KHTr	Mean Annual October-March Temp. Total October-March Rainfall Elevation Aspect	$Y = 462.27 - 0.151Xa + 0.0004Xb - 0.19Xc + 0.0129Xd$	P < 0.93	F(4,6) = 0.21	0.12
	Mean November - December Temp. Total November - December Rainfall Elevation Aspect	$Y = 1646.75 + 0.0615Xa + 0.0033Xb - 0.49Xc - 0.053Xd$	P < 0.12	F(4,7) = 2.8	<b>0.61</b>
	Mean December - January Temp. Total December - January Rainfall Elevation Aspect	$Y = 1226.82 - 0.190Xa + 0.002Xb - 0.37Xc - 0.0005Xd$	P < 0.31	F(4,8) = 1.44	0.42
	Mean November - January Temp. Total November - January Rainfall Elevation Aspect	$Y = 884.91 - 0.092Xa + 0.001Xb - 0.27Xc - 0.005Xd$	P < 0.65	F(4,7) = 0.64	0.27
	Mean November - February Temp. Total November - February Rainfall Elevation Aspect	$Y = 642.65 - 0.151Xa + 0.0004Xb - 0.19Xc + 0.0129Xd$	P < 0.93	F(4,6) = 0.21	0.12
	Mean December - March Temp. Total December - March Rainfall Elevation Aspect	$Y = 951.61 - 0.10Xa - 0.29Xc + 0.021Xd$	P < 0.81	F(4,7) = 0.40	0.19
	Mean January-February Temp. Total January-February Rainfall Elevation Aspect	$Y = 58.77 + 0.163Xa - 0.001Xb - 0.02Xc + 0.047Xd$	P < 0.27	F(4,6) = 1.58	0.44
	KHW	Mean Annual October-March Temp. Total October-March Rainfall Elevation Aspect	$Y = -561 + 0.29Xa + 0.0004Xb + 0.17Xc$	P < 0.70	F(4,6) = 0.56

	Mean November - December Temp. Total November - December Rainfall Elevation Aspect	$Y = -35.85 + 0.14Xa - 0.0005Xb + 0.19Xd$	$P < 0.53$	$F(4,8) = 0.87$	0.25
	Mean December - January Temp. Total December - January Rainfall Elevation Aspect	$Y = -38.07 + 0.14Xa - 0.002Xb + 0.20Xd$	$P < 0.43$	$F(4,8) = 1.09$	0.29
	Mean November - January Temp. Total November - January Rainfall Elevation Aspect	$Y = -24.47 + 0.17Xa - 0.001Xb + 0.13Xd$	$P < 0.47$	$F(4,8) = 1$	0.27
	Mean November - February Temp. Total November - February Rainfall Elevation Aspect	$Y = -310.75 + 0.36Xa - 0.0007Xb + 0.09Xc$	$P < 0.33$	$F(4,7) = 1.43$	0.38
	Mean December - March Temp. Total December - March Rainfall Elevation Aspect	$Y = -43.9 + 0.35Xa - 0.0005Xb + 0.22Xd$	$P < 0.24$	$F(4,8) = 1.75$	0.40
	Mean January-February Temp. Total January-February Rainfall Elevation Aspect	$Y = -38.06 + 0.46Xa - 0.0002Xb + 0.18Xd$	$P < 0.12$	$F(4,8) = 2.74$	<b>0.51</b>
SUHTr	Mean Annual October-March Temp. Total October-March Rainfall Elevation Aspect	$Y = 236.8 - 0.26Xa - 0.001Xb - 0.08Xc + 0.01Xd$	$P < 0.32$	$F(4,5) = 1.6$	0.55
	Mean November - December Temp. Total November - December Rainfall Elevation Aspect	$Y = 170.13 + 0.07Xa - 0.0007Xb - 0.06Xc + 0.016Xd$	$P < 0.17$	$F(4,7) = 2.18$	0.55
	Mean December - January Temp. Total December - January Rainfall Elevation	$Y = 219.49 + 0.17Xa + 0.002Xb - 0.08Xc + 0.02Xd$	$P < 0.03$	$F(4,8) = 4.48$	0.69

	Aspect				
	Mean November - January Temp. Total November - January Rainfall Elevation Aspect	$Y = 220.32 + 0.10Xa + 0.0004Xb - 0.08Xc + 0.02Xd$	$P < 0.26$	$F(4,7) = 1.65$	0.49
	Mean November - February Temp. Total November - February Rainfall Elevation Aspect	$Y = 187.54 + 0.21Xa + 0.0005Xb - 0.07Xc + 0.02Xd$	$P < 0.30$	$F(4,6) = 1.6$	<b>0.77</b>
	Mean December - March Temp. Total December - March Rainfall Elevation Aspect	$Y = 109.18 + 0.40Xa + 0.002Xb - 0.04Xc + 0.03Xd$	$P < 0.02$	$F(4,7) = 5.76$	<b>0.77</b>
	Mean January-February Temp. Total January-February Rainfall Elevation Aspect	$Y = 360.85 - 0.005Xa + 0.001Xb - 0.13Xc + 0.02Xd$	$P < 0.04$	$F(4,8) = 4.1$	0.67
SLHTe	Mean Annual October-March Temp. Total October-March Rainfall Elevation Aspect	$Y = -32.31 + 1.07Xa + 0.004Xb + 0.001Xc + 0.17Xd$	$P < 0.50$	$F(4,5) = 0.96$	0.43
	Mean November - December Temp. Total November - December Rainfall Elevation Aspect	$Y = -10.69 + 0.215Xa - 0.003Xb + 0.002Xc + 0.047Xd$	$P < 0.26$	$F(4,7) = 1.67$	0.49
	Mean December - January Temp. Total December - January Rainfall Elevation Aspect	$Y = -14.42 + 0.659Xa - 0.001Xb + 0.003Xc - 0.014Xd$	$P < 0.18$	$F(4,7) = 2.17$	0.55
	Mean November - January Temp. Total November - January Rainfall Elevation Aspect	$Y = -17.01 + 0.58Xa - 0.001Xb + 0.002Xc + 0.053Xd$	$P < 0.22$	$F(4,7) = 1.86$	0.52
	Mean November - February Temp. Total November - February Rainfall	$Y = -22.67 + 0.58Xa - 0.0022Xb + 0.003Xc + 0.09Xd$	$P < 0.39$	$F(4,5) = 1.29$	0.51

	Elevation Aspect				
	Mean December - March Temp. Total December - March Rainfall Elevation Aspect	$Y = -25.26 + 0.83Xa + 0.002Xb + 0.002Xc + 0.09Xd$	$P < 0.10$	$F(4,6) = 3.20$	<b>0.68</b>
	Mean January-February Temp. Total January-February Rainfall Elevation Aspect	$Y = -20.67 + 0.70Xa + 0.0016Xb + 0.00024Xc + 0.06Xd$	$P < 0.31$	$F(4,6) = 1.53$	0.51
SLHTr	Mean Annual October-March Temp. Total October-March Rainfall Elevation Aspect	$Y = 41.53 + 0.164Xa + 0.0014Xb + 0.0009Xc - 0.51Xd$	$P < 0.82$	$F(4,3) = 0.36$	0.33
	Mean November - December Temp. Total November - December Rainfall Elevation Aspect	$Y = 39.54 + 0.02Xa + 0.0014Xb + 0.0007Xc - 0.4622Xd$	$P < 0.69$	$F(4,5) = 0.58$	0.31
	Mean December - January Temp. Total December - January Rainfall Elevation Aspect	$Y = 39.42 + 0.3488Xa + 0.0037Xb + 0.0021Xc - 0.55Xd$	$P < 0.37$	$F(4,5) = 1.33$	0.52
	Mean November - January Temp. Total November - January Rainfall Elevation Aspect	$Y = 67.16 + 0.773Xa + 0.0049Xb + 0.0042Xc - 0.97Xd$	$P < 0.37$	$F(4,5) = 1.33$	0.52
	Mean November - February Temp. Total November - February Rainfall Elevation Aspect	$Y = 57.42 + 0.62Xa + 0.0029Xb + 0.0028Xc - 0.80Xd$	$P < 0.57$	$F(4,4) = 0.82$	0.45
	Mean December - March Temp. Total December - March Rainfall Elevation Aspect	$Y = 28.03 + 0.497Xa + 0.0022Xb + 0.0013Xc - 0.42Xd$	$P < 0.60$	$F(4,4) = 0.75$	0.43
	Mean January-February Temp. Total January-February Rainfall Elevation Aspect	$Y = 27.64 + 1.11Xa - 0.0004Xb + 0.0008Xc - 0.48Xd$	$P < 0.08$	$F(4,4) = 4.62$	<b>0.82</b>

Appendix vi: Summary of shrub abundance

<b>Kotisephola Pass study site</b>																
Shrub abundance per elevation																
Total number of counted shrubs	951															
Percentage shrub abundance (%)																
<i>Helichrysum trilineatum</i>	69															
<i>Helichrysum witbergense</i>	8															
Other plant species (including grass, shrubs, moss, lichen etc.)	22															
	N	NNE	NE	ENE	E	ESE	SE	SSE	S	SSW	SW	WSW	W	WNW	NW	NNW
<b>Shrub abundance per aspect</b>																
Shrub species richness (Number of shrub species per aspect)	2+	2+	2+	2+	3+	3+	3+	3+	3+	3+	3+	3+	3+	3+	3+	3+
Total number of counted shrubs per aspect	16	12	8	8	42	85	69	42	62	93	75	74	117	149	89	10
<b>Percentage shrub (%) per aspect</b>																
<i>Helichrysum trilineatum</i>	0.0	0.2	0.2	0.0	0.6	1.2	3.6	5.2	5.8	8.7	9.4	11.2	17.8	22.6	13.5	0.0
<i>Helichrysum witbergense</i>	0.0	0.0	0.0	0.0	0.0	0.0	5.0	8.8	27.5	42.5	16.3	0.0	0.0	0.0	0.0	0.0
Other plant species (including grass, shrubs, moss, lichen etc.)	7.5	5.2	3.3	3.8	17.8	36.2	19.2	0.5	0.9	0.9	0.0	0.0	0.0	0.0	0.0	4.7
<b>Standard deviation for shrub abundance per aspect</b>	5.7				24.0				21.0				28.6			
<b>Shannon-Weiner Diversity Index</b>	0.0	0.3	0.4	0.0	0.3	0.3	0.8	0.6	0.8	0.8	0.5	0.0	0.0	0.0	0.0	0.0
<b>Shannon-Weiner Evenness Index</b>	0.0	0.4	0.5	0.0	0.5	0.5	0.8	0.5	0.7	0.7	0.7	0.0	0.0	0.0	0.0	0.0
<b>Sani Pass-upper study site</b>																
Shrub abundance per elevation																
Total number of counted shrubs	1369															

Percentage shrub abundance (%)																
<i>Helichrysum trilineatum</i>	518															
Other plant species (including grass, shrubs, moss, lichen etc.)	851															
	N	NNE	NE	ENE	E	ESE	SE	SSE	S	SSW	SW	WSW	W	WNW	NW	NNW
Shrub abundance per aspect																
Shrub species richness (Number of shrub species per aspect)	2+	2+	2+	2+	3+	3+	2+	2+	2+	2+	2+	2+	2+	2+	2+	2+
Total number of counted shrubs per aspect	110	112	101	89	100	106	100	86	59	46	52	95	93	77	58	85
Percentage shrub (%) per aspect																
<i>Helichrysum trilineatum</i>	46	9	5	5	9	6	4	4	6	7	8	35	38	32	3	1
Other plant species (including grass, shrubs, moss, lichen etc.)	91	28	30	25	24	30	37	41	31	17	14	1	3	3	1	4
<b>Standard deviation for shrub abundance per aspect</b>	26.9				33.0				22.7				36.2			
<b>Shannon-Weiner Diversity Index</b>	0.3	0.6	0.4	0.2	0.6	0.5	0.3	0.3	0.5	0.6	0.4	0.0	0.1	0.1	0.1	0.2
<b>Shannon-Weiner Evenness Index</b>	0.4	0.8	0.6	0.2	0.8	0.7	0.4	0.4	0.7	0.9	0.5	0.0	0.1	0.1	0.2	0.3
Sani Pass-lower study site																
Shrub abundance per elevation																
Total number of counted shrubs	296															
Percentage shrub abundance (%)																
<i>Helichrysum trilineatum</i>	7															
<i>Helichrysum tenuifolium</i>	16															
Other plant species (including grass, shrubs, moss, lichen etc.)	78															
	E															
Shrub abundance per aspect																

Shrub species richness (Number of shrub species per aspect)	3+
Total number of counted shrubs per aspect	296
<b>Percentage shrub (%) per aspect</b>	
<i>Helichrysum trilineatum</i>	7
<i>Helichrysum tenuifolium</i>	16
Other plant species (including grass, shrubs, moss, lichen etc.)	78
<b>Standard deviation for shrub abundance per aspect</b>	31.6
<b>Shannon-Weiner Diversity Index</b>	0.4
<b>Shannon-Weiner Evenness Index</b>	0.3